



Published in final edited form as:

ACS Sens. 2024 April 26; 9(4): 1682–1705. doi:10.1021/acssensors.3c02529.

## Electrochemical Detection of Gasotransmitters: Status and Roadmap

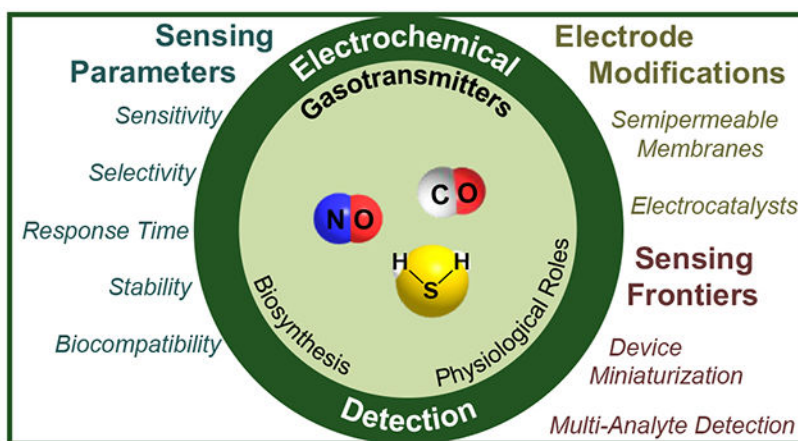
Audrey L. Herrald,  
Emma K. Ambroggi,  
Katherine A. Mirica

Department of Chemistry, Burke Laboratory, Dartmouth College, 41 College Street, Hanover, New Hampshire 03755, United States

### Abstract

Gasotransmitters, including nitric oxide (NO), carbon monoxide (CO), and hydrogen sulfide (H<sub>2</sub>S) are a class of gaseous, endogenous signaling molecules that interact with one another in the regulation of critical cardiovascular, immune, and neurological processes. The development of analytical sensing mechanisms for gasotransmitters, especially multi-analyte mechanisms, holds vast importance and constitutes a growing area of study. This review provides an overview of electrochemical sensing mechanisms, with an emphasis on opportunities in multi-analyte sensing. Electrochemical methods demonstrate good sensitivity, adequate selectivity, and the most well-developed potential for multi-analyte detection of gasotransmitters. Future research will likely address challenges with sensor stability and biocompatibility (i.e., sensor lifetime and cytotoxicity), sensor miniaturization, and multi-analyte detection in biological settings.

### Graphical Abstract



**Corresponding Author:** Katherine A. Mirica – Department of Chemistry, Burke Laboratory, Dartmouth College, Hanover, NH, 03755, United States, Katherine.a.mirica@dartmouth.edu.

The authors declare no competing financial interest.

## Keywords

Gasotransmitters; nitric oxide; carbon monoxide; hydrogen sulfide; electrochemistry; sensors; tools; electrocatalysts; multi-analyte detection

---

## HISTORICAL PERSPECTIVE OF GASOTRANSMITTER DISCOVERY

Nitric oxide (NO) was first identified as an important physiological signaling molecule in the 1980s by Robert Furchgott, Louis Ignarro and Ferid Murad.<sup>1–3</sup> The trio was later awarded the Nobel Prize in Medicine and Physiology for their work with NO. Carbon monoxide (CO) and hydrogen sulfide (H<sub>2</sub>S) were recognized as important biological signaling molecules shortly after. In 1993, Ajay Verma and colleagues published their findings that endogenous CO—initially presumed to be an unimportant byproduct of heme breakdown—elicited vasodilatory effects similar to those of NO.<sup>4</sup> This discovery initiated a series of investigations into the signaling properties of the molecule, leading to the official designation of CO as a gasotransmitter.<sup>5</sup> H<sub>2</sub>S joined the gasotransmitter fold in 2010, and in subsequent years, each of the three molecules has demonstrated important roles in biological function and disease pathogenesis.<sup>6</sup> The physiological functions of NO, CO and H<sub>2</sub>S are intimately linked. Each of the molecules plays a role in the biosynthesis and breakdown of the others, and co-modulatory signaling activity is observed between all three—often in shared physiological locations and on similar timescales.<sup>7</sup> This relationship underlies the importance of analytical sensing mechanisms that can simultaneously detect and differentiate between multiple gasotransmitters, and it is the reason for our decision to highlight multi-analyte detection in this review.

Importantly, chemical species must satisfy a particular set of criteria to be classified as gasotransmitters. The term “gasotransmitter” was first coined in 2002 by Rui Wang, who sought to distinguish NO and CO from classical neurotransmitters.<sup>8</sup> As defined by Wang and colleagues, gasotransmitters are small, endogenous molecules of gas that exist either in a gaseous form or are dissolved in circulation in the body.<sup>9</sup> Gasotransmitters must be freely permeable to cell membranes, have well-defined specific functions at physiologically relevant concentrations, be functionally mimicable by their exogenously applied counterparts, and participate in signal transduction with specific molecular targets.<sup>10</sup> NO, CO, and H<sub>2</sub>S were the first three molecules to be classified as gasotransmitters. Although additional molecules have been proposed as potential gasotransmitters, the term “gasotransmitter” throughout this review will refer specifically to NO, CO, and H<sub>2</sub>S.<sup>10,11</sup> The relevant concentrations and endogenous locations of each gasotransmitter are displayed in Table 1, in addition to an overview of the physiochemical properties of each species.

The criteria that Wang and colleagues have established define gasotransmitters as a specific subset of physiological gases; not all biologically active gasses are gasotransmitters. Diatomic oxygen, for example, is not produced inside the body—meaning that, despite its important role as a signaling agent, the molecule is not a gasotransmitter. The same can be said of ethylene and hydrogen gas, even though the latter has demonstrated physiological relevance as both a therapeutic mechanism and as a biomarker for some

diseases.<sup>12</sup> Recently, ammonia, methane, sulfur dioxide, and carbonyl sulfide have all been proposed as additions to the gasotransmitter family.<sup>13–15</sup> Further research is required to fully elucidate the biological roles of these potential gasotransmitters. In many cases, progress in the development of *in-vivo* detection mechanisms for these potential gasotransmitters will be critical in improving the understanding of pathways for their endogenous synthesis<sup>14</sup> and physiological actions<sup>13</sup>—both of which are expected to elucidate the relationship between the species in question and the gasotransmitters that have already been identified. The pathways of endogenous synthesis and the physiological actions of NO, CO, and H<sub>2</sub>S, as well as their interactions with one another, are addressed in subsequent sections.

## SCOPE AND FOCUS OF REVIEW

This review focuses solely on electrochemical methods for the detection of gasotransmitters. While several methods for the detection of gasotransmitters have been established (among them UV-Vis spectroscopy and fluorescence), electrochemical methods offer many advantageous characteristics for rapid and multiplexed detection in biological settings. First, the commercialization of electrochemical sensors has made the method relatively inexpensive, user-friendly, and easily customizable for multiple different target analytes.<sup>18</sup> Second, electrochemistry offers the possibility of multi-analyte detection via microelectrode arrays—particularly important for the detection of gasotransmitters, whose biological actions are closely interrelated.<sup>19,20</sup> Third, electrochemical methods are characterized by low detection limits and fast response times both *in-vivo* and *in-vitro*.<sup>12,19,21–24</sup> For these reasons, electrochemical methods for the detection of gasotransmitters are highlighted in this review. Readers are referred to the work of Alday and colleagues and Jose and colleagues for reviews on fluorescence-based methods for the detection of gasotransmitters.<sup>25,26</sup>

In addition to the focus on electrochemistry, this review highlights electrochemical sensors that are capable of multi-analyte detection. The physiological actions of gasotransmitters are not only tied closely to their rates of synthesis and diffusion, but also to their interactions with one another.<sup>7,27–29</sup> Therefore a complete scientific understanding of the gasotransmitters will depend on sensing mechanisms that are capable of detecting and distinguishing between multiple gasotransmitters simultaneously. The body's own solutions to the challenge of distinguishing between gasotransmitters can provide inspiration for effective sensing schemes. As such, the physiological actions and types of biological distinction for the three gasotransmitters are addressed below.

While numerous groups have reviewed detection methods for NO,<sup>18,30,31</sup> CO,<sup>20,25,26</sup> or H<sub>2</sub>S,<sup>20,24</sup> the literature lacks an up-to-date review of electrochemical sensors for all three gasotransmitters.<sup>20,25,26</sup> In this review, we seek to present and summarize promising detection methods while taking into account the co-existence of all three gasotransmitters. We first address the physiological function and significance of each gasotransmitter, then follow with a discussion of analytical detection methods. The discussion of detection methods is divided into two sections, each highlighting a different element of electrochemical sensors: (1) semi-permeable membranes and (2) electrocatalysts. Both of these electrode-modifying materials can bolster selectivity against potential interferents and enhance the sensitivity of the device. Electrochemical sensing platforms for the

simultaneous detection of multiple gasotransmitters are addressed in the final section. In addition to presenting the most sensitive and selective examples of electrochemical gasotransmitter sensors currently reported, we also seek to survey novel and emerging materials that hold promise for future gasotransmitter detection in complex physiological environments.

## PHYSIOLOGICAL SYNTHESIS AND SIGNIFICANCE: NO

A family of enzymes called nitric oxide synthases (NOSs) produce NO by catalyzing the oxidation of the amino acid L-arginine to NG-hydroxy-L-arginine and eventually to L-citrulline and NO (Figure 1). The NOS family consists of three NOS isoenzymes: endothelial (eNOS), neuronal (nNOS), and cytokine-inducible (iNOS).<sup>3,32</sup> Though all of these NOS isoforms produce NO by catalyzing L-arginine oxidation, each isoenzyme plays a slightly different physiological role. eNOS, generated in blood vessel linings, catalyzes the production of the NO that eventually modulates vasodilation and helps maintain appropriate blood pressure.<sup>33</sup> nNOS is found in neuronal cells, where the enzyme helps produce the NO that is implicated in neuronal signaling pathways.<sup>34</sup> Finally, iNOS catalyzes NO production throughout the body in support of the innate immune system. When the body encounters an invasive pathogen, iNOS is expressed by macrophages, hepatocytes, and smooth muscle cells. The subsequent uptick in NO levels then aids the immune system by reducing its microbial load.<sup>35</sup>

Following synthesis, NO plays key roles in a variety of physiological systems. Among them are the cardiovascular, reproductive, and nervous systems, where NO is involved in neuronal communication, regulation of vascular tone, smooth muscle cell neurotransmission, immune response, and even gene regulation.<sup>5</sup> The most clearly understood mechanism for NO function is its targeting of the abundant smooth muscle enzyme soluble guanylate cyclase (sGC). Here, NO stimulates the conversion of guanosine 5'-triphosphate (GTP) to 3',5'-cGMP, which initiates smooth-muscle relaxation (and thus vasodilation) via activation of calcium-sensitive K<sup>+</sup> channels.<sup>33,36</sup> In the brain, NO serves as a retrograde messenger that enhances two elements of neural plasticity: long-term potentiation (LTP) and long-term depression (LTD). Both LTP and LTD refer to lasting changes in neural connections that arise from repetitive firing patterns in the brain, and neither could occur without NO. A plethora of additional NO-related neural functions have been reported, including NO-modulated release of neurotransmitters,<sup>37</sup> facilitation of discriminative learning,<sup>38</sup> the upkeep of circadian rhythm,<sup>39</sup> and even the modulation of sensory experience.<sup>40</sup>

Importantly, the many physiological roles of NO could not have been identified in the absence of selective and sensitive methods for its detection. The identification of NO as the mysterious “endothelium-derived relaxing factor” (EDRF), critical in vasodilation, was the finding that first established NO as a gasotransmitter and initiated a subsequent flood of investigations into the signaling capabilities of the molecule.<sup>41</sup> This initial identification of NO as EDRF, accomplished independently in 1986 by Ignarro et al. and by Palmer, Ferrige, and Moncada, compared spectrophotometric scans of deoxyhemoglobin before and after the addition of a saturated solution of NO to scans of the same deoxyhemoglobin solution before and after the addition of the then-unidentified EDRF.<sup>1,42</sup> NO was also chemically

identified by Ignarro et al. through a spectrophotometric bioassay based on the diazotization of sulfanic acid by NO and subsequent coupling with N-(1-naphthyl)-ethylenediamine.<sup>1</sup> Soon after the identification of NO as EDRF, Bredt and Snyder identified the role of NO in neural signalling *in vitro* using the Griess Assay.<sup>37</sup> Other early detection of NO *in vivo* relied on electron paramagnetic resonance (EPR) spectroscopy combined spin-trapping with an iron-based complex.<sup>43</sup> Around the same time, World Precision Instruments developed the first commercially available electrode-based amperometric detection system for NO, now used widely in research. Currently, two-electrode amperometric detection is one of the most common methods for experimental analysis of NO both *in vivo* and *in vitro*.<sup>31</sup>

## PHYSIOLOGICAL SYNTHESIS AND SIGNIFICANCE: CO

The endogenous production of CO depends upon catalysis by an enzyme known as heme oxygenase (HO). HO produces CO through the breakdown of free heme, largely from aging or damaged red blood cells.<sup>44</sup> The breakdown process generates three products: CO, ferrous iron, and biliverdin-IX (see Figure 2). Biliverdin-IX, eventually reduced to bilirubin-IX through the action of biliverdin reductase, exerts powerful antioxidant effects.<sup>45</sup> Macrophages recycle the ferrous iron, which also plays a number of critical physiological roles.<sup>46</sup> Initially, the clear physiological value of both biliverdin and ferrous iron contributed to postulations that CO, the third product of heme breakdown, might also play an important physiological role.<sup>5</sup> By now, CO is well known to function as a neural signaling molecule through modulation of the messenger nucleotide guanosine 3',5'-monophosphate (cGMP), similarly to NO.<sup>47,48</sup>

Many mechanistic elements of CO signaling relate closely to the molecule's well-understood toxicity when present in excess from exogenous sources. The high-affinity bonding between CO and hemoglobin (Hb) greatly exceeds that of oxygen and Hb, meaning that excess CO can pose a dangerous hindrance to oxygen transport. Upon saturation of hemoglobin, CO can also bind to other proteins.<sup>49</sup> These binding actions, like the hemoglobin interactions, pose health risks—namely inhibition of ATP synthesis in the mitochondrial respiratory chain.<sup>49</sup> However, CO-protein interactions within the mitochondria are also emerging as important signaling mechanisms for the maintenance of cellular homeostasis, cytoprotection, and metabolism. As a gasotransmitter, CO exerts its physiological effects through four primary pathways, each of which originates in the mitochondria of the cell: (i) mitochondrial biogenesis, (ii) modulation of enzymatic activity of cytochrome c oxidase, (iii) generation of mitochondrial ROS for signaling and (iv) induction of mitochondrial uncoupling effect, which helps curb the generation of harmful reactive oxygen species.<sup>50</sup> The latter appears to enhance longevity in aging individuals, and it has also been explored as a potential therapeutic for neurodegenerative diseases.<sup>51</sup>

## PHYSIOLOGICAL SYNTHESIS AND SIGNIFICANCE: H<sub>2</sub>S

Hydrogen sulfide, like NO and CO, is produced largely via enzymatic reactions.<sup>52</sup> However, unlike NO and CO, H<sub>2</sub>S emerges from numerous pathways (see Figure 3). Many of these pathways involve the amino acid l-cysteine, which humans obtain mainly through dietary means.<sup>53</sup> Catalytic H<sub>2</sub>S production from l-cysteine occurs through three enzymes:

cystathionine  $\beta$ -synthase (CBS), cystathionine- $\gamma$ -lyase (CSE), and 3-mercaptopyruvate sulfurtransferase (3-MST), each mediating a different pathway for H<sub>2</sub>S production. CBS, the predominant H<sub>2</sub>S synthase in the central nervous system, acts directly on l-cysteine to generate H<sub>2</sub>S.<sup>53,54</sup> CSE catalyzes l-cysteine or its homologue, homocysteine, to generate H<sub>2</sub>S along with  $\alpha$ -ketobutyrate and ammonia.<sup>55</sup> Finally, 3-MST—the most recently discovered H<sub>2</sub>S-producing enzyme—mediates the release of H<sub>2</sub>S from persulfide through an enzymatic process facilitated by cysteine aminotransferase (CAT) and involving the transfer of a sulfur atom from 3-MST to an intermediate (3-mercaptopyruvate).<sup>56</sup> The 3-MST enzyme also produces H<sub>2</sub>S through interactions with the amino acid d-cysteine, after the exogenous amino acid is broken down by d-amino acid oxidase (DAO) in the peroxisome of the cell.

Even though a majority of endogenous H<sub>2</sub>S emerges through enzymatic mechanisms, some endogenous H<sub>2</sub>S is also derived non-enzymatically from sulfane sulfur via chemical reduction.<sup>57</sup> In this process, reactive sulfur species in persulfides, thiosulfate, and polysulfides are reduced to H<sub>2</sub>S by reducing agents such as NADH (nicotinamide adenine dinucleotide) and NADPH. Both reducing agents are supplied by the oxidation of glucose (via glycolysis).<sup>57</sup> Ishigami and colleagues used silver particles to measure free H<sub>2</sub>S in the brain, and they found that all endogenous H<sub>2</sub>S is immediately absorbed and stored as bound sulfur upon its production. The release of H<sub>2</sub>S from its bound state requires alkalization of the cytoplasm, which has been achieved in studied brain cells (astrocytes) when the excitation of nearby neurons generates high extracellular concentrations of K<sup>+</sup>.<sup>58</sup> These findings constitute the basis of a potential mechanism for the action of H<sub>2</sub>S as a neural signaling molecule.

As a gasotransmitter, H<sub>2</sub>S plays multiple roles in regulating cell behaviors. These roles include cell survival, differentiation, atrophy, and senescence, each via one (or multiple) of the following mechanisms: histone modification, DNA methylation, non-coding RNA changes, DNA damage repair, transcription factor activity, and post-translational modification of proteins.<sup>59</sup> Through post-translational modifications (PTMs), H<sub>2</sub>S signaling is thought to play an important role in the reduction of harmful reactive oxygen species (ROSs). These ROSs, which tend to disrupt critical cellular processes, are implicated in the pathogenesis of numerous diseases.<sup>60</sup> Researchers propose that H<sub>2</sub>S-induced PTMs could protect against a wide range of these age-related diseases, including cardiovascular disease, cancer, and neurodegenerative diseases.<sup>61</sup> While the physical, biochemical, and physiological properties of H<sub>2</sub>S have been addressed in the literature, experimental and mathematical modeling of the transport properties of the molecule *in vivo* remain limited.<sup>60,62</sup> In fact, compared to NO and CO, the physiological behavior of H<sub>2</sub>S appears to be the least understood, perhaps due in part to its tendency for reversible conversion into closely related molecular species. In electrochemical sensing, for example, the electrooxidation of H<sub>2</sub>S readily generates electrode-poisoning sulfur, posing a challenge to sensor design.<sup>63</sup> Many electrochemical sensing schemes are also challenged by the task of differentiation between H<sub>2</sub>S and other thiol species, particularly because free blood sulfide levels are considerably lower than total concentrations of sulfide species.<sup>64</sup> Often, the alkaline conditions or high electrical potentials required for the detection of H<sub>2</sub>S also result in the inadvertent release of some sulfide from other sulfide-containing biomolecules.<sup>65</sup>



The rapid O<sub>2</sub>-dependent consumption of H<sub>2</sub>S by blood, a process governed by constitutive production and oxidation, also contributes to the difficulty of determining physiological concentrations of H<sub>2</sub>S.<sup>64</sup> Nonetheless, electrochemical sensing platforms for H<sub>2</sub>S have been developed, and the most promising of these are described in subsequent sections.

## BIOLOGY AS A MODEL FOR MULTI-ANALYTE DETECTION

In many physiological contexts, gasotransmitters act together to carry out their roles. This concerted activity makes multi-analyte detection strategies particularly valuable. Such detection strategies depend on precise distinction between often-similar biological gases, presenting unique challenges to sensor design. However, we suggest that inspiration for creative chemical solutions lies in a well-studied and highly effective model of multi-analyte detection: the human body. Physiological distinction between gasotransmitters by heme proteins and nitric oxide synthases (eNOS, iNOS)—among other examples—are discussed here as instances of physiological detection that could prove useful in sensor design.

First, interactions between gasotransmitters and heme proteins serve as one of the most ubiquitous examples of multi-gasotransmitter detection in the body.<sup>7,16,66</sup> The enzymes heme oxygenase (HO), nitric oxide synthase (NOS), and cystathionine β-synthase (CBS) are critical for the synthesis and regulation of CO, NO, and H<sub>2</sub>S, respectively. Each must reliably distinguish between multiple gasotransmitters to perform its role. The selectivity of heme binding sites tends to be governed by one or more of the following (often sequential) principles: (1) oxidative states of the central iron of the prosthetic heme and the associated binding affinity of gases, (2) conformational changes within the protein arising from ligand binding, and (3) structural changes and protein functions. Each element can be observed in the example of hemoglobin (Hb).<sup>7,67</sup>

The oxidative states of the central hemoglobin iron atom are critical in distinguishing between gasotransmitters. The central iron atom shifts between ferrous (Fe<sup>2+</sup>) and ferric (Fe<sup>3+</sup>) oxidation states. When iron is in the ferrous state, hemoglobin binds preferentially to neutral ligands like O<sub>2</sub> and CO.<sup>7</sup> In the case of ferric (Fe<sup>3+</sup>) hemoglobin, anions such as OH<sup>-</sup>, N<sub>3</sub><sup>-</sup>, CN<sup>-</sup>, and H<sub>2</sub>S are preferentially bound. When it comes to distinguishing between gasotransmitters, NO has a much higher affinity for ferrous heme (nitrosylheme) than does CO. While NO binds preferentially to a five-coordinated heme structure, CO binds preferentially to a six-coordinate structure.<sup>7</sup> The differences are due to a combination of varied d-orbital electron density, pi-backbonding stabilization, and the presence of physiological reducing equivalents.<sup>7,68-71</sup> In the context of sensor design, this example reinforces the importance of attention to d-electron configuration and possible oxidation states of a central ligating metal. The simple chemical properties that govern molecular selectivity in the body are the same measurable and predictable properties of candidate metals for sensor fabrication—meaning that a thorough understanding of analyte-detector chemistry, even at the simplest level, plays a key role in the rational design of multi-analyte sensors.

In addition to hemoglobin, eNOS, iNOS, and HO serve as examples of endogenous substrates that must distinguish between, and respond differentially to, multiple endogenous

gasotransmitters.<sup>73–80</sup> The ligation of NO to the Fe<sup>2+</sup> (ferrous) heme of HO-2, the primary enzyme responsible for the endogenous production of CO, occurs 500-fold more tightly than binding between NO and one of its common heme targets, Fe<sup>3+</sup>-myoglobin (see Figure 4).<sup>7,72,81</sup> Conversely, CO exerts inhibitory effects on iNOS, the enzyme responsible for the synthesis of NO. As for the third gasotransmitter, H<sub>2</sub>S appears to *stimulate* the activity of eNOS and aid in increased NO production. Specifically, the S-sulfhydration of eNOS appears to increase eNOS phosphorylation, decrease its S-nitrosylation, promote eNOS dimerization, and, in all, increase NO production.<sup>10</sup> These interactions are thought to occur in similar regions and on similar temporal timescales to those of NO and CO on NOS. In short, each of the three gasotransmitters influences the endogenous “detectors” discussed here, often modulating their affinity for one or two of the other gases. Sensor design that incorporates an analyte-specific inhibitory cascade could aid in the modulation of sensor specificity under different physiological conditions—another thread of design inspiration drawn from biology.<sup>32,82,83</sup>

## ANALYTICAL DETECTION METHODS

The physiological relevance of gasotransmitters has generated a host of efforts to develop sensitive and selective methods for their detection. Among these methods are chromatography, colorimetry, spectroscopy, and electrochemistry. While chromatographic and colorimetric methods provide some of the most reliable and sensitive analyses, these methods do not allow for real-time monitoring of gasotransmitters within living cells.<sup>84</sup> Electrochemical methods for gasotransmitter detection offer the advantages of easily miniaturized detection platforms and limited sample disturbance.<sup>31</sup> The selectivity and sensitivity of electrochemical methods often depend upon the application of semi-permeable membranes and other chemical mediators (e.g., catalysts), both of which enhance the performance of the sensor.<sup>31</sup> The most common electrochemical techniques for the detection of gasotransmitters include potentiodynamic methods, such as linear sweep voltammetry (LSV), cyclic voltammetry (CV), and differential pulse voltammetry (DPV), as well as potentiostatic methods, such as constant potential amperometry (CPA) and chronocoulometry (CC).<sup>31</sup> While the opportunity to vary the applied voltage in potentiodynamic techniques enables superior tailoring of analytical parameters (i.e., sensor selectivity and signal magnitude), potentiostatic techniques often afford greater sensitivity and temporal resolution.<sup>84</sup>

Regardless of sensing technique, both the selectivity and sensitivity of sensors depend on modifications to the surface of sensing electrodes. These modifications can take many forms, but this review categorizes electrochemical sensors according to two of the most prominent modification types: (1) semi-permeable membranes and (2) electrocatalysts (see Figure 5). Semi-permeable membranes take advantage of the physical characteristics of target analytes to allow the passage of species with certain properties while restricting or preventing the passage of interferent species.<sup>31</sup> Electrocatalysts are a class of chemical modifiers that can function by increasing electrode surface area, catalyzing reactions that are essential for electrode function, minimizing reactions with interferent species, and/or exerting some other chemical effect that enhances the selectivity and sensitivity of the electrode.<sup>31,85,86</sup> These modifications are often used in conjunction with one another.<sup>85</sup> In Table 2, selected sensor



examples from both categories are presented according to their analyte(s) of focus. Each form of electrode modification will be further addressed in its corresponding subsection.

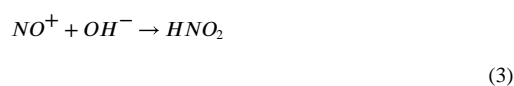
The selectivity of electrochemical sensors is often reported in terms of  $K$ , the selectivity coefficient. In essence, the selectivity coefficient for a target species with respect to a common interferent  $i$  is the ratio of the sensor's sensitivity to the interferent and its sensitivity to the target analyte. The selectivity coefficient is given by the following relationship:

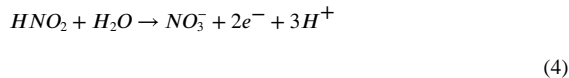
$$\log K_{CO(or\ NO)r(i)} = \log \left( \frac{\text{sensitivity to } i}{\text{sensitivity to } CO(or\ NO)} \right) \quad (1)$$

More negative selectivity coefficients demonstrate better selectivity, and “adequate” selectivity coefficients for effective sensors differ depending on the concentrations of typical interferents relative to the target analyte *in vivo*. In addition to selectivity, the sensitivity, limit of detection, and linear dynamic range of sensors are key metrics for the comparison of different sensing devices. Sensitivity, often quantified in units of amperes per mole per unit volume, refers to the slope of change in the signal (e.g., current) with respect to a single-unit change in the concentration of the target analyte. The limit of detection (LOD; nM–mM) refers to the minimum concentration of an analyte that can be detected (though not necessarily quantified) by a sensing platform.<sup>89</sup>

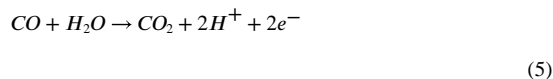
Linear dynamic range, reported as a range of concentrations of the target analyte in solution, refers to the range of concentrations within which signals from the sensor are directly proportional to changes in the concentration of the target analyte. A robust linear dynamic range is particularly important for the detection of gasotransmitters due to the broad range of *in vivo* concentrations of these species (see Table 1).<sup>90</sup> Quantitative measures of the selectivity, sensitivity, and linear dynamic range of various sensing platforms are reported and discussed below.

The selectivity and sensitivity of electrochemical sensors are closely tied to the nature of the chemical transformations that occur at the working electrode. For NO, electrochemical detection usually depends on electrooxidation of the species. This oxidation process involves (1) the transfer of an electron to the electron sink, and (2) the reaction of the resultant nitrosonium ion with hydroxide in the formation of nitrous acid, which is followed in some cases by (3) further oxidation of nitrous acid to nitrate through a two-electron exchange (Eqs. 2–4).



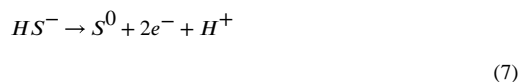
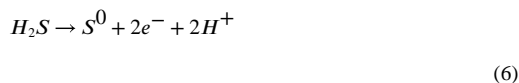


Electrochemical detection of CO, as with NO, depends on electrooxidation of the analyte at the surface of a working electrode (Eq. 5).



Unlike NO, examples of *in-vivo* electrochemical detection of CO as the sole target analyte are somewhat rare. The first example of direct, *in-vivo* electrochemical detection of CO took the form of a dual NO/CO sensor, and expansions upon this sensor have followed.<sup>19,23,91,92</sup> In these applications, the oxidation potentials of CO and NO at the surface of the working electrode are reportedly so similar in a biological environment that alterations to the applied potential prove insufficient for generating complete selectivity against either species in favor of the other; necessitating selectivity-inducing modifications of the working electrode.<sup>47,91–95</sup> Thus, in addition to differences in applied potential, selectivity in dual-electrode NO/CO sensors is also imparted by electrocatalytic membranes (Sn and Pt are examples) and/or selective alterations to electrode diameter (125  $\mu\text{m}$  for a CO-sensitive electrode compared to 12.5  $\mu\text{m}$  for the NO-sensitive electrode of a dual-electrode sensor, for example).<sup>23</sup>

Finally, direct amperometric detection of H<sub>2</sub>S is possible via a two-electron oxidation with elemental sulfur as a byproduct (Eqs. 6–7).



One important issue associated with this amperometric detection of H<sub>2</sub>S is the gradual production of an insulating sulfur layer upon reaction. This sulfur layer passivates the electrode surface, thereby reducing sensitivity and contributing to high variability in performance over time.<sup>31</sup> Among the most recent potential solutions to this challenge are the fabrication of an electrode that has been pre-poisoned with sulfur to stabilize performance, the periodic application of an ultra-high “cleansing” potential (+1.5 V) on a GCE to convert elemental sulfur to water-soluble sulfate, thereby mitigating surface passivation, and, in Clark-type electrodes, the incorporation of a gas-permeable membrane and alkaline internal solution with a redox mediator (e.g., ferrocyanide) to accept electrons from H<sub>2</sub>S and undergo regeneration at the working electrode, thereby generating a measurable current.<sup>96,97</sup> These

modifications have achieved varying degrees of success, and the most recent advancements here will be addressed in the following section.

## PERM-SELECTIVE MEMBRANE MODIFICATIONS

In physiological media, the accurate detection of gasotransmitters requires sensing architectures that can distinguish between the target analyte and any potential interfering species. Since biological fluid tends to contain many molecules with oxidation potentials near those of NO, CO, or H<sub>2</sub>S,<sup>83</sup> the most effective electrochemical sensors are those that limit the access of these potential interferents to the electrode—where their oxidation or reduction can hinder accurate detection of the target analyte. In the detection of NO, semi-porous membranes are capable of enhancing the signal obtained from the oxidation of NO by 100 to 1000-fold. Many operate by excluding interferents based on their size, charge, or lipophilicity.<sup>31</sup> While the application of a semi-permeable membrane is known to reduce sensor sensitivity, the exclusion of interferents is often sufficiently valuable to warrant the diminished sensitivity.<sup>98</sup> Electrocatalysts rely primarily on amplification of the signal to enhance selectivity towards the target analyte; unlike semi-permeable membranes, they do not always prevent interference from other biological species. Accordingly, many sensors are modified with both an electrocatalyst and a semipermeable membrane.<sup>31</sup> In the following sections, the most common membrane-based modifications to electrochemical sensors for NO, CO, and H<sub>2</sub>S are outlined.

An important consideration in the development of membrane-based sensors is the position of the counter and reference electrodes relative to the semipermeable membrane. In ‘Shibuki-style’ electrodes, the perm-selective membrane encloses an internal filling solution in which the working electrode, reference electrode, and counter electrode are all immersed.<sup>99</sup> By contrast, solid contact electrodes directly coat the electrodes in the membrane (either all three electrodes or only the working electrode may be coated).<sup>85,100</sup> These configurations have inherent benefits and drawbacks. Sensors where all the electrodes are enclosed in the membrane are better protected from the accumulation of interferent species at the electrode surfaces, but may suffer from decreased sensitivity. Shibuki style electrodes in particular are also less amenable to miniturization than solid contact electrodes.<sup>100</sup> In general, sensors fabricated on flexible wearable or implantable substrates tend to feature solid contact configurations.<sup>101–103</sup> The configuration of membranes and electrodes is indicated in the text below, as well as Table 2.

### NO

Many electrochemical NO sensors rely on the fluorinated polymer Nafion to induce NO selectivity.<sup>22,104,105</sup> Nafion permits NO passage, while its negatively charged sulfonate pendant groups repel many common anionic interferents.<sup>106</sup> However, due to its net negative charge, Nafion membranes do not induce selectivity against positively charged interferents<sup>107</sup> and might even reduce electrode sensitivity by limiting the diffusion of NO to its hydrophobic domains.<sup>98</sup> Alternative semi-porous membranes for the detection of NO in physiological conditions include hydrophobic materials, like polypropylene Celgard membranes, and electropolymerized films, particularly the organic polymers

poly(phenol) and poly-5-amino-1-naphthol (poly(5A1N)).<sup>31,108,109</sup> Electropolymerized films have the inherent advantage of simple, reproducible deposition onto substrates, which can be leveraged to create flexible, miniaturized sensors.<sup>93</sup> Recently, Yan and coworkers incorporated electropolymerized films such as poly(5A1N) and poly(eugenol) into flexible, amperometric sensors which were capable of selective NO detection *in vivo* in rabbits.<sup>102,103</sup>

Recent findings suggest that the combination of size exclusion and hydrophobic interactions that generate selectivity in membranes like TeflonAF or fluorinated xerogels may afford greater selectivity than membranes that operate primarily through charge repulsion, like Nafion. In line with these findings, hydrophobic membranes have emerged as a frontier of NO-sensing research in recent years. Fluorinated xerogel membranes are particularly common.<sup>87,91,110–112</sup> These networks of polymerized silanes provide three-dimensional scaffolding for layers of selectivity-enhancing enzymes,<sup>113</sup> and they have been shown to reduce sensor response times more than 3-fold compared to the Teflon-like polytetrafluoroethylene (ePTFE) membranes used in earlier electrodes.<sup>19,91</sup>

Schoenfish and colleagues investigated a variety of fluorinated xerogel membranes to design a set of fluorinated xerogel-derived microelectrodes for the amperometric detection of NO.<sup>110</sup> While early generations of organically modified xerogels proved useful in numerous sensing applications, a relatively low permeability for NO hindered their use in physiological settings, where the concentrations of NO can reach submicromolar levels.<sup>120</sup> The group utilized sol-gel chemistry to improve the permeability of xerogel materials to NO. They prepared a series of electrodes modified with sol-gel derived permselective membranes by depositing four silane solutions, each made from polymers with varying degrees of fluorination, onto different Pt disk electrodes. Cyclic voltammetric and amperometric experiments conducted with a standard NO solution in the presence of common interferents (e.g., nitrite) revealed that the most highly fluorinated xerogel membrane (see Figure 6) generated the most ideal combination of permeability and selectivity. The authors predicted that the high degree of fluorination led to an increase in the surface hydrophobicity of the membrane, thereby enhancing its permeability to nonpolar NO while rejecting hydrophilic interferents such as nitrite, ascorbic acid, uric acid, and dopamine. The same group built on this investigation of xerogels by combining the optimized 17FTMS xerogel with a poly(5A1N) to create a bilaminar sensor with superior selectivity and stability over 24 hours continuous operation.<sup>121</sup>

Building on these fundamental investigations, Ha and colleagues utilized a fluorinated xerogel coating on the working electrodes in their amperometric, oxidation-based dual-electrode NO/CO sensor, which enabled concentration-dependent anodic detection of CO at an Au-deposited Pt microdisk electrode (WE1) with a sensitivity of  $26 \pm 14 \text{ pA } \mu\text{M}^{-1}$ ,  $n = 6$ , and the detection of NO at a Pt black-deposited Pt disk electrode (WE2) with a sensitivity of  $180 \pm 46 \text{ pA } \mu\text{M}^{-1}$ ,  $n = 6$ . Constant applied potentials were +0.20 V and +0.75 V, respectively, vs Ag/AgCl, and limits of detection were  $\sim 180 \text{ nM CO}$  at WE1 and  $\sim 6.0 \text{ nM NO}$  at WE2 ( $S/N = 3$ ). A broad linear dynamic range ( $0.18\text{--}9.0 \text{ } \mu\text{M}$  for CO at WE1 and  $0.020\text{--}2.0 \text{ } \mu\text{M}$  for NO at WE2,  $R^2 > 0.999$ ,  $n = 5$ ) and a fast response time (90% of amperometric response reached at  $4.5 \pm 1.3 \text{ s}$  for WE1 and  $3.1 \pm 0.2 \text{ s}$  for WE2,  $n = 5$ ) made the sensor particularly effective.<sup>116</sup> These response times were elevated by factors of 3.7 $\times$  and 4.8 $\times$  from a previous

investigation<sup>19</sup> in which a PTFE (polytetrafluoroethylene) gas-permeable membrane was used, and the group attributes these improvements to their choice of a thin-layer fluorinated xerogel membrane, rather than the PTFE film; the combination of hydrophobicity and size exclusion as generators of selectivity were thought to facilitate better analyte access to the electrode than the PTFE membrane, which acts as a resistive diffusional barrier to NO and CO.<sup>91</sup>

Another effective example of hydrophobic NO-selective membranes is the TeflonAF-modified Celgard membrane, which Cha and colleagues built into an amperometric, microfluidic NO sensor (signal obtained from oxidation to nitrite at 0.65–0.75 V vs Ag/AgCl) with excellent selectivity (coefficients of –5.9 against both nitrite and ascorbic acid) and long-term monitoring capability (>16 h) for the release of NO from cultured macrophages.<sup>108</sup> Like many other electrochemical sensors for NO,<sup>31</sup> the membrane is applied over the working electrode in conjunction with an electrode-modifying catalyst. An electrochemically deposited Au–hexacyanoferrate layer is deposited directly on a porous polymer membrane, and it catalyzes the oxidation of NO as well as stabilizes the current output.<sup>108</sup> The TeflonAF membrane imparts NO-selectivity through its highly fluorinated backbone, similarly to the Nafion membranes referenced above. However, unlike Nafion, the TeflonAF material lacks sulfonate pendant groups that impart anionic selectivity in Nafion.<sup>35</sup> Instead, the TeflonAF membrane is thought to gain its selectivity via NO-partitioning into its hydrophobic polymeric matrix.<sup>108</sup> These examples represent some, though far from all, of the available and effective semi-permeable membranes for the detection of NO. For a comprehensive review of membrane modifications in NO sensing, readers are referred to the work of Brown & Schoenfish, and Xu et al..<sup>22,31</sup>

## CO

As with the detection of NO, recent electrochemical sensors for CO take advantage of the molecule's small size and hydrophobic properties through the application of perm-selective membranes. While less research has been performed on endogenous CO detection than has been performed for NO, a series of investigations of dual-analyte CO-NO detection systems have been reported, primarily by Lee and coworkers.<sup>19,23,91,92,116,122</sup> Semi-permeable membranes are applied in each case; Ha et al. obtained the best selectivity and temporal resolution with fluorinated xerogel membranes in their solid contact, amperometric, NO- and CO-oxidizing, dual-electrode sensor.<sup>91</sup> Other semi-permeable membranes employed in dual-detection schemes include the slightly thicker ePFT membrane, employed in a different amperometric, NO- and CO-oxidizing, dual-electrode sensor.<sup>19,91</sup> The ePFT-utilizing sensor operated via the oxidation of CO at a Pt microdisk deposited with Pt and Sn (constant applied potential of +0.70 V vs Ag/AgCl), and the oxidation of NO at a Pt electrode modified with Pt–Fe(III) oxide nanocomposites (+0.75 V vs Ag/AgCl).<sup>19</sup>

Another investigation employed a polytetrafluoroethylene (Tetra-tex) gas-permeable membrane in an amperometric, NO- and CO-oxidizing, dual-electrode sensor (see Figure 7).<sup>23</sup> In this application, two different Pt-disk working electrodes and an Ag/AgCl reference/counter electrode are encased in the Tetra-tex membrane. The membrane provided selectivity against potential interferents, operating on principles of size-based and

hydrophobicity-based exclusion. However, the Tetra-tex membrane was not instrumental in enabling differentiation between NO and CO. Rather, the simultaneous detection of the two gases was made possible by the construction of two different working electrodes: one larger (250  $\mu\text{m}$ ) Sn-modified Pt electrode (WE1), and one smaller (25  $\mu\text{m}$ ) unmodified Pt electrode (WE2). Though both CO and NO were oxidized at both electrodes, the ratio of NO to CO oxidation at the small, unmodified electrode was much larger ( $\sim 10$ ) than at the larger, Sn-modified electrode ( $\sim 2$ ). These differing ratios allowed the researchers to convert the anodic currents that were measured independently at WE1 and WE2 into concentration values for both NO and CO in the co-presence of the gases—the first time that such an endeavor was successfully carried out on the surface of living biological tissue. The constant applied potentials at each electrode, optimized for sensitivity, were +0.7 V for WE1 and +0.85 V for WE2 vs Ag/AgCl. This TetraTex-modified sensor was markedly more sensitive ( $9.6 \pm 1.5 \text{ nA } \mu\text{M}^{-1}$  for NO and  $19.8 \pm 3.11 \text{ nA } \mu\text{M}^{-1}$  for CO) than the sensors modified with ePFT ( $1.29 \pm 0.35 \text{ nA } \mu\text{M}^{-1}$  for NO and  $1.59 \pm 0.47 \text{ nA } \mu\text{M}^{-1}$  for CO) or fluorinated-xerogel ( $180 \pm 46 \text{ pA } \mu\text{M}^{-1}$  for NO and  $26 \pm 14 \text{ pA } \mu\text{M}^{-1}$  for CO). However, the TetraTex membrane accompanied the use of relatively large working electrodes.<sup>23</sup> The additional surface area was beneficial for sensitivity, because it allowed for high analyte-electrode interaction, but such large electrodes limit the feasibility of in-vivo applications and incorporation of into devices.<sup>116</sup>

As for the selectivity imparted by semi-permeable membranes, direct comparisons are somewhat limited by variation in methods of reporting selectivity metrics. For the detection of CO with fluorinated xerogel membrane-modified electrodes, selectivity coefficients for various interferents ranged from  $-3.03$  to  $-4.16$ , demonstrating adequate selectivity for biological detection against each interferent assessed.<sup>116</sup> For the ePFT and TetraTex membranes, selectivity coefficients were not reported. The authors state that amperometric readouts from before and after the addition of various biological interferents demonstrated “adequate selectivity” for the target analyte(s) up to interferent concentrations of 500  $\mu\text{M}$  (for the TetraTex-modified sensor) and a slightly less-selective 100  $\mu\text{M}$  (for the ePFT-modified sensor).<sup>19,23</sup>

## H<sub>2</sub>S

As with NO and CO, electrochemical detection of H<sub>2</sub>S depends on modifications to the electrode surface—many in the form of semi-permeable membranes. Unlike NO and CO, however, H<sub>2</sub>S is a weak acid ( $\text{pK}_{\text{a}1}$  of 6.97 - 7.06 at 25 deg. C).<sup>123</sup> In physiological conditions, H<sub>2</sub>S exists in equilibrium with its conjugate base, HS<sup>-</sup>. In electrochemical sensing schemes, it is often this conjugate base that is oxidized at the electrode surface (or that interacts with another electroactive species) to generate measurable changes in current. Ion-sensitive electrodes (ISEs) are among the most common electrochemical sensors for H<sub>2</sub>S, and many commercially available detectors of this type are in use. For in-vivo applications, ISEs are often applied with blood, plasma and other biological fluids,<sup>63,82,124,125</sup> though Olson and colleagues have reported that ISEs may suffer from inconsistencies in detection due to the rapid consumption of sulfide in blood.<sup>64</sup> Commercially available ion-sensitive electrodes are Ag/Ag<sub>2</sub>S electrodes, sensitive to S<sup>2-</sup> ( $2 \text{ Ag} + \text{S}^{2-} \rightleftharpoons \text{Ag}_2\text{S} + 2 \text{ e}^-$ ). Since H<sub>2</sub>S exists in equilibrium between H<sub>2</sub>S, HS<sup>-</sup>, and S<sup>2-</sup>



with  $pK_a 1 = 7.1$  and  $pK_a 2 = 17.1$ , a highly alkaline environment is required to favor the  $S^{2-}$  equilibrium.<sup>126</sup> As a result, the in-vivo application of these commercially available ISEs is challenging.

One of the earliest real-time sensing mechanisms for  $H_2S$ , an amperometric system based on a standard Clark-type ion electrode, utilized a semi-permeable silicone membrane. The membrane formed a barrier between dissolved  $H_2S$  outside of the electrode and an alkaline solution surrounding the working electrodes. Upon passing through the semi-permeable membrane,  $H_2S$  was oxidized in the alkaline solution to  $HS^-$ . The hydrosulfur anion was oxidized by  $K_3[Fe(CN)_6]$ , yielding sulfur and  $K_4[Fe(CN)_6]$ . The latter complex generated a concentration-dependent current as it was re-oxidized at the exposed end of the Pt working electrode, meaning that it was  $K_4[Fe(CN)_6]$  (not hydrogen sulfide directly) that generates the measured signal. The LOD for this sensor was about  $2 \mu M$ , and its silicone membrane was reported as successful in selecting against  $HS^-$  and  $S_2^{2-}$ , two common interferents. The few uncharged molecules capable of passing through the silicone membrane were  $SO_2$  (which gave a 300-fold smaller signal than the target analyte pH 2, and no response for pH > 6.5) and ethanethiol (which gave a 20-fold smaller signal at pH 2, with no data reported regarding its interference at other pH values). Other common interferents in a physiological setting, including ammonia ( $\approx 2 M$ ), methylamine ( $\approx 6 M$ ), and acetic acid ( $\approx 1 M$ ), demonstrated no effect on the zero signal or on the measuring signal of the electrode when mixed into the external,  $H_2S$ -containing solution.<sup>127</sup>

Two additional uses of silicone membranes in the electrochemical detection of  $H_2S$  show low limits of detection and adequate selectivity. Doeller and colleagues employed a  $25\text{-}\mu m$  thick silicone membrane in successful  $H_2S$  detection, followed by a report of a silicone polycarbonate membrane of the same thickness.<sup>97,128</sup> The second example used a polarographic sensor set to a polarizing voltage of 100 mV, with a Pt anode, Pt-wire cathode,  $K_3[Fe(CN)_6]$  electrolyte, and an  $H_2S$ -permeable polymer membrane.  $H_2S$  was dissociated to  $HS^-$  following diffusion through the membrane and was then oxidized by  $K_3[Fe(CN)_6]$ , generating  $K_4[Fe(CN)_6]$  (See Figure 8). The latter was oxidized at the Pt anode, generating a current proportional to the concentration of  $H_2S$ . The lower limit of detection for the sensor was dictated by the relatively small background current that was generated during the electrolytic conduction of current from cathode to anode (as ferricyanide was reduced at the cathode and oxidized at the anode), which gave an LOD around 10 nM. The sensor demonstrated an accuracy of  $\pm 3\%$  at  $20 \mu M$  sulfide and a response time (to 90% change in sulfide level) of 20-30s, ideal for kinetic studies of  $H_2S$  metabolism in cells, tissue, and whole organisms.<sup>97</sup> The membrane demonstrated good selectivity against many common interferents:  $S_2O_3^{2-}$ ,  $SO_3^-$ ,  $SO_4^-$ , cysteine, glutathione, cystine, homocysteine, ascorbate,  $O_2$ ,  $NO$ ,  $NO_2^-$ ,  $NO_3^-$ , and  $H_2O_2$ , which facilitated the use of this sensor packaged alongside oxygen and nitric oxide sensors in a respirometer chamber. Silicone membranes (e.g., silicone-polycarbonate copolymer and dimethyl silicone) are particularly effective for use in  $H_2S$  sensing due to their allowance of rapid  $H_2S$  diffusion.<sup>97</sup>

To conclude this discussion of semi-permeable membranes, it must be noted that considerable advancements have been made in the construction of membranes that enable selectivity based on *more* than just the size of the target analyte. Numerous recently

developed membranes can be tuned to provide optimal selectivity for analyte(s) of interest, and this selectivity arises from a host of molecular properties. Among these properties are hydrophobicity, pore size, electronic environment, thickness, stability, biosafety, and even multilayer interactions (i.e., the capacity of a given material to interact favorably with a second perm-selective element). While it is true that early versions of semi-permeable membranes sometimes granted selectivity at the expense of electrode sensitivity, recent examples of detection-enhancing membranes make it clear that perm-selective membranes will play an important role in the development of next-generation electrochemical sensors. Particularly for the detection of gasotransmitters, the biostability of sensors and any deposited electrocatalysts is an emerging challenge. Semipermeable membranes have the potential to serve the three-part role of enhancing selectivity, enhancing sensitivity by reducing biofouling from unintended electrochemical interactions, and (critically) improving the biocompatibility of electrochemical devices by serving as a protective and biosafe external layer for in-vivo sensors.

## ELECTROCATALYTIC SENSOR MODIFICATIONS

While semi-permeable membranes serve as an important source of selectivity in electrochemical sensing, the membranes are frequently used alongside additional chemical modifiers to attain optimal electrode selectivity and sensitivity. These chemical modifiers often act as electrocatalysts, improving the sensitivity of a sensor by facilitating charge transfer in an electrochemical reaction and thereby amplifying the signal that is elicited by the target analyte.<sup>31</sup> In some cases, electrocatalysts impart selectivity by lowering the oxidation potential of the target analyte. If the effect is specific to the target analyte, then the decreased oxidation potential may enable detection of the target analyte without risking the oxidation of (and subsequent interference by) analytes with similar oxidation potentials. Chemical modifiers might be coated beside or suspended within a semi-permeable membrane, and their character varies widely; examples from the literature include transition metal nanoparticles,<sup>129</sup> carbon nanostructures,<sup>130</sup> metallophthalocyanines,<sup>88</sup> and other electrode-roughening or reaction-catalyzing substances.<sup>31</sup>

### NO

For the detection of NO, two common electrode modifications are electropolymerized films (EPFs), including both monomers and polymers, and metallophthalocyanine macrocycles.<sup>131</sup> EPFs are applied via the oxidation of monomers to radical cations. When an electrode is placed in a monomer solution and a sufficiently positive potential is applied, radical coupling and oxidation reactions lead to the formation of an oligomer. As this oligomer precipitates from solution onto the surface of the electrode, the EPF is formed. While non-conducting and semi-conducting polymers will passivate the electrode, the growth of conducting polymers can be modulated by the application of potentials—making this process both observable and controllable through amperometric methods such as CV and CPA.<sup>93</sup> As a result, the deposition of EPFs is regarded as a reproducible, controllable mode of electrode modification for gas sensing applications.

Metalloporphyrins and metallophthalocyanines (Figure 9), many of which are modeled after endogenous heme-containing enzymes, have both demonstrated excellent properties for the enhancement of NO detection. In MPc complexes, extended pi systems facilitate fast redox processes, which in turn enable a rapid current response to NO oxidation by guiding electron transfer from NO to the electrode charge sink.<sup>88,132</sup> The effectiveness of this process in enhancing sensor selectivity results from a reduction in the overpotential that is required for NO oxidation. Without catalysis, sufficient NO oxidation requires overpotentials that also induce oxidation of common biological interferents, which can significantly impair sensing performance.<sup>131</sup> Catalysts like MPcs and metalloporphyrins can decrease the potential that is required to oxidize NO, thereby avoiding oxidation of interferent species.<sup>133</sup>

In 1992, Malinski and Taha performed a seminal study of a nickel metalloporphyrin (Figure 9a) that was electropolymerized onto the surface of a carbon fiber electrode and coated with Nafion for the detection of NO.<sup>134</sup> Their electrode, which could function in either an amperometric or voltametric mode, had a width of just 0.5  $\mu\text{m}$  and detected amounts of NO as low as  $10^{-20}$  mol at the single-cell level. The Nafion membrane and electropolymerized metalloporphyrin generated sufficient selectivity against nitrite that only a small increase in current was observed during the detection of NO when combined in solution with nitrite, and the peak potential was unaffected by the presence of nitrite. Nickel metalloporphyrins have demonstrated promising detection capabilities, but porphyrins with other metal centers are also effective. Both iron and manganese metal centers have been successfully employed in the porphyrin-mediated detection of NO.<sup>135–137</sup>

Like metalloporphyrins, metallophthalocyanine complexes (MPcs) can lower the oxidation potential of NO and increase both the oxidation and reduction currents when applied in a sensing context. They have also been reported to demonstrate greater stability than metalloporphyrins in instances of catalysis-induced degradation.<sup>131</sup> MPc complexes mimic naturally occurring metalloporphyrins in their structure; they are comprised of a highly conjugated cyclic organic system surrounding a chelated metal ion (Figure 9b). Changing the identity of this metal ion can change the catalytic properties of the molecule, affording unique control over the mechanism and stability of the catalytic process. MPcs with Mn, Fe, or Co centers, for example, have been shown by x-ray photoelectron spectroscopy (XPS) to catalyze redox processes of NO at the metal center, whereas EPR spectroscopy has shown NO to bind to NiPc complexes much more weakly.<sup>131,138–140</sup> MPc-based catalysts have proven capable of amplifying the NO signal approximately 3-fold compared to unmodified sensors and demonstrate complete selectivity in catalyzing NO reactions over CO and ascorbic acid, two other common interferents.<sup>141</sup> When the catalytic activities of Fe, Co, Ni, and Zn MPc-modifiers are compared, the Ni complex appears most effective in catalyzing NO oxidation and shuttling the resulting charge, while the Cu complex exhibits the lowest electrocatalytic activity.<sup>131,132</sup>

Building on these fundamental studies, more recent reports have incorporated phthalocyanine and porphyrin monomers in sensor architectures for single-cell NO detection. Xu et al. combined FePc monomers and nanographene on an indium tin oxide (ITO) substrate. This FePc-N-G sensor was able to detect NO release from cultured human endothelial cells stimulated by the addition of L-arginine to the cell culture medium.<sup>142</sup>

Hao et al. used a similar strategy, layering hemin, a biologically derived iron-porphyrin, onto graphdyene, a conductive carbon-based material. The HEM-GDY sensor detected NO release from human breast cancer cells upon addition of acetylcholine.<sup>143</sup> Inspired by the catalytic activity of nickel-based porphyrins and phthalocyanines, Zhou et al. combined a Ni-salen complex with acetylene black (AB) to create a Ni-N<sub>2</sub>O<sub>2</sub>/AB composite material. This material was incorporated into a paper-based sensor that detected NO with an LOD of 1.8 nM. The authors attribute the sensitivity and selectivity of their device to the binding interactions between the nickel-metal center and NO.<sup>144</sup>

Current efforts in MPc-based sensor development are faced with the challenge of enhancing the sensitivity, selectivity, and conductivity of MPc complexes. Our group has suggested that molecular engineering can enable steady advancements in these areas. The enhancement of electrode sensitivity, for example, might be approached by fabricating MPc thin films with long-range order, high crystallinity, and control over alignment to increase the number of active sites that are available for analyte interaction.<sup>145</sup> Principles such as these have aided our group in developing MPc-based metal-organic framework (MOF) and covalent organic framework (COF) sensors for gasotransmitters in air (Figure 10). Importantly, even though NO, CO, and H<sub>2</sub>S exert their physiological effects within liquid-phase biological media (i.e., dissolved within blood or CSF and diffusing through cell walls to reach molecular targets), gasotransmitters are constantly exhaled in the gas phase. The determination of gasotransmitter concentrations in exhaled air can help physicians monitor the progression of diseases, the efficacy of medications, the efficiency and/or functionality of an individual's cardiovascular system, and an array of other valuable diagnostic functions.<sup>17,146–150</sup> For these reasons, electrochemical methods that aid in the gas-phase detection of gasotransmitters remain highly relevant in physiological contexts. Both Cu- Ni- linked NiPc-2D conductive MOFs have proven particularly valuable in the gas-phase detection of gasotransmitters. These MPc-MOFs exhibited exceptional detection capabilities for NO, each within part-per-billion (ppb) detection ranges (1.0–1.1 ppb for NO) at low driving voltages (0.01–1.0 V) within 1.5 min of exposure. The detection took place in nitrogen and a humidified atmosphere at solid-gas interfaces using chemiresistive device architectures.<sup>145</sup> For the detection of NO, the achieved LODs with these framework-integrated MPcs mark the best MOF- or COF-based chemiresistive sensors to date.<sup>151,152</sup> Although this class of materials have not yet been employed for the liquid phase detection of NO, a NiPc-based MOF has been reportedly employed as an electrochemical sensor for nitrite.<sup>153</sup>

As with phthalocyanines, porphyrins can be integrated into framework materials for enhanced sensing performance. Recently, Ling and colleagues developed an electrochemical sensor for the detection of NO by synthesizing NporMOF(Fe), a porphyrin based MOF. The nano-MOF was synthesized from zirconium oxychloride octahydrate and an iron metalloporphyrin (TCPP(Fe)), then dropcast onto a glassy carbon electrode and coated with Nafion. In CV and DPV studies, the NporMOF(Fe) modified electrode detected NO in PBS, in the presence of NO<sub>2</sub><sup>-</sup> (Figure 11a), with a linear detection range of 5 μM to 200 μM and a detection limit of 1.3 μM.<sup>115</sup> An important caveat is the method of generating NO solution: nitrite is added to the acidic phosphate buffer solution (pH 2.5), which is converted to NO in acidic conditions. The linear detection range and LOD for the sensor

are based on the assumption of total conversion of  $\text{NO}_2^-$  to NO, and the concentration is not independently verified. The physiological relevance of NO detection in this pH range is limited, nevertheless, this report represents a fundamental advancement in MOF-based electrochemical sensors.

The authors attribute the cathodic peak at  $-0.55$  V to the reduction of  $[\text{Fe}(\text{III})(\text{NO})]^+$ , which is formed when NO binds to TCPP(Fe) group via axial coordination. The origin of the unique catalytic properties of the nano-MOF for the reduction of NO are not thoroughly explored, though the authors suggest that active sites generated by the pores of the MOF and the nanoscale MOF particles both enhance the activity and selectivity of the sensor. Selectivity was probed by injecting  $200 \mu\text{M}$  of common biological interferents and plotting the relative current intensity elicited by each. The results (Figure 11b) suggest that the nano-MOF electrode is selective for NO against most common interferents; however, no quantitative metrics (e.g., selectivity coefficients) have been calculated. The nano-MOF material demonstrated adequate stability for short-term use, retaining 94% of its current response after 10 days.<sup>115</sup>

Despite limitations, porphyrin and MPC-MOFs are a promising form of electrode modification in the development of portable, low-power, remotely operated and/or wirelessly transducing sensors. In addition to their effective sensing capabilities, these materials exhibit tunable structure-function relationships—a property that is of immense value in an electrode-modifying material, as a tunable structure endows particularly good control over the properties of a sensing mechanism and may aid in the application of effective materials to a broad array of environments or analytes.<sup>151,152</sup> While MPC-framework based electrode modifications in particular remain limited by a cumbersome synthesis processes and disordered spatial alignment in solid-state devices, ongoing advancements—including integration with graphitic materials and metal- or covalent organic frameworks, as well as the development of tunable bottom-up assembly methods—show promise for enhancing the detection of NO and other endogenous gases.<sup>145,151,152</sup>

## CO

Like NO, one barrier to the sensitive detection of CO in physiological systems is the presence of interferents. While semi-permeable membranes successfully improve the selectivity of CO sensors against these interfering species,<sup>154</sup> they sometimes come at the expense of decreased response time or sensitivity due to the required diffusion of CO through the physical membrane barrier.<sup>94</sup> Lee and colleagues have investigated catalytic Au nanoparticles as a potential solution to the issue of obstructive semi-permeable membranes both for CO<sup>94</sup> and for NO.<sup>155</sup> Since many interferents in the detection of CO are polar or ionic, electrode-modifying materials with hydrophobic properties tend to enhance selectivity. Interestingly, the hydrophobic properties of electrodeposited metallic nanostructures can be modified by altering the deposition potential; lower potentials yield greater nanoscale-surface roughness and thus more hydrophobic properties.<sup>156</sup> Kwon and colleagues studied this tunable hydrophobicity of layered gold nanoparticles in the context of CO detection. The researchers deposited a series of gold nanostructures onto glassy carbon electrodes at 5 different deposition potentials (0.05-0.45 V vs. Ag/AgCl using

LSV), then investigated the sensitivity and selectivity of each electrode in the amperometric detection of CO. Detection experiments were conducted amperometrically at  $-0.05$  V vs. Ag/AgCl in a gas-tight cell filled with PBS (pH 7.4) and injected with incremental aliquots of saturated CO (0.9 mM). The most selective nanoparticle layer was obtained from electrodeposition at 0.05 V—the lowest potential of those that the group applied. The sensitivity of this electrode for CO increased as the hydrophobicity of the Au membrane increased, and the selectivity coefficients for CO against ascorbic acid, nitrite, and GABA ( $-0.71$ ,  $-3.77$ , and  $-3.67$ , respectively) were best for the most hydrophobic Au-layer.<sup>94</sup>

Au-nanoparticles have also been reported to catalyze the oxidation of ascorbic acid and NO, two potential interferents in the detection of CO.<sup>157</sup> Kwon et al. found that increasing the roughness of the Au-nanoparticle layer did indeed enhance the apparent catalytic effects of the layer for AA and NO (a result of high electroactivity of Au for NO and AA)—until the morphology of the Au layer becomes sufficiently rough. At this point, the high hydrophobicity of the Au deposit attained at 0.05 V generates selectivity for CO over anionic AA. The hydrophobic CO molecules reap the benefits of the increased catalytic surface area, transferring charge at the peaks and valleys of the electrocatalyst, while AA cannot penetrate deeply enough to obtain a catalytic benefit (Figure 12). The authors conclude that the tunable hydrophobicity of Au deposits may make these Au nanoparticles worthy of further investigation as selectivity- and sensitivity-enhancing electrode modifying materials for the detection of CO.<sup>94</sup>

Many efforts for real-time, in-vivo electrochemical detection of endogenous CO occur through dual CO-NO electrodes. In these cases, chemical modifications to the CO-sensing electrode surface include the addition of gold(III) chloride hydrate for enhanced conductivity,<sup>91</sup> the sequential deposit of Pt and Sn,<sup>19</sup> and Sn deposition alone.<sup>23</sup> The gold(III) chloride hydrate-modified electrode constructed by Ha and colleagues was an amperometric, oxidation-based dual-electrode NO/CO sensor which enabled concentration-dependent anodic detection of CO at an Au-deposited Pt microdisk electrode (WE1) with a sensitivity of  $26 \pm 14$  pA  $\mu\text{M}^{-1}$ ,  $n = 6$ , and NO at a Pt black-deposited Pt disk electrode (WE2) with a sensitivity of  $180 \pm 46$  pA  $\mu\text{M}^{-1}$ ,  $n = 6$ . The CO electrode is only about one-seventh as sensitive to CO as its electrode pair to NO (WE2). However, the relatively high concentration of endogenous CO makes this weaker sensitivity sufficient for physiological detection.<sup>19,91</sup> The gold(III) chloride-modified electrode is succeeded in sensitivity by the Pt-Sn modified system, for which CO sensitivity is reported as  $1.29 \pm 0.35$  nA  $\mu\text{M}^{-1}$ .<sup>19</sup> Even more sensitive was the Sn-deposited electrode, which generated sensitivities ranging between  $9.6 \pm 1.5$  and  $5.0 \pm 1.1$  nA  $\mu\text{M}^{-1}$ , depending on the polarization potential (V vs Ag/AgCl) of the working electrode.<sup>23</sup>

The dual-detection system developed by Ha and colleagues operates through an interesting scheme: the detection of NO at one electrode generates a CO-blocking oxide Pt film, enabling the selective detection of CO at (only) the other electrode. The sensor is an amperometric, oxidation-based NO-CO sensor, where one glassy carbon working electrode is plated with gold complex (for anodic detection of CO; WE1) and the other with Pt (for anodic detection of NO; WE2). The Pt-deposited electrode initially demonstrated problematic sensitivity to both CO and NO. However, the oxidation of CO was successfully



suppressed through maintained oxidation of NO on the Pt-deposited electrode in basic conditions. The process generated an oxide film that inhibited CO adsorption, acting as a sort of additional, selectivity-enhancing electrode modification.<sup>116,158</sup> The result is a sensing system wherein the two different electrodes and different polarization potentials (Au, + 0.2 V, Pt black, + 0.75 V, both vs Ag/AgCl) facilitate the selective oxidation of CO (Au-modified electrode) and NO (Pt black-modified electrode).<sup>116</sup> In addition to electrocatalytic modifications, a thin-layer coating of fluorinated xerogel was applied to both electrodes in order to generate complete selectivity for CO. In comparing the electrode performance with and without xerogel coating, the coated electrodes showed less sensitivity (~20% of uncoated CO response and ~40% of uncoated NO response) than the uncoated electrodes, but the uncoated Au-modified (CO-detecting) electrode showed a response to both CO and NO. With the coating, an oxidation current for NO was not observed. This suggests that the diffusional barrier provided by the xerogel played a critical role in generating CO selectivity, in addition to the deposition of Au. Another sensitivity-generating component of the sensor was the etching of recessed micropores. The electrocatalysts were electrodeposited into these micropores, increasing functional surface area without necessitating an increased electrode diameter. The result was a miniaturized sensor ( $240 \pm 26 \mu\text{m}$  tip diameter), insertable into rat brain tissue for real-time sensing.<sup>116</sup>

Another example of electrocatalyst-generated selectivity for NO/CO detection was reported by Park and colleagues. In this amperometric, oxidation-based sensor, selectivity for NO over CO could not be obtained through modification of applied potentials alone due to the similar oxidation potentials of NO and CO. Thus, selectivity was generated by electrodeposition of two different electrocatalysts: Pt-Sn and Pt-Fe(III) oxide nanocomposites. The current generated at the Pt-Sn modified electrode depended on the concentrations of both NO and CO, while the current generated at the Pt-Fe(III) electrode depended only on the concentration of NO. Following calibration, the concentration of CO was determined by subtraction of the NO concentration recorded at the second electrode. In this case, the nanocomposite proved notably beneficial for enhancing sensitivity to NO over CO at one of the working electrodes. The sensor was amperometric, operating via the oxidation of CO at a Pt microdisk deposited with Pt and Sn (WE1) (constant applied potential of +0.70 V) and the oxidation of NO at a Pt electrode modified with Pt-Fe(III) oxide nanocomposites (WE2) (+0.75 V vs Ag/AgCl).<sup>92</sup> The high catalytic activity of the Pt-Fe(III) nanoparticle composites for electrochemical oxidation of NO was initially reported by Wang & Lin,<sup>159</sup> based on explorations of Pt-catalyzed oxidation performed by Pei & Li.<sup>160</sup> The Pt-Fe(III)/GCE fabricated by Wang & Lin appeared to reduce the overpotential for NO oxidation and enhance the current response more effectively than GCE modified with pure Pt or pure Fe(III), suggesting a cooperative effect of Pt and Fe(III) in the electrocatalysis.<sup>159</sup>

## H<sub>2</sub>S

One common type of electrocatalyst for H<sub>2</sub>S detection is that of enzyme functionalized electrodes. Like the ion-selective electrodes described above, enzyme-based sensors for H<sub>2</sub>S also tend to show notable pH sensitivity. However, since many enzymes operate optimally around a physiological pH, this dependence poses less of an impediment to in-vivo detection

than the highly alkaline pH values that are required for the ion-sensitive Ag/Ag<sub>2</sub>S method.<sup>63</sup> Generally, these sensors operate via H<sub>2</sub>S-selective enzymes that are applied to the electrode surface as recognition elements. The first application of this technique for H<sub>2</sub>S detection employed cytochrome oxidase-based inhibited enzyme electrodes, which demonstrated LODs as low as 1 ppm in the gas phase.<sup>161</sup> The sensing electrode was a catalytic oxygen electrode based on the electrochemical reduction of cytochrome C, in the presence of cytochrome oxidase, on a gold electrode modified with bis(4-pyridyl) disulphide. Since the current varied with the concentration of *active* enzyme, the electrode was sensitive to any inhibitors of cytochrome oxidase (i.e., substances that block the enzymatic reaction). H<sub>2</sub>S is one of these substances; when it binds to the oxidase, it inhibits enzymatic action by coordinating to the metal ions in the molecule. Enzymatic inhibition-based sensors are particularly sensitive because a single inhibitor molecule is sufficient to impair the catalyst—thereby preventing the reaction of many molecules of substrate. The result is an amplification effect in the detection of inhibitors like H<sub>2</sub>S.<sup>161</sup>

Since this first application of enzyme inhibition-based detection of H<sub>2</sub>S, focus has shifted to horseradish peroxidase (HRP)-modified electrodes. One such sensing scheme, reported by Yang et al., is an amperometric, three-electrode system with an HRP modified self-assembled monolayer (SAM)–Au electrode as the working electrode, SCE as the reference electrode, and Pt foil as a counter electrode.<sup>162</sup> Benzoquinone acts as an electron mediator. Through a multi-step catalytic process, the substrate (0.1 M H<sub>2</sub>O<sub>2</sub>) interacts with HRP(Fe<sup>3+</sup>) to generate an intermediate and water. In the absence of sulfide, the reaction progresses; eventually, hydroquinone (previously reduced from benzoquinone) is oxidized back to benzoquinone, donating two electrons to the electrode and generating a measurable reduction current. When present, sulfide coordinates with the intermediate that is generated in the first step of the reaction.<sup>163</sup> This coordination impairs reaction progress, reducing the sensor current in a concentration-dependent manner. Yang et al. used an applied potential of –150 mV for amperometric measurements, and the group reported a detection limit of 0.3 μM for H<sub>2</sub>S.<sup>162</sup>

A related approach, also based on the inhibition of enzymatic activity by H<sub>2</sub>S and the concentration-dependent reduction of current strength, again yielded a 0.3 μM detection limit—though this approach involved a screen-printed working electrode, slightly cheaper and more accessible than the previous method, modified with *Coprinus cinereus* peroxidase (benzoquinone served again as an electron mediator).<sup>164</sup> The linear range, 1.09–16.3 μM, was also slightly greater than that of Yang and colleagues. Building upon the SAM example, Liu and colleagues reported a multilayer film-modified biosensor, constructed via layer-by-layer (LBL) biospecific binding of concanavalin A and horseradish peroxidase on the surface of a gold electrode.<sup>165</sup> Again, the amperometric signal resulted from inhibition of enzymatic activity in the presence of sulfide. This response is illustrated in Figure 13; a CV scan was obtained in PBS with only hydroquinone (green). The addition of H<sub>2</sub>O<sub>2</sub> increased the current response as expected (red); H<sub>2</sub>O<sub>2</sub> is reduced by the HRP enzyme. Upon the introduction of sulfide, sulfide attacks the heme group of the HRP and blocks its active site. The reduction of H<sub>2</sub>O<sub>2</sub> is accordingly inhibited, and the percent inhibition of the current by sulfide is proportional to the concentration of sulfide in solution (black). The limit of detection—0.05 μM—was much improved from previous reports. (All amperometric

measurements were carried out at an applied potential of  $-0.150$  V vs. Ag/AgCl in the presence of  $0.2$  M hydroquinone).<sup>165</sup>

Polarographic (amperometric) detection methods for the detection of  $\text{H}_2\text{S}$  are among the most broadly applied methods for direct, real-time sensing in-vivo. Electrocatalytic electrode modifications play a significant role in determining the selectivity and sensitivity of amperometric sensors, and nanocomposite-based electrode modifications are one particularly common form. These materials provide the benefit of high surface area, low cost (relative to many other electrode modifications), and a variety of tunable morphologies.<sup>166</sup> In particular, a class of Au nanomaterials show promising catalytic effects for the electrochemical detection of  $\text{H}_2\text{S}$ .<sup>167</sup> In one application, Au@Ag core-shell nanoparticles demonstrated excellent conductivity and sensitivity enhancement; Zhao and colleagues reported oxidation of the nanoparticles to  $\text{Ag}_2\text{S}$  in the presence of  $\text{H}_2\text{S}$ , initiating a decrease in the differential pulse voltammetry (DPV) peak at  $0.26$  V with a LOD of  $0.04$  nM.<sup>167</sup>

In another example of electrocatalysts for the detection of  $\text{H}_2\text{S}$ , low-potential sensing of  $\text{H}_2\text{S}$  with a detection limit of  $0.3$   $\mu\text{M}$  and linear dynamic range of  $1.25$ – $112.5$   $\mu\text{M}$  was achieved through the application of carbon nanotubes to a glassy carbon electrode. The oxidation of sulfide began around  $-0.3$  V (vs. Ag/AgCl, pH 7.4 (observed via cyclic voltammetry)—a  $400$  mV decrease in the required overpotential compared to an ordinary carbon electrode.<sup>21</sup> In another application, various concentrations of functionalized single wall carbon nanotubes (f-SWCNT) were incorporated with polyaniline via electrochemical polymerization of Aniline monomer with sulfuric acid. This sensor is one example of electrode modification with conductive polymers, which tend to be associated with easy electrode preparation, low cost, environmental stability, and controllable electrical conductivity.<sup>168</sup> While conductive polymers typically suffer from low sensitivity, the present example incorporated the polyaniline conductive polymer with carbon nanotubes—thereby enhancing the surface-to-volume ratio of these sensors and directly improving the sensing capacity.  $\text{H}_2\text{S}$  partly dissociated into  $\text{H}^+$  and  $\text{HS}^-$ , resulting in the partial protonation of the polymer and the removal of electrons from its aromatic rings. The electron transfer was then observed via changes in the work function of the polymer (and, accordingly, the resistance of the sensor). The sensitivity increased with f-SWCNT content, and since the gas sensing depends on  $\text{H}_2\text{S}$  adsorption (which decreases as temperature increases), the gas sensing response decreased with increasing temperature.<sup>169</sup>

A physiologically applicable example of nanomaterial-modified  $\text{H}_2\text{S}$  sensors involves PdCu alloy “nanoflowers”. The high surface area-to-volume ratio (characteristic of most nanomaterials) facilitated chemical reaction between copper oxide ( $\text{CuO}$  and  $\text{Cu}_2\text{O}$ ) and hydrogen sulfide (including  $\text{H}_2\text{S}$  and  $\text{HS}^-$ ) in a neutral solution (pH 7.4). In the presence of  $\text{Na}_2\text{S}$ , copper and its oxide were converted into  $\text{Cu}_2\text{S}$  and  $\text{CuS}$ , resulting in an increase in the oxidation peak current of  $\text{Cu}_2\text{S}$ - $\text{CuS}$  with increasing concentrations of  $\text{Na}_2\text{S}$  (sulfide). The  $\text{Cu}_2\text{S}$ - $\text{CuS}$  species were oxidized to generate current responses via CV, with an initial peak at  $0.05$  V resulting from the chemical reaction between PdCu alloy nanoflowers and hydrogen sulfate, forming  $\text{Cu}_2\text{S}$  and generating the oxidation current. The detection limit for the sensor was reported as  $0.2$   $\mu\text{M}$ , with a linear range of  $0.4$   $\mu\text{M}$  to  $400$   $\mu\text{M}$ .<sup>170</sup>

Carbon nanotubes have been frequently employed as scaffolding for electrocatalytic materials, in addition to serving as electrocatalysts themselves. In 2021, Jeromiyas and colleagues functionalized carbon nanotubes with a layer of Gd doped molybdenum selenide for the sensitive and selective detection of hydrogen sulfide.<sup>119</sup> Molybdenum diselenide ( $\text{MoSe}_2$ ) is a two-dimensional transition metal dichalcogenide (2D TMD), which can enhance electrochemical sensing by virtue of appreciable conductivity, large surface area, and ultrathin-layered structures.<sup>171</sup> The authors chose to incorporate this material with carbon nanofibers (CNFs) to avoid the issue of easy agglomeration between sheets of  $\text{MoSe}_2$ , which impairs charge transfer. This CNF scaffolding also facilitated conductivity and enabled easy application to electrode surfaces.<sup>172</sup> The resulting sensor detected  $\text{H}_2\text{S}$  within a linear concentration range of 12.5 nM–1.2 mM with an LOD of 1 nM, making it one of the most sensitive electrochemical devices reported recently for the detection of  $\text{H}_2\text{S}$ .<sup>173</sup> In another recent example, gold-nanowires were incorporated with carbon nanotubes to form an electrocatalyst on a flexible, poly(dimethylsiloxane) (PDMS) substrate. This stretchable sensor was able to detect  $\text{H}_2\text{S}$  with a broad linear range from 5 nM to 24.9  $\mu\text{M}$ , and successfully monitored the release of  $\text{H}_2\text{S}$  from HeLa cells cultured on the flexible sensor. Sensor performance was maintained when the film was stretched, giving the device potential applicability for a variety of physiological studies.<sup>101</sup>

In a similar vein, one *photoelectrochemical* sensor with a comparably broad linear range of detection was reported by Yu and colleagues. In this sensor, the signal originated from a charge transfer process that occurs between the analyte ( $\text{H}_2\text{S}$ ), the photoelectric material, and a glassy carbon electrode.  $\text{H}_2\text{S}$  from endogenous and exogenous sources reacts with  $\text{Cd}^{2+}$ , which the group deposited onto the electrode via treatment with thioglycolic acid during electrode construction. The reaction resulted in covalent grafting of the resulting CdS onto  $\text{TiO}_2$  nanotubes to form CdS nanoparticles. Photocurrent was then generated when excited electrons are transferred from CdS nanoparticles to  $\text{TiO}_2$  under irradiation at 420 nm. Without  $\text{Cd}^+$  modification, the  $\text{TiO}_2$  nanotubes absorbed only UV light (due to a relatively large band gap of 3.0–3.2 eV). The generation of CdS upon exposure to sulfide decreased this band gap (2.4 eV), allowing photoelectrochemical response within the visible range. The method was employed for the detection of  $\text{H}_2\text{S}$  from cancer cells, with a limit of detection at 0.3  $\mu\text{M}$  and linear range of 10 nM– $10^6$  nM.<sup>174</sup>

While many of the previous examples detect  $\text{H}_2\text{S}$  that is released from isolated cells and tissues or injected into simulated biological fluid, an online electrochemical system (OECS) developed by Wang and colleagues demonstrates one of the most recent examples of real-time hydrogen sulfide detection in a live, behaving animal. The sensor operated through catalysis of the oxidation of free sulfur ( $\text{H}_2\text{S}$  and  $\text{HS}^-$ ) by hexammineruthenium(III) ( $\text{Ru}(\text{NH}_3)_6^{3+}$ ) to elemental sulfur. The authors proposed the use of ammineruthenium(III) because of its ability to oxidize both  $\text{H}_2\text{S}$  and  $\text{HS}^-$  in the neutral solution; the standard potential of  $\text{Ru}(\text{NH}_3)_6^{3+}$  is higher than those of sulfide (Figure 14a). Since it has not been determined whether  $\text{H}_2\text{S}$  or  $\text{HS}^-$  (or both) perform signaling roles in the brain, the authors sought an electrocatalyst that would be capable of facilitating the detection of “free sulfide” in both forms, at a potential that is lower than those for the oxidation of potential redox-active interferents.<sup>175</sup> The sensor yielded a detection limit of 0.17  $\mu\text{M}$  and operates within a linear range of 0.5 to 10  $\mu\text{M}$ —notably narrower than some *in-vitro* methods, but the

biocompatibility of the device is promising. As illustrated in Figure 14b, fluid was sampled from the hippocampus of the guinea pig with microdialysis probes. The microdialysate then flowed into a microchannel located on the surface of a polydimethylsiloxane (PDMS) chip. Here, the microdialysate mixed with continuously perfused ammonium(III), and the device performed continuous electrochemical detection as the fluids flowed across indium tin oxide (ITO) working, counter, and reference (Ag/AgCl) electrodes. The system detected H<sub>2</sub>S within seconds and maintained a current response for just under an hour. The demonstration served as a proof-of-concept model for the biological applications of the device.<sup>175</sup>

In sum, a review of electrocatalytic sensor modifications has made it clear that electrocatalysts occupy a critical role in the development of high-performing sensors. In a growing number of cases, tunable electrocatalytic properties of electrode-modifying materials are enhancing *both* the sensitivity and the selectivity of detectors—without restricting access to the surface of the electrode. The use of nanoscale structures as scaffolding for electrocatalysts appears to have grown rapidly in recent years. Many, if not most, reports of electrochemical sensors for gasotransmitters incorporate some form of nanotechnology—often due to the ease of interaction between nanoparticles and similarly scaled biological molecules. At the forefront of electrocatalytic sensor modifications are *tunable* materials, often the result of new chemical procedures that afford researchers the capability to endow their material with analyte-specific catalytic properties. Biologically inspired metal porphyrins and metallophthalocyanine materials work much in the way that a heme-containing enzyme might function, deriving analyte-specific targeting capabilities from tunable properties of its cyclic organic structure and conductive metal nodes (though not always simultaneously). Future development in electrochemical detection methods for gasotransmitters will depend on creative development in the tunability, accessibility (cost), and miniaturizability, among other elements, of electrode-modifying catalytic materials.

## ELECTROCHEMICAL MULTI-ANALYTE SENSING

In recent years, in-vivo detection of endogenous gases has emerged as a promising and largely untapped avenue for clinical diagnosis, treatment, and recovery. One central factor in this transition has been the development of increasingly sensitive and selective detection mechanisms, often operating via electrochemical means.<sup>176</sup> Despite these advancements, in-vivo detection remains limited by the challenges of sensor insertion, stability in physiological conditions, and cytocompatibility. Such challenges have been sufficiently addressed for in-vivo sensing in a number of gasotransmitter-related applications, but most of these instances involve the detection of single analytes<sup>20,61,177</sup>—despite well-documented knowledge of interaction between gasotransmitters during endogenous signaling.<sup>178</sup> Multi-analyte sensing has the capacity to provide more complete physiological insight while avoiding the duplication of challenges associated with sensor design and insertion. In this section, recent advancements and future implications for the development of multi-analyte sensors are addressed.

Particularly in the case of NO and CO, similarities in function accompany similarities in form; both gasotransmitters are characterized by small size, charge variability,

lipopermeability, short lifetimes, and an affinity for heme binding, for example. The gases also aid in many of the same physiological functions, namely neurotransmission and vasodilation.<sup>7</sup> Another significant similarity between the pair, particularly in electrochemical sensing, is their similar oxidation potentials. In one example based on amperometric detection of NO and CO oxidations, CO was oxidized at one of the modified working electrodes only within the potential region between the onsets of oxidation (+0.20 V vs Ag/AgCl) and reduction (−0.05 V) of NO, making the selective detection of CO over NO based on applied potentials seemingly impossible. Selective detection of CO was achieved by applying a very minimal overpotential of +0.2 V in addition to a xerogel membrane, which limited the diffusion of NO enough to provide CO-selectivity.<sup>116</sup>

These similarities lend themselves to the development of numerous multi-analyte detection strategies for NO and CO, though small *differences* between the species often make these dual-detection possible. NO, for example, is a free radical; it has an unpaired electron that is readily donated to form the nitrosonium ion, facilitating the formation of numerous NO–metal complexes.<sup>179</sup> In contrast, CO is a stable gas (not a free radical); it does not undergo many of the oxidative and reductive reactions that are characteristic of NO. In biological settings, CO binds preferentially to ferrous heme, while NO binds both ferrous and ferric hemoproteins—just one example of the differences in binding characteristics of the two molecules.<sup>178–180</sup> Another example involves differential interactions with the enzyme soluble guanylate cyclase (sGC), a pathway by which both gases are thought to carry out many of their biological functions. While both NO and CO bind to the iron atom of the enzyme's heme moiety, NO binds to the heme iron, breaking an Fe-ImH (imidazole-histidine sidechain) bond and resulting in a ferrous, five-coordinate nitrosyl heme that is associated with a 100–400 fold increase in sGC activity. In contrast, CO leaves the Fe-ImH bond intact when it binds to the sGC heme group, resulting in a six-coordinate complex that only weakly increases the activity of sGC (about 1–6 fold).<sup>181</sup> These differences lay the groundwork for in-vivo interaction between the two species<sup>7,182</sup> and inform strategies for selective detection.

Differences between NO and CO mediate their electrochemical detection in dual-sensing architectures. As one example, CO has been found at higher concentrations than NO in some biological settings.<sup>19,23</sup> This difference enables detection schemes wherein low sensitivity to both CO and NO is sufficient for the detection of CO while functionally selective against NO due to low signal, as discussed by Ha and colleagues. In their sensor, a miniaturized, solid-state electrode modified with electroplated gold is overlaid with a fluorinated xerogel membrane (see Figure 15 for construction). This dual sensor has proven effective for real-time, in-vivo CO and NO detection in the cortex of a rat. Ongoing efforts in the dual sensing of CO and NO, like those of single-analyte detectors, seek to improve real-time applications in physiological conditions by reducing response time and increasing the work range of the sensors.<sup>23,116,122</sup>

While commonalities between CO and NO lend themselves to construction of dual-analyte sensing mechanisms, progress towards analytical sensors for simultaneous detection of all three gasotransmitters remains limited. No devices for simultaneous monitoring of NO, CO, and H<sub>2</sub>S in liquid states could be identified, which remains a major unresolved



research challenge. One promising direction for multianalyte detection relies on the use of modular, molecularly precise electrode materials such as MOFs and COFs. Phthalocyanine-based framework materials recently developed by our group demonstrate ppb-ppm sensing capacities for NO, H<sub>2</sub>S, and CO in the gas phase. These materials generate selectivity via their highly tunable nature, since modifications to MOF linkers and metal nodes can significantly alter the material's sensing properties.<sup>151,152,183</sup> Mechanistic studies indicate the importance of the (exchangeable) metal linker and the modifiable MPc units in the sensing response, and corroborate the prediction that these tunable MPc materials will likely play an important role in the future of multi-analyte electrochemical detection. In particular, the differential responses of multiple layered, conductive framework materials in sensors arrays have already been shown to effectively differentiate between a variety of analytes in gas phase detection.<sup>151,183–186</sup> With further development, these materials may be promising candidates for biologically relevant detection of gasotransmitters in the future.

Another example of multi-analyte sensing capabilities can be seen in the work of Li and colleagues, who developed a multi-chamber electrochemical microsystem for the simultaneous detection of NO, H<sub>2</sub>O<sub>2</sub>, ONOO<sup>-</sup>, and NO<sub>2</sub><sup>-</sup>. While not all of these endogenous species act as gasotransmitters, the device displayed promising mechanistic principles for the potential application to a broader range of species. The microsystem consisted of a glass substrate equipped with four sets of microband electrodes, each of which includes a platinum-black coated working electrode, Ag/AgCl reference, and a Pt counter electrode. The four electrodes were divided between four wells, where amperometric responses were monitored for the simultaneous detection of one species per well. This amperometric microchip-based design from Li's group, which demonstrated excellent reliability and compared appropriately to single-analyte detection of the same species, represents one of the most promising methods for large-scale, real-time, in-vivo detection of multiple endogenous species with a single device.<sup>187</sup>

While the development of multi-analyte sensors remains relatively nascent, especially with respect to gasotransmitters, researchers expect their prevalence to increase over the coming years;<sup>31</sup> future advancements in multi-analyte sensing have the potential to illuminate poorly understood pathways for interaction between gasotransmitters, expedite detection processes, and greatly improve the feasibility of in-vivo sensing devices by reducing measures of invasiveness-per-analyte.

## CONCLUSIONS AND OUTLOOK

Each of the detection methods described in this review presents its own set of advantages and disadvantages. To arrive at a conclusion regarding the most promising method(s) for the direct, real-time detection of gasotransmitters, a previously defined set of criteria are presented. According to Griveau and Bedioui,<sup>141</sup> in-situ biologically relevant gasotransmitter detection requires sensing mechanisms that satisfy the following conditions: First, sensors should have rapid response times (both NO and H<sub>2</sub>S are quite reactive in the physiological setting, with short half-lives and involvement in numerous fast-acting metabolic pathways). Second, sensors should have low—at least sub-nanomolar—LODs. Third, sensors should be sufficiently selective against common biological interferents.

Fourth, sensors should be capable of real-time detection. Finally, sensors should be non-invasive and “biocompatible”—sample destruction should be avoided.

In sum, the studies that have been reviewed herein converge repeatedly on three themes of electrochemical detection for physiologically relevant analytes. First, modification at the electrode surface enables finely tuned sensitivity and selectivity of electrochemical sensors. These electrode-modifying procedures and materials—whether they take the form of electrocatalysts, perm-selective membranes, or some combination of the two—constitute the forefront of sensor development. Secondly, the miniaturization of sensors aids in minimally invasive sensing, which is critically important in the detection of gasotransmitters. Already, developments like nanoscale scaffolding materials and microelectrode arrays are facilitating this transition to minimally invasive detection. Third, improvements in the quality and availability of wireless technology are poised to enhance the clinical relevance of many electrochemical sensors. Wireless capabilities combat the need for physical attachment to external equipment, and the potential for insertable detection systems with real-time monitoring capabilities should be considered in evaluations of stability and reliability of future detection platforms.

One alternate approach to wireless, non-invasive detection of gasotransmitters is the development of sensing platforms for exhaled air. Although not directly related to their endogenous functions, the concentrations of gasotransmitters in exhaled air can be indicative of certain diseases and serve as a useful diagnostic tool.<sup>149,150</sup> Chemiresistive sensing mechanisms for exhaled gasotransmitters avoid the issue of invasiveness entirely; investing in these platforms should be considered just as valuable as investing in the miniaturization of existing liquid-phase detection methods. Gas-phase sensing can also be conducted with swallowable capsules to monitor gasotransmitters in the digestive tract.<sup>188</sup>

Importantly, advancements in materials chemistry hold promise as the next frontier of sensor development. In the past decade, great leaps in sensor performance have stemmed from the synthesis of new materials, the controlled growth of nanostructures, novel applications of existing materials as electrocatalysts or perm-selective membranes, and creative mimicry of biological machinery. New chemistry will likely be required to address the challenges posed by multi-analyte detection needs. Specifically, materials that can be easily tuned to tailor their electrocatalytic characteristics towards a given target analyte hold great promise; they afford maximal versatility and selectivity with minimal restructuring of the underlying conductive frameworks that have already demonstrated sound detection capabilities. In tandem with the development of these tunable materials, efforts to elucidate the mechanisms of material-analyte interactions are central to rational sensor design. Spectroscopic and computational studies of both new and existing sensors will pave the way for efficient progress in the field, as trial-and-error methods are displaced by the intentional development of mechanism-centered electrocatalysts and membranes.

The array of chemical transduction mechanisms for electrochemical detection of gasotransmitters is broad. Both semi-permeable membranes and electrocatalyst deposition (often together) have proven successful in affording adequate sensitivity and selectivity. Now, the practical application of these methods in physiological conditions represents a

new and exciting next challenge in the field.<sup>176</sup> Miniaturizable and biocompatible sensing devices with replicable procedures for synthesis and fabrication, especially those capable of multi-analyte detection, will likely constitute the next frontier for gasotransmitter detection.

## ACKNOWLEDGEMENTS

The authors acknowledge support from the Maximizing Investigators' Research Award from the National Institutes of Health (R35GM138318).

## REFERENCES:

- (1). Ignarro LJ; Buga GM; Wood KS; Byrns RE; Chaudhuri G Endothelium-Derived Relaxing Factor Produced and Released from Artery and Vein Is Nitric Oxide. *Proc. Natl. Acad. Sci* 1987, 84, 9265–9269. [PubMed: 2827174]
- (2). Furchgott RF; Zawadzki JV The Obligatory Role of Endothelial Cells in the Relaxation of Arterial Smooth Muscle by Acetylcholine. *Nature* 1980, 288, 373–376. [PubMed: 6253831]
- (3). Schmidt HHHW; Pollock JS; Nakane M; Gorsky FD; Förstermann U; Murad F Purification of a Soluble Isoform of Guanylyl Cyclase-Activating-Factor Synthase. *Proc. Natl. Acad. Sci* 1991, 88, 365–369. [PubMed: 1703296]
- (4). Verma A; Hirsch DJ; Glatt CE; Ronnett GV; Snyder SH Carbon Monoxide: A Putative Neural Messenger. *Science* 1993, 259, 381–384. [PubMed: 7678352]
- (5). Mir JM; Maurya RC A Gentle Introduction to Gasotransmitters with Special Reference to Nitric Oxide: Biological and Chemical Implications. *Rev. Inorg. Chem* 2018, 38, 193–220.
- (6). Gadalla MM; Snyder SH Hydrogen Sulfide as a Gasotransmitter. *J. Neurochem* 2010, 113, 14–26. [PubMed: 20067586]
- (7). Kajimura M; Fukuda R; Bateman RM; Yamamoto T; Suematsu M Interactions of Multiple Gas-Transducing Systems: Hallmarks and Uncertainties of CO, NO, and H<sub>2</sub>S Gas Biology. *Antioxid. Redox Signal* 2010, 13, 157–192. [PubMed: 19939208]
- (8). Wang R. Two's Company, Three's a Crowd: Can H<sub>2</sub>S Be the Third Endogenous Gaseous Transmitter? *FASEB J.* 2002, 16, 1792–1798. [PubMed: 12409322]
- (9). Wang R. The Evolution of Gasotransmitter Biology and Medicine. In *Signal Transduction and the Gasotransmitters: NO, CO, and H<sub>2</sub>S in biology and Medicine*; Springer Science and Business Media: New York, 2004.
- (10). Wang R. *Gasotransmitters*; Royal Society of Chemistry, 2018.
- (11). Pacher P. Cyanide Emerges as an Endogenous Mammalian Gasotransmitter. *Proc. Natl. Acad. Sci* 2021, 118, e2108040118. [PubMed: 34099579]
- (12). Bandothkar AJ; Wang J Non-Invasive Wearable Electrochemical Sensors: A Review. *Trends Biotechnol.* 2014, 32, 363–371. [PubMed: 24853270]
- (13). Huang Y; Tang C; Du J; Jin H Endogenous Sulfur Dioxide: A New Member of Gasotransmitter Family in the Cardiovascular System. *Oxid. Med. Cell. Longev* 2016, 2016, 1–9.
- (14). Steiger AK; Zhao Y; Pluth MD Emerging Roles of Carbonyl Sulfide in Chemical Biology: Sulfide Transporter or Gasotransmitter? *Antioxid. Redox Signal* 2018, 28, 1516–1532. [PubMed: 28443679]
- (15). Wang R. Gasotransmitters: Growing Pains and Joys. *Trends Biochem. Sci* 2014, 39, 227–232. [PubMed: 24767680]
- (16). Sarti P; Arese M The Intricate Interplay among the Gasotransmitters NO, CO, H<sub>2</sub>S and Mitochondrial Complex IV. *Pharm. Pharmacol. Int. J* 2018, 6.
- (17). Mathew TL; Pownraj P; Abdulla S; Pullithadathil B Technologies for Clinical Diagnosis Using Expired Human Breath Analysis. *Diagnostics* 2015, 5, 27–60. [PubMed: 26854142]
- (18). Iverson NM; Hofferber EM; Stapleton JA Nitric Oxide Sensors for Biological Applications. *Chemosensors* 2018, 6, 8.

- (19). Park SS; Kim J; Lee Y Improved Electrochemical Microsensor for the Real-Time Simultaneous Analysis of Endogenous Nitric Oxide and Carbon Monoxide Generation. *Anal. Chem* 2012, 84, 1792–1796. [PubMed: 22263574]
- (20). Pakchin PS; Nakhjavani SA; Saber R; Ghanbari H; Omid Y Recent Advances in Simultaneous Electrochemical Multi-Analyte Sensing Platforms. *TrAC Trends Anal. Chem* 2017, 92, 32–41.
- (21). Lawrence NS; Deo RP; Wang J Electrochemical Determination of Hydrogen Sulfide at Carbon Nanotube Modified Electrodes. *Anal. Chim. Acta* 2004, 517, 131–137.
- (22). Xu T; Scafa N; Xu L; Su L; Li C; Zhou S; Liu Y; Zhang X Electrochemical Sensors for Nitric Oxide Detection in Biological Applications. *Electroanalysis* 2014, 26, 449–468.
- (23). Lee Y; Kim J Simultaneous Electrochemical Detection of Nitric Oxide and Carbon Monoxide Generated from Mouse Kidney Organ Tissues. *Anal. Chem* 2007, 79, 7669–7675. [PubMed: 17877421]
- (24). Ibrahim H; Serag A; Farag MA Emerging Analytical Tools for the Detection of the Third Gasotransmitter H<sub>2</sub>S, a Comprehensive Review. *J. Adv. Res* 2021, 27, 137–153. [PubMed: 33318873]
- (25). Alday J; Mazzeo A; Suarez S Selective Detection of Gasotransmitters Using Fluorescent Probes Based on Transition Metal Complexes. *Inorganica Chim. Acta* 2020, 510, 119696.
- (26). Amilan Jose D; Sharma N; Sakla R; Kaushik R; Gadiyaram S Fluorescent Nanoprobes for the Sensing of Gasotransmitters Hydrogen Sulfide (H<sub>2</sub>S), Nitric Oxide (NO) and Carbon Monoxide (CO). *Methods* 2019, 168, 62–75. [PubMed: 31176771]
- (27). Ali MY; Ping CY; Mok Y; Ling L; Whiteman M; Bhatia M; Moore PK Regulation of Vascular Nitric Oxide in Vitro and in Vivo ; a New Role for Endogenous Hydrogen Sulphide? *Br. J. Pharmacol* 2006, 149, 625–634. [PubMed: 17016507]
- (28). Taoka S; Banerjee R Characterization of NO Binding to Human Cystathionine B-Synthase: Possible Implications of the Effects of CO and NO Binding to the Human Enzyme. *J. Inorg. Biochem* 2001, 87, 245–251. [PubMed: 11744062]
- (29). Kubo S; Kurokawa Y; Doe I; Masuko T; Sekiguchi F; Kawabata A Hydrogen Sulfide Inhibits Activity of Three Isoforms of Recombinant Nitric Oxide Synthase. *Toxicology* 2007, 241, 92–97. [PubMed: 17888559]
- (30). Goshi E; Zhou G; He Q Nitric Oxide Detection Methods in Vitro and in Vivo. *Med. Gas Res* 2019, 9, 192–207. [PubMed: 31898604]
- (31). Brown MD; Schoenfisch MH Electrochemical Nitric Oxide Sensors: Principles of Design and Characterization. *Chem. Rev* 2019, 119, 11551–11575. [PubMed: 31553169]
- (32). Hevel JM; White KA; Marletta MA Purification of the Inducible Murine Macrophage Nitric Oxide Synthase. Identification as a Flavoprotein. *J. Biol. Chem* 1991, 266, 22789–22791. [PubMed: 1720773]
- (33). Nitric Oxide; Ignarro LJ, Ed.; Academic Press: San Diego, 2000.
- (34). Zhou L; Zhu D-Y Neuronal Nitric Oxide Synthase: Structure, Subcellular Localization, Regulation, and Clinical Implications. *Nitric Oxide* 2009, 20, 223–230. [PubMed: 19298861]
- (35). Xue Q; Yan Y; Zhang R; Xiong H Regulation of iNOS on Immune Cells and Its Role in Diseases. *Int. J. Mol. Sci* 2018, 19, 3805. [PubMed: 30501075]
- (36). Archer SL; Huang JM; Hampf V; Nelson DP; Shultz PJ; Weir EK Nitric Oxide and cGMP Cause Vasorelaxation by Activation of a Charybdotoxin-Sensitive K Channel by cGMP-Dependent Protein Kinase. *Proc. Natl. Acad. Sci* 1994, 91, 7583–7587. [PubMed: 7519783]
- (37). Bredt DS; Snyder SH Nitric Oxide Mediates Glutamate-Linked Enhancement of cGMP Levels in the Cerebellum. *Proc. Natl. Acad. Sci* 1989, 86, 9030–9033. [PubMed: 2573074]
- (38). Groll-Knapp E; Haider M; Kienzl K; Handler A; Trimmel M Changes in Discrimination Learning and Brain Activity (ERP's) Due to Combined Exposure to NO and CO in Rats. *Toxicology* 1988, 49, 441–447. [PubMed: 3376142]
- (39). Kapas L; Shibata M; Kimura M; Krueger JM Inhibition of Nitric Oxide Synthesis Suppresses Sleep in Rabbits. *Am. J. Physiol.-Regul. Integr. Comp. Physiol* 1994, 266, R151–R157.
- (40). Prast H; Philippu A Nitric Oxide as Modulator of Neuronal Function. *Prog. Neurobiol* 2001, 64, 51–68. [PubMed: 11250062]

- (41). Tanabe M; Nagatani Y; Saitoh K; Takasu K; Ono H Pharmacological Assessments of Nitric Oxide Synthase Isoforms and Downstream Diversity of NO Signaling in the Maintenance of Thermal and Mechanical Hypersensitivity after Peripheral Nerve Injury in Mice. *Neuropharmacology* 2009, 56, 702–708. [PubMed: 19111753]
- (42). Palmer RMJ; Ferrige AG; Moncada S Nitric Oxide Release Accounts for the Biological Activity of Endothelium-Derived Relaxing Factor. *Nature* 1987, 327, 524–526. [PubMed: 3495737]
- (43). Komarov A; Mattson D; Jones MM; Singh PK; Lai C-S In Vivo Spin Trapping of Nitric Oxide in Mice. *Biochem. Biophys. Res. Commun* 1993, 195, 1191–1998. [PubMed: 8216248]
- (44). Wagener FADTG; Volk H-D; Willis D; Abraham NG; Soares MP; Adema GJ; Figdor CG Different Faces of the Heme-Heme Oxygenase System in Inflammation. *Pharmacol. Rev* 2003, 55, 551–571. [PubMed: 12869663]
- (45). Jansen T; Daiber A Direct Antioxidant Properties of Bilirubin and Biliverdin. Is There a Role for Biliverdin Reductase? *Front. Pharmacol* 2012, 3, 1–10. [PubMed: 22291651]
- (46). Arosio P; Elia L; Poli M Ferritin, Cellular Iron Storage and Regulation. *IUBMB Life* 2017, 69, 414–422. [PubMed: 28349628]
- (47). Ryter SW; Morse D; Choi AMK Carbon Monoxide: To Boldly Go Where NO Has Gone Before. *Sci. STKE* 2004, 230, 1–10.
- (48). Lee PJ; Otterbein LE Carbon Monoxide and Signal Transduction Pathways. In *Signal Transduction and the Gasotransmitters: NO, CO, and H<sub>2</sub>S in biology and Medicine*; Wang R, Ed.; Springer Science and Business Media: New York, 2004.
- (49). Stucki D; Stahl W Carbon Monoxide – beyond Toxicity? *Toxicol. Lett* 2020, 333, 251–260. [PubMed: 32860873]
- (50). Almeida AS; Figueiredo-Pereira C; Vieira HLA Carbon Monoxide and Mitochondria-Modulation of Cell Metabolism, Redox Response and Cell Death. *Front. Physiol* 2015, 6, 1–6. [PubMed: 25688210]
- (51). Geisler JG; Marosi K; Halpern J; Mattson MP DNP, Mitochondrial Uncoupling, and Neuroprotection: A Little Dab'll Do Ya. *Alzheimers Dement.* 2017, 13, 582–591. [PubMed: 27599210]
- (52). Kimura H. Production and Physiological Effects of Hydrogen Sulfide. *Antioxid. Redox Signal* 2014, 20, 783–793. [PubMed: 23581969]
- (53). Cao X; Ding L; Xie Z; Yang Y; Whiteman M; Moore PK; Bian J-S A Review of Hydrogen Sulfide Synthesis, Metabolism, and Measurement: Is Modulation of Hydrogen Sulfide a Novel Therapeutic for Cancer? *Antioxid. Redox Signal* 2019, 31, 1–38. [PubMed: 29790379]
- (54). Braunstein AE; Goryachenkova EV; Tolosa EA; Willhardt IH Specificity and Some Other Properties of Liver Serine Sulphhydrylase: Evidence for Its Identity with Cystathionine  $\beta$ -Synthase. *Biochim. Biophys. Acta* 1971, 242, 247–260. [PubMed: 5121611]
- (55). Chiku T; Padovani D; Zhu W; Singh S; Vitvitsky V; Banerjee R H<sub>2</sub>S Biogenesis by Human Cystathionine  $\gamma$ -Lyase Leads to the Novel Sulfur Metabolites Lanthionine and Homolanthionine and Is Responsive to the Grade of Hyperhomocysteinemia. *J. Biol. Chem* 2009, 284, 11601–11612. [PubMed: 19261609]
- (56). Shibuya N; Tanaka M; Yoshida M; Ogasawara Y; Togawa T; Ishii K; Kimura H 3-Mercaptopyruvate Sulfurtransferase Produces Hydrogen Sulfide and Bound Sulfane Sulfur in the Brain. *Antioxid. Redox Signal* 2009, 11, 703–714. [PubMed: 18855522]
- (57). Searcy DG; Lee SH Sulfur Reduction by Human Erythrocytes. *J. Exp. Zool* 1998, 282, 310–322. [PubMed: 9755482]
- (58). Ishigami M; Hiraki K; Umemura K; Ogasawara Y; Ishii K; Kimura H A Source of Hydrogen Sulfide and a Mechanism of Its Release in the Brain. *Antioxid. Redox Signal* 2009, 11, 205–214. [PubMed: 18754702]
- (59). Wang Y; Yu R; Wu L; Yang G Hydrogen Sulfide Signaling in Regulation of Cell Behaviors. *Nitric Oxide* 2020, 103, 9–19. [PubMed: 32682981]
- (60). Miller DL; Roth MB Hydrogen Sulfide Increases Thermotolerance and Lifespan in *Caenorhabditis Elegans*. *Proc. Natl. Acad. Sci* 2007, 104, 20618–20622. [PubMed: 18077331]
- (61). Perridon BW; Leuvenink HGD; Hillebrands J-L; Van Goor H; Bos EM The Role of Hydrogen Sulfide in Aging and Age-Related Pathologies. *Aging* 2016, 8, 2264–2289. [PubMed: 27683311]



- (62). Nieto-Draghi C; Mackie AD; Bonet Avalos J Transport Coefficients and Dynamic Properties of Hydrogen Sulfide from Molecular Simulation. *J. Chem. Phys* 2005, 123, 014505. [PubMed: 16035853]
- (63). Xu T; Scafa N; Xu L-P; Zhou S; Al-Ghanem KA; Mahboob S; Fugetsu B; Zhang X Electrochemical Hydrogen Sulfide Biosensors. *The Analyst* 2016, 141, 1185–1195. [PubMed: 26806283]
- (64). Olson KR; Healy MJ; Qin Z; Skovgaard N; Vulesevic B; Duff DW; Whitfield NL; Yang G; Wang R; Perry SF Hydrogen Sulfide as an Oxygen Sensor in Trout Gill Chemoreceptors. *Am. J. Physiol.-Regul. Integr. Comp. Physiol* 2008, 295, R669–R680. [PubMed: 18565835]
- (65). Nagy P; Pálkás Z; Nagy A; Budai B; Tóth I; Vasas A Chemical Aspects of Hydrogen Sulfide Measurements in Physiological Samples. *Biochim. Biophys. Acta BBA - Gen. Subj* 2014, 1840, 876–891.
- (66). Carson RJ; Seyffarth G; Mian R; Maddock H Interactions Between Gasotransmitters. In *Signal Transduction and the Gasotransmitters: NO, CO, and H<sub>2</sub>S in biology and Medicine*; Wang R, Ed.; Springer Science and Business Media: New York, 2004; pp 33–55.
- (67). Shimizu T; Huang D; Yan F; Stranova M; Bartosova M; Fojtková V; Martínková M Gaseous O<sub>2</sub>, NO, and CO in Signal Transduction: Structure and Function Relationships of Heme-Based Gas Sensors and Heme-Redox Sensors. *Chem. Rev* 2015, 115, 6491–6533. [PubMed: 26021768]
- (68). Stuehr DJ; Haque MM Nitric Oxide Synthase Enzymology in the 20 Years after the Nobel Prize. *Br. J. Pharmacol* 2019, 176, 177–188. [PubMed: 30402946]
- (69). Yoshimura T. Endogenous Nitric Oxide, Its Chemical Characterization and the High Affinity for Metal Ions and Metalloproteins. *CVD Gd. Round Ser* 1996, 3, 1–26.
- (70). Ueno T; Yoshimura T The Physiological Activity and In Vivo Distribution of Dinitrosyl Dithiolato Iron Complex. *Jpn. J. Pharmacol* 2000, 82, 95–101. [PubMed: 10877526]
- (71). Stuehr DJ; Santolini J; Wang Z-Q; Wei C-C; Adak S Update on Mechanism and Catalytic Regulation in the NO Synthases. *J. Biol. Chem* 2004, 279, 36167–36170. [PubMed: 15133020]
- (72). Brucker EA; Olson JS; Ikeda-Saito M; Phillips GN Nitric Oxide Myoglobin: Crystal Structure and Analysis of Ligand Geometry. *Proteins Struct. Funct. Genet* 1998, 30, 352–356. [PubMed: 9533619]
- (73). Hara E; Takahashi K; Tominaga T; Kumabe T; Kayama T; Suzuki H; Fujita H; Yoshimoto T; Shirato K; Shibahara S Expression of Heme Oxygenase and Inducible Nitric Oxide Synthase mRNA in Human Brain Tumors. *Biochem. Biophys. Res. Commun* 1996, 224, 153–158. [PubMed: 8694803]
- (74). Motterlini R; Green CJ; Foresti R Regulation of Heme Oxygenase-1 by Redox Signals Involving Nitric Oxide. *Antioxid. Redox Signal* 2002, 4, 615–624. [PubMed: 12230873]
- (75). Durante W; Kroll MH; Christodoulides N; Peyton KJ; Schafer AI Nitric Oxide Induces Heme Oxygenase-1 Gene Expression and Carbon Monoxide Production in Vascular Smooth Muscle Cells. *Circ. Res* 1997, 80, 557–564. [PubMed: 9118487]
- (76). Carter EP; Hartsfield CL; Miyazono M; Jakkula M; Morris KG; McMurtry IF Regulation of Heme Oxygenase-1 by Nitric Oxide during Hepatopulmonary Syndrome. *Am. J. Physiol.-Lung Cell. Mol. Physiol* 2002, 283, L346–L353. [PubMed: 12114196]
- (77). Foresti R; Motterlini R The Heme Oxygenase Pathway and Its Interaction with Nitric Oxide in the Control of Cellular Homeostasis. *Free Radic. Res* 1999, 31, 459–475. [PubMed: 10630670]
- (78). Hartsfield CL; Alam J; Cook JL; Choi AMK Regulation of Heme Oxygenase-1 Gene Expression in Vascular Smooth Muscle Cells by Nitric Oxide. *Am. J. Physiol.-Lung Cell. Mol. Physiol* 1997, 273, L980–L988.
- (79). Vincent SR; Das S; Maines MD Brain Heme Oxygenase Isoenzymes and Nitric Oxide Synthase Are Co-Localized in Select Neurons. *Neuroscience* 1994, 63, 223–231. [PubMed: 7534881]
- (80). Liu X; Peyton KJ; Ensenat D; Wang H; Hannink M; Alam J; Durante W Nitric Oxide Stimulates Heme Oxygenase-1 Gene Transcription via the Nrf2/ARE Complex to Promote Vascular Smooth Muscle Cell Survival. *Cardiovasc. Res* 2007, 75, 381–389. [PubMed: 17408602]
- (81). Wang J; Lu S; Moënné-Loccoz P; Ortiz De Montellano PR Interaction of Nitric Oxide with Human Heme Oxygenase-1. *J. Biol. Chem* 2003, 278, 2341–2347. [PubMed: 12433915]



- (82). Scheele JS; Kharitonov VG; Martásek P; Roman LJ; Sharma VS; Masters BSS; Magde D Kinetics of CO Ligation with Nitric-Oxide Synthase by Flash Photolysis and Stopped-Flow Spectrophotometry. *J. Biol. Chem* 1997, 272, 12523–12528. [PubMed: 9139703]
- (83). Peng H; Chen W; Wang B Methods for the Detection of Gasotransmitters. In *Gasotransmitters: Physiology and Pathophysiology*; Hermann A, Sitdikova GF, Weiger TM, Eds.; Springer Berlin Heidelberg: Berlin, Heidelberg, 2012; pp 99–137.
- (84). Jaworska E; Pawłowski P; Michalska A; Maksymiuk K Advantages of Amperometric Readout Mode of Ion-selective Electrodes under Potentiostatic Conditions. *Electroanalysis* 2019, 31, 343–349.
- (85). Hetrick EM; Schoenfish MH Analytical Chemistry of Nitric Oxide. *Annu. Rev. Anal. Chem* 2009, 2, 409–433.
- (86). Bentley CL; Kang M; Unwin PR Nanoscale Surface Structure–Activity in Electrochemistry and Electrocatalysis. *J. Am. Chem. Soc* 2019, 141, 2179–2193. [PubMed: 30485739]
- (87). Hunter RA; Privett BJ; Henley WH; Breed ER; Liang Z; Mittal R; Yoseph BP; McDunn JE; Burd EM; Coopersmith CM; Ramsey JM; Schoenfish MH Microfluidic Amperometric Sensor for Analysis of Nitric Oxide in Whole Blood. *Anal. Chem* 2013, 85, 6066–6072. [PubMed: 23692300]
- (88). Brown MD; Schoenfish MH Catalytic Selectivity of Metallophthalocyanines for Electrochemical Nitric Oxide Sensing. *Electrochimica Acta* 2018, 273, 98–104. [PubMed: 30739948]
- (89). Goines S; Dick JE Review—Electrochemistry’s Potential to Reach the Ultimate Sensitivity in Measurement Science. *J. Electrochem. Soc* 2020, 167, 037505.
- (90). Privett BJ; Shin JH; Schoenfish MH Electrochemical Sensors. *Anal. Chem* 2010, 82, 4723–4741. [PubMed: 20476724]
- (91). Moon J; Ha Y; Kim M; Sim J; Lee Y; Suh M Dual Electrochemical Microsensor for Real-Time Simultaneous Monitoring of Nitric Oxide and Potassium Ion Changes in a Rat Brain during Spontaneous Neocortical Epileptic Seizure. *Anal. Chem* 2016, 88, 8942–8948. [PubMed: 27535464]
- (92). Park SS; Hong M; Ha Y; Sim J; Jhon G-J; Lee Y; Suh M The Real-Time in Vivo Electrochemical Measurement of Nitric Oxide and Carbon Monoxide Release upon Direct Epidural Electrical Stimulation of the Rat Neocortex. *The Analyst* 2015, 140, 3415–3421. [PubMed: 25751504]
- (93). Brown MD; Schoenfish MH Nitric Oxide Permselectivity in Electropolymerized Films for Sensing Applications. *ACS Sens.* 2016, 1, 1453–1461. [PubMed: 31875180]
- (94). Kwon T; Mun HY; Seo S; Yu A; Lee C; Lee Y Amperometric Sensing of Carbon Monoxide: Improved Sensitivity and Selectivity via Nanostructure-Controlled Electrodeposition of Gold. *Biosensors* 2021, 11, 334. [PubMed: 34562925]
- (95). Nowaczyk A; Kowalska M; Nowaczyk J; Grze k G Carbon Monoxide and Nitric Oxide as Examples of the Youngest Class of Transmitters. *Int. J. Mol. Sci* 2021, 22, 6029. [PubMed: 34199647]
- (96). Brown MD; Hall JR; Schoenfish MH A Direct and Selective Electrochemical Hydrogen Sulfide Sensor. *Anal. Chim. Acta* 2019, 1045, 67–76. [PubMed: 30454574]
- (97). Doeller JE; Isbell TS; Benavides G; Koenitzer J; Patel H; Patel RP; Lancaster JR; Darley-USmar VM; Kraus DW Polarographic Measurement of Hydrogen Sulfide Production and Consumption by Mammalian Tissues. *Anal. Biochem* 2005, 341, 40–51. [PubMed: 15866526]
- (98). Pontié M; Gobin C; Pauporté T; Bedioui F; Devynck J Electrochemical Nitric Oxide Microsensors: Sensitivity and Selectivity Characterisation. *Anal. Chim. Acta* 2000, 411, 175–185.
- (99). Shibuki K. An Electrochemical Microprobe for Detecting Nitric Oxide Release in Brain Tissue. *Neurosci. Res* 1990, 9, 69–76. [PubMed: 2175870]
- (100). Coneski PN; Schoenfish MH Nitric Oxide Release: Part III. Measurement and Reporting. *Chem. Soc. Rev* 2012, 41, 3753–3758. [PubMed: 22362308]
- (101). Li J; Zhu C; Peng W; Cao X; Gao H; Jiang M; Wu Z; Yu C Stretchable Electrochemical Sensor Based on a Gold Nanowire and Carbon Nanotube Network for Real-Time Tracking Cell-Released H<sub>2</sub>S. *Anal. Chem* 2023, 95, 2406–2412. [PubMed: 36669829]

- (102). Deng Y; Qi H; Ma Y; Liu S; Zhao M; Guo Z; Jie Y; Zheng R; Jing J; Chen K; Ding H; Lv G; Zhang K; Li R; Cheng H; Zhao L; Sheng X; Zhang M; Yin L A Flexible and Highly Sensitive Organic Electrochemical Transistor-Based Biosensor for Continuous and Wireless Nitric Oxide Detection. *Proc. Natl. Acad. Sci* 2022, 119, e2208060119. [PubMed: 35972962]
- (103). Li R; Qi H; Ma Y; Deng Y; Liu S; Jie Y; Jing J; He J; Zhang X; Wheatley L; Huang C; Sheng X; Zhang M; Yin L A Flexible and Physically Transient Electrochemical Sensor for Real-Time Wireless Nitric Oxide Monitoring. *Nat. Commun* 2020, 11, 3207. [PubMed: 32587309]
- (104). Pekarova M; Kralova J; Kubala L; Ciz M; Lojek A; Gregor C; Hrbac J Continuous Electrochemical Monitoring of Nitric Oxide Production in Murine Macrophage Cell Line RAW 264.7. *Anal. Bioanal. Chem* 2009, 394, 1497–1504. [PubMed: 19430767]
- (105). Ciszewski A; Milczarek G Electrochemical Detection of Nitric Oxide Using Polymer Modified Electrodes. *Talanta* 2003, 61, 11–26. [PubMed: 18969158]
- (106). Wynne AM; Reid CH; Finnerty NJ *In Vitro* Characterisation of Ortho Phenylenediamine and Nafion-Modified Pt Electrodes for Measuring Brain Nitric Oxide. *J. Electroanal. Chem* 2014, 732, 110–116.
- (107). Mitchell KM; Michaelis EK Multimembrane Carbon Fiber Electrodes for Physiological Measurements of Nitric Oxide. *Electroanalysis* 1998, 10, 81–88.
- (108). Cha W; Tung Y-C; Meyerhoff ME; Takayama S Patterned Electrode-Based Amperometric Gas Sensor for Direct Nitric Oxide Detection within Microfluidic Devices. *Anal. Chem* 2010, 82, 3300–3305. [PubMed: 20329749]
- (109). Shim JH; Do H; Lee Y Simple Fabrication of Amperometric Nitric Oxide Microsensors Based on Electropolymerized Membrane Films. *Electroanalysis* 2010, 22, 359–366.
- (110). Shin JH; Privett BJ; Kita JM; Wightman RM; Schoenfish MH Fluorinated Xerogel-Derived Microelectrodes for Amperometric Nitric Oxide Sensing. *Anal. Chem* 2008, 80, 6850–6859. [PubMed: 18714964]
- (111). Hughes LB; Labban N; Conway GE; Pollock JA; Leopold MC Adaptable Xerogel-Layered Amperometric Biosensor Platforms on Wire Electrodes for Clinically Relevant Measurements. *Sensors* 2019, 19, 2584. [PubMed: 31174353]
- (112). Kang SW; Kim OK; Seo B; Lee SH; Quan FS; Shin JH; Lee G-J; Park H-K Simultaneous, Real-Time Measurement of Nitric Oxide and Oxygen Dynamics during Cardiac Ischemia-Reperfusion of the Rat Utilizing Sol-Gel-Derived Electrochemical Microsensors. *Anal. Chim. Acta* 2013, 802, 74–81. [PubMed: 24176507]
- (113). Walcarius A; Collinson MM Analytical Chemistry with Silica Sol-Gels: Traditional Routes to New Materials for Chemical Analysis. *Annu. Rev. Anal. Chem* 2009, 2, 121–143.
- (114). Wang M; Zhu L; Zhang S; Lou Y; Zhao S; Tan Q; He L; Du M A Copper(II) Phthalocyanine-Based Metallo-Covalent Organic Framework Decorated with Silver Nanoparticle for Sensitively Detecting Nitric Oxide Released from Cancer Cells. *Sens. Actuators B Chem* 2021, 338, 129826.
- (115). Ling P; Zang X; Qian C; Gao F A Metal–Organic Framework with Multienzyme Activity as a Biosensing Platform for Real-Time Electrochemical Detection of Nitric Oxide and Hydrogen Peroxide. *The Analyst* 2021, 146, 2609–2616. [PubMed: 33720222]
- (116). Ha Y; Sim J; Lee Y; Suh M Insertable Fast-Response Amperometric NO/CO Dual Microsensor: Study of Neurovascular Coupling During Acutely Induced Seizures of Rat Brain Cortex. *Anal. Chem* 2016, 88, 2563–2569. [PubMed: 26855261]
- (117). Liu Y-L; Wang X-Y; Xu J-Q; Xiao C; Liu Y-H; Zhang X-W; Liu J-T; Huang W-H Functionalized Graphene-Based Biomimetic Microsensor Interfacing with Living Cells to Sensitively Monitor Nitric Oxide Release. *Chem. Sci* 2015, 6, 1853–1858. [PubMed: 28706641]
- (118). Quinton D; Girard A; Thi Kim LT; Raimbault V; Griscom L; Razan F; Griveau S; Bedioui F On-Chip Multi-Electrochemical Sensor Array Platform for Simultaneous Screening of Nitric Oxide and Peroxynitrite. *Lab. Chip* 2011, 11, 1342–1350. [PubMed: 21321748]
- (119). Jeromiyas N; Lin C-M; Lee Y-C; Chen C-H; Mani V; Arumugam R; Huang S-T Gd Doped Molybdenum Selenide/Carbon Nanofibers: An Excellent Electrocatalyst for Monitoring Endogenous H<sub>2</sub>S. *Inorg. Chem. Front* 2021, 8, 2871–2879.
- (120). Walcarius A. Electrochemical Applications of Silica-Based Organic–Inorganic Hybrid Materials. *Chem. Mater* 2001, 13, 3351–3372.

- (121). Brown MD; Schoenfish MH Selective and Sensocompatible Electrochemical Nitric Oxide Sensor with a Bilaminar Design. *ACS Sens.* 2019, 4, 1766–1773. [PubMed: 31244005]
- (122). Kim YS; Ha Y; Sim J; Suh M; Lee Y Location-Dependent Sensing of Nitric Oxide and Calcium Ions in Living Rat Kidney Using an Amperometric/Potentiometric Dual Microsensor. *The Analyst* 2016, 141, 297–304. [PubMed: 26606650]
- (123). Chen KY; Morris JC Kinetics of Oxidation of Aqueous Sulfide by O<sub>2</sub>. *Environ. Sci. Technol* 1972, 6, 529–537.
- (124). Mason J; Cardin CJ; Dennehy A The Role of Sulphide and Sulphide Oxidation in the Copper Molybdenum Antagonism in Rats and Guinea Pigs. *Res. Vet. Sci* 1978, 24, 104–108. [PubMed: 625596]
- (125). Yang B; Wang S; Tian S; Liu L Determination of Hydrogen Sulfide in Gasoline by Au Nanoclusters Modified Glassy Carbon Electrode. *Electrochem. Commun* 2009, 11, 1230–1233.
- (126). Li G; Polk BJ; Meazell LA; Hatchett DW ISE Analysis of Hydrogen Sulfide in Cigarette Smoke. *J. Chem. Educ* 2000, 77, 1049–1052.
- (127). Jeroschewski P; Steuckart C; Kühl M An Amperometric Microsensor for the Determination of H<sub>2</sub>S in Aquatic Environments. *Anal. Chem* 1996, 68, 4351–4357.
- (128). Kraus DW; Doeller JE Sulfide Consumption by Mussel Gill Mitochondria Is Not Strictly Tied to Oxygen Reduction: Measurements Using a Novel Polarographic Sulfide Sensor. *J. Exp. Biol* 2004, 207, 3667–3679. [PubMed: 15371475]
- (129). Azzouz A; Goud KY; Raza N; Ballesteros E; Lee S-E; Hong J; Deep A; Kim K-H Nanomaterial-Based Electrochemical Sensors for the Detection of Neurochemicals in Biological Matrices. *TrAC Trends Anal. Chem* 2019, 110, 15–34.
- (130). Asif M; Aziz A; Wang Z; Ashraf G; Wang J; Luo H; Chen X; Xiao F; Liu H Hierarchical CNTs@CuMn Layered Double Hydroxide Nanohybrid with Enhanced Electrochemical Performance in H<sub>2</sub>S Detection from Live Cells. *Anal. Chem* 2019, 91, 3912–3920. [PubMed: 30761890]
- (131). Nyokong T; Vilakazi S Phthalocyanines and Related Complexes as Electrocatalysts for the Detection of Nitric Oxide. *Talanta* 2003, 61, 27–35. [PubMed: 18969159]
- (132). Caro CA; Zagal JH; Bedioui F Electrocatalytic Activity of Substituted Metallophthalocyanines Adsorbed on Vitreous Carbon Electrode for Nitric Oxide Oxidation. *J. Electrochem. Soc* 2003, 150, E95–E103.
- (133). Zagal JH; Griveau S; Silva JF; Nyokong T; Bedioui F Metallophthalocyanine-Based Molecular Materials as Catalysts for Electrochemical Reactions. *Coord. Chem. Rev* 2010, 254, 2755–2791.
- (134). Mallinski T; Taha Z Nitric Oxide Release from a Single Cell Measured in Situ by a Porphyrinic-Based Microsensor. *Nature* 1992, 358, 676–678. [PubMed: 1495562]
- (135). Diab N; Schuhmann W Electropolymerized Manganese Porphyrin/Polypyrrole Films as Catalytic Surfaces for the Oxidation of Nitric Oxide. *Electrochimica Acta* 2001, 47, 265–273.
- (136). Bedioui F; Trevin S; Albin V; Villegas MGG; Devynck J Design and Characterization of Chemically Modified Electrodes with Iron(III) Porphyrinic-Based Polymers: Study of Their Reactivity toward Nitrites and Nitric Oxide in Aqueous Solution. *Anal. Chim. Acta* 1997, 341, 177–185.
- (137). Hayon J; Ozer D; Rishpon J; Bettelheim A Spectroscopic and Electrochemical Response to Nitrogen Monoxide of a Cationic Iron Porphyrin Immobilized in Nafion-Coated Electrodes or Membranes. *J. Chem. Soc. Chem. Commun* 1994, 5, 619–620.
- (138). Privett BJ; Shin JH; Schoenfish MH Electrochemical Nitric Oxide Sensors for Physiological Measurements. *Chem. Soc. Rev* 2010, 39, 1925–1935. [PubMed: 20502795]
- (139). Uchida K; Soma M; Onishi T; Tamaru K Adsorption of NO and Pyridine by Various Metal Phthalocyanines Studied by X-Ray Photoelectron Spectroscopy and Gravimetry. *J. Chem. Soc. Faraday Trans. 1 Phys. Chem. Condens. Phases* 1979, 75, 2839–2850.
- (140). Zilbermann I; Hayon J; Katchalski T; Raveh O; Rishpon J; Shames AI; Bettelheim A Ligation and Mediated Oxidation of Nitrogen Monoxide by Nickel(II) Tetrasulfonated Phthalocyanine. *J. Electrochem. Soc* 1997, 144, L228–L230.

- (141). Griveau S; Bedioui F Overview of Significant Examples of Electrochemical Sensor Arrays Designed for Detection of Nitric Oxide and Relevant Species in a Biological Environment. *Anal. Bioanal. Chem* 2013, 405, 3475–3488. [PubMed: 23334219]
- (142). Xu H; Liao C; Liu Y; Ye B-C; Liu B Iron Phthalocyanine Decorated Nitrogen-Doped Graphene Biosensing Platform for Real-Time Detection of Nitric Oxide Released from Living Cells. *Anal. Chem* 2018, 90, 4438–4444. [PubMed: 29508999]
- (143). Hao X; Hu F; Gu Y; Yang H; Li C; Guo C Molecularly Assembled Graphdiyne with Atomic Sites for Ultrafast and Real-Time Detection of Nitric Oxide in Cell Assays. *Biosens. Bioelectron* 2022, 195, 113630. [PubMed: 34536724]
- (144). Zhou W; Tan Y; Ma J; Wang X; Yang L; Li Z; Liu C; Wu H; Sun L; Deng W Ultrasensitive NO Sensor Based on a Nickel Single-Atom Electrocatalyst for Preliminary Screening of COVID-19. *ACS Sens.* 2022, 7, 3422–3429. [PubMed: 36315489]
- (145). Aykanat A; Meng Z; Benedetto G; Mirica KA Molecular Engineering of Multifunctional Metallophthalocyanine-Containing Framework Materials. *Chem. Mater* 2020, 32, 5372–5409.
- (146). Szabo C. Gasotransmitters in Cancer: From Pathophysiology to Experimental Therapy. *Nat. Rev. Drug Discov* 2016, 15, 185–203. [PubMed: 26678620]
- (147). Yasuda Y. Pathophysiological Significance of Measuring Exhaled Gasotransmitters during Exercise. *J. Phys. Fit. Sports Med* 2013, 2, 311–318.
- (148). Kiss H; Örl s Z; Gellért Á; Megyesfalvi Z; Mikáczó A; Sárközi A; Vaskó A; Miklós Z; Horváth I Exhaled Biomarkers for Point-of-Care Diagnosis: Recent Advances and New Challenges in Breathomics. *Micromachines* 2023, 14, 391. [PubMed: 36838091]
- (149). Sharma A; Kumar R; Varadwaj P Smelling the Disease: Diagnostic Potential of Breath Analysis. *Mol. Diagn. Ther* 2023, 27, 321–347. [PubMed: 36729362]
- (150). Shende P; Vaidya J; Kulkarni YA; Gaud RS Systematic Approaches for Biodiagnostics Using Exhaled Air. *J. Controlled Release* 2017, 268, 282–295.
- (151). Meng Z; Aykanat A; Mirica KA Welding Metallophthalocyanines into Bimetallic Molecular Meshes for Ultrasensitive, Low-Power Chemiresistive Detection of Gases. *J. Am. Chem. Soc* 2019, 141, 2046–2053. [PubMed: 30596491]
- (152). Meng Z; Stolz RM; Mirica KA Two-Dimensional Chemiresistive Covalent Organic Framework with High Intrinsic Conductivity. *J. Am. Chem. Soc* 2019, 141, 11929–11937. [PubMed: 31241936]
- (153). Lu S; Jia H; Hummel M; Wu Y; Wang K; Qi X; Gu Z Two-Dimensional Conductive Phthalocyanine-Based Metal–Organic Frameworks for Electrochemical Nitrite Sensing. *RSC Adv.* 2021, 11, 4472–4477. [PubMed: 35424394]
- (154). Seto H; Kondo T; Yuasa M Sensitive and Selective Electrochemical Detection of Carbon Monoxide in Saline at a Pt-Ru/Nafion/MnO<sub>2</sub>-Modified Electrode. *Anal. Sci* 2012, 28, 115–120. [PubMed: 22322802]
- (155). Kim S; Ha Y; Kim S; Lee C; Lee Y Selectivity Enhancement of Amperometric Nitric Oxide Detection via Shape-Controlled Electrodeposition of Platinum Nanostructures. *The Analyst* 2019, 144, 258–264.
- (156). Lafuma A; Quéré D Superhydrophobic States. *Nat. Mater* 2003, 2, 457–460. [PubMed: 12819775]
- (157). Song J; Xu L; Xing R; Li Q; Zhou C; Liu D; Song H Synthesis of Au/Graphene Oxide Composites for Selective and Sensitive Electrochemical Detection of Ascorbic Acid. *Sci. Rep* 2014, 4, 7515. [PubMed: 25515430]
- (158). Jensen GC; Zheng Z; Meyerhoff ME Amperometric Nitric Oxide Sensors with Enhanced Selectivity Over Carbon Monoxide via Platinum Oxide Formation Under Alkaline Conditions. *Anal. Chem* 2013, 85, 10057–10061. [PubMed: 24067100]
- (159). Wang S; Lin X Electrodeposition of Pt–Fe(III) Nanoparticle on Glassy Carbon Electrode for Electrochemical Nitric Oxide Sensor. *Electrochimica Acta* 2005, 50, 2887–2891.
- (160). Pei J; Yu N-T; Li X-Y Electrocatalytic Detection of Biological Nitric Oxide at an Ultramicroelectrode Modified with an Electrodeposited CuPtCl<sub>6</sub> Film. *Anal. Chim. Acta* 1999, 402, 145–155.

- (161). Albery WJ; Cass AEG; Mangold BP; Shu ZX Inhibited Enzyme Electrodes. Part 3: A Sensor for Low Levels of H<sub>2</sub>S and HCN. *Biosens. Bioelectron* 1990, 5, 397–413. [PubMed: 2171574]
- (162). Yang Y; Yang M; Wang H; Jiang J; Shen G; Yu R An Amperometric Horseradish Peroxidase Inhibition Biosensor Based on a Cysteamine Self-Assembled Monolayer for the Determination of Sulfides. *Sens. Actuators B Chem* 2004, 102, 162–168.
- (163). Zhao J; Henkens RW; Crumbliss AL Mediator-Free Amperometric Determination of Toxic Substances Based on Their Inhibition of Immobilized Horseradish Peroxidase. *Biotechnol. Prog* 1996, 12, 703–708. [PubMed: 8879158]
- (164). Savizi ISP; Kariminia H-R; Ghadiri M; Roosta-Azad R Amperometric Sulfide Detection Using *Coprinus Cinereus* Peroxidase Immobilized on Screen Printed Electrode in an Enzyme Inhibition Based Biosensor. *Biosens. Bioelectron* 2012, 35, 297–301. [PubMed: 22472527]
- (165). Liu L; Chen Z; Yang S; Jin X; Lin X A Novel Inhibition Biosensor Constructed by Layer-by-Layer Technique Based on Biospecific Affinity for the Determination of Sulfide. *Sens. Actuators B Chem* 2008, 129, 218–224.
- (166). Zhao Y; Liu L; Kong D; Kuang H; Wang L; Xu C Dual Amplified Electrochemical Immunosensor for Highly Sensitive Detection of *Pantoea Stewartii* Sbusp. *Stewartii*. *ACS Appl. Mater. Interfaces* 2014, 6, 21178–21183. [PubMed: 25384268]
- (167). Zhao Y; Yang Y; Cui L; Zheng F; Song Q Electroactive Au@Ag Nanoparticles Driven Electrochemical Sensor for Endogenous H<sub>2</sub>S Detection. *Biosens. Bioelectron* 2018, 117, 53–59. [PubMed: 29885580]
- (168). Braga SS; Marques J; Heister E; Diogo CV; Oliveira PJ; Paz FAA; Santos TM; Marques MPM Carriers for Metal Complexes on Tumour Cells: The Effect of Cyclodextrins vs CNTs on the Model Guest Phenanthroline-5,6-Dione Trithiacyclononane Ruthenium(II) Chloride. *BioMetals* 2014, 27, 507–525. [PubMed: 24652595]
- (169). Suhail MH; Abdullah O. Gh.; Kadhim GA Hydrogen Sulfide Sensors Based on PANI/f-SWCNT Polymer Nanocomposite Thin Films Prepared by Electrochemical Polymerization. *J. Sci. Adv. Mater. Devices* 2019, 4, 143–149.
- (170). Shang H; Xu H; Liu Q; Du Y PdCu Alloy Nanosheets-Constructed 3D Flowers: New Highly Sensitive Materials for H<sub>2</sub>S Detection. *Sens. Actuators B Chem* 2019, 289, 260–268.
- (171). Wang Y-H; Huang K-J; Wu X Recent Advances in Transition-Metal Dichalcogenides Based Electrochemical Biosensors: A Review. *Biosens. Bioelectron* 2017, 97, 305–316. [PubMed: 28618367]
- (172). Yang J; Liu Y; Shi C; Zhu J; Yang X; Liu S; Li L; Xu Z; Zhang C; Liu T Carbon Nanotube with Vertical 2D Molybdenum Sulphoselenide Nanosheet Arrays for Boosting Electrocatalytic Hydrogen Evolution. *ACS Appl. Energy Mater* 2018, 1, 7035–7045.
- (173). Cheng S; Zhang L; Zhang M In Vivo Detection of Hydrogen Sulfide in Brain and Cell. *Electroanalysis* 2022, 34, 1027–1040.
- (174). Ding L; Ma C; Li L; Zhang L; Yu J A Photoelectrochemical Sensor for Hydrogen Sulfide in Cancer Cells Based on the Covalently and in Situ Grafting of CdS Nanoparticles onto TiO<sub>2</sub> Nanotubes. *J. Electroanal. Chem* 2016, 783, 176–181.
- (175). Wang S; Liu X; Zhang M Reduction of Ammineruthenium(III) by Sulfide Enables In Vivo Electrochemical Monitoring of Free Endogenous Hydrogen Sulfide. *Anal. Chem* 2017, 89, 5382–5388. [PubMed: 28422478]
- (176). Vadgama P. Monitoring with In Vivo Electrochemical Sensors: Navigating the Complexities of Blood and Tissue Reactivity. *Sensors* 2020, 20, 3149. [PubMed: 32498360]
- (177). Sukanuma K; Tsukada K; Kashiba M; Tsuneshige A; Furukawa T; Kubota T; Goda N; Kitajima M; Yonetani T; Suematsu M Erythrocytes with T-State-Stabilized Hemoglobin as a Therapeutic Tool for Postischemic Liver Dysfunction. *Antioxid. Redox Signal* 2006, 8, 1847–1855. [PubMed: 16987037]
- (178). Hartsfield CL Cross Talk between Carbon Monoxide and Nitric Oxide. *Antioxid. Redox Signal* 2002, 4, 301–307. [PubMed: 12006181]
- (179). Lancaster JR Nitric Oxide: A Brief Overview of Chemical and Physical Properties Relevant to Therapeutic Applications. *Future Sci. OA* 2015, 1, fso.15.59.

- (180). Kajimura M; Shimoyama M; Tsuyama S; Suzuki T; Kozaki S; Takenaka S; Tsubota K; Oguchi Y; Suematsu M Visualization of Gaseous Monoxide Reception by Soluble Guanylate Cyclase in the Rat Retina. *FASEB J.* 2003, 77, 1–23.
- (181). Friebe A; Schultz G; Koesling D Sensitizing Soluble Guanylyl Cyclase to Become a Highly CO-Sensitive Enzyme. *EMBO J.* 1996, 15, 6863–6868. [PubMed: 9003762]
- (182). Maines MD The Heme Oxygenase System: A Regulator of Second Messenger Gases. *Annu. Rev. Pharmacol. Toxicol* 1997, 37, 517–554. [PubMed: 9131263]
- (183). Aykanat A; Meng Z; Stolz RM; Morrell CT; Mirica KA Bimetallic Two-Dimensional Metal–Organic Frameworks for the Chemiresistive Detection of Carbon Monoxide. *Angew. Chem. Int. Ed* 2022, 61, e202113665.
- (184). Smith MK; Mirica KA Self-Organized Frameworks on Textiles (SOFT): Conductive Fabrics for Simultaneous Sensing, Capture, and Filtration of Gases. *J. Am. Chem. Soc* 2017, 139, 16759–16767. [PubMed: 29087700]
- (185). Smith MK; Jensen KE; Pivak PA; Mirica KA Direct Self-Assembly of Conductive Nanorods of Metal–Organic Frameworks into Chemiresistive Devices on Shrinkable Polymer Films. *Chem. Mater* 2016, 28, 5264–5268.
- (186). Campbell MG; Liu SF; Swager TM; Dinc M Chemiresistive Sensor Arrays from Conductive 2D Metal–Organic Frameworks. *J. Am. Chem. Soc* 2015, 137, 13780–13783. [PubMed: 26456526]
- (187). Li Y; Meunier A; Fulcrand R; Sella C; Amatore C; Thouin L; Lemaître F; Guille-Collignon M Multi-chambers Microsystem for Simultaneous and Direct Electrochemical Detection of Reactive Oxygen and Nitrogen Species Released by Cell Populations. *Electroanalysis* 2016, 28, 1865–1872.
- (188). Stine JM; Ruland KL; Beardslee LA; Levy JA; Abianeh H; Botasini S; Pasricha PJ; Ghodssi R Miniaturized Capsule System Toward Real-Time Electrochemical Detection of H<sub>2</sub>S in the Gastrointestinal Tract. *Adv. Healthc. Mater* 2023, 13, 2302897.



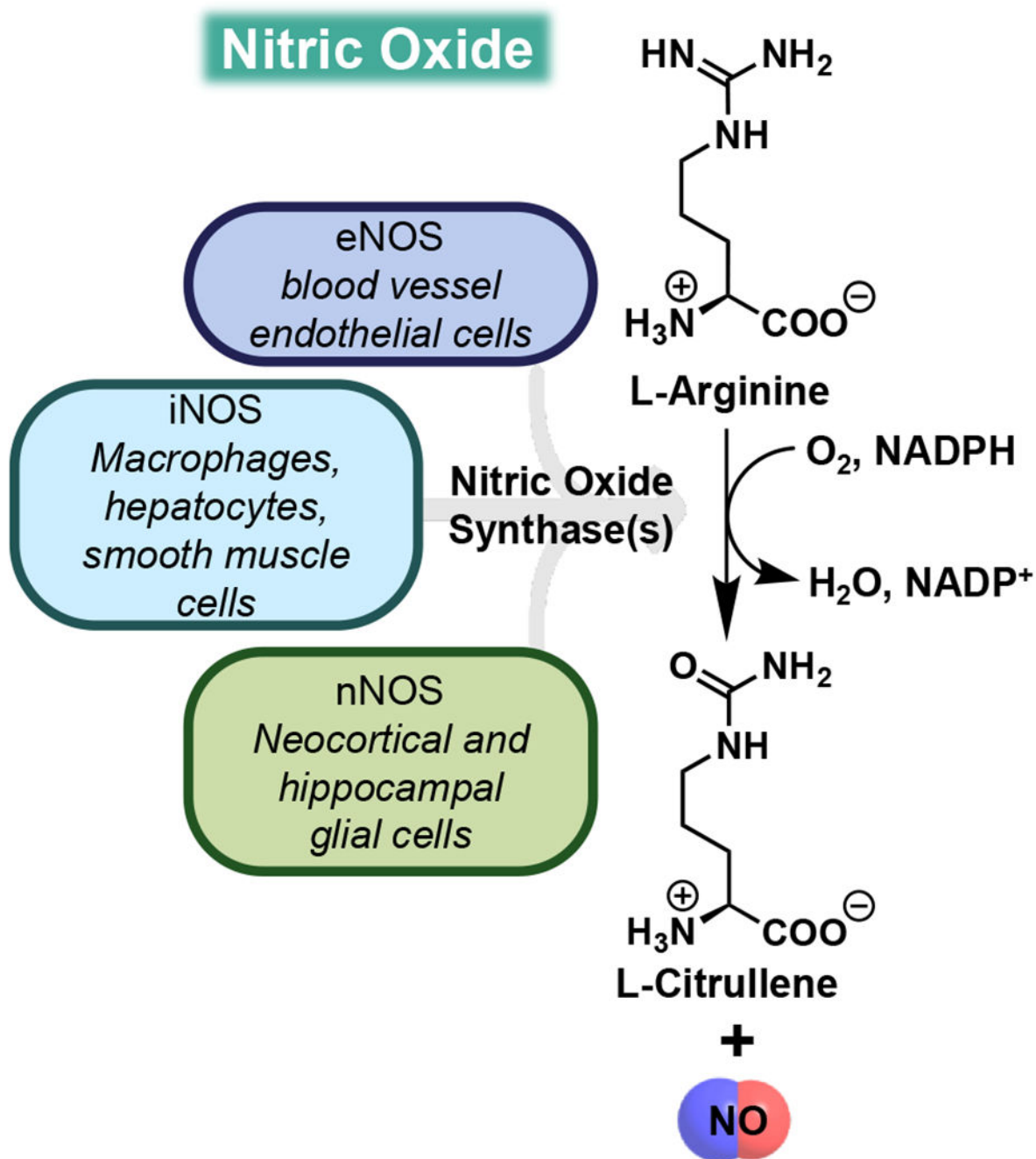


**Figure 1.** Endogenous synthesis pathways for NO via nitric oxide synthase isoenzymes nNOS, eNOS, and iNOS. The three synthesis pathways begin in different bodily regions, but each includes catalysis of L-arginine oxidation to generate NO.

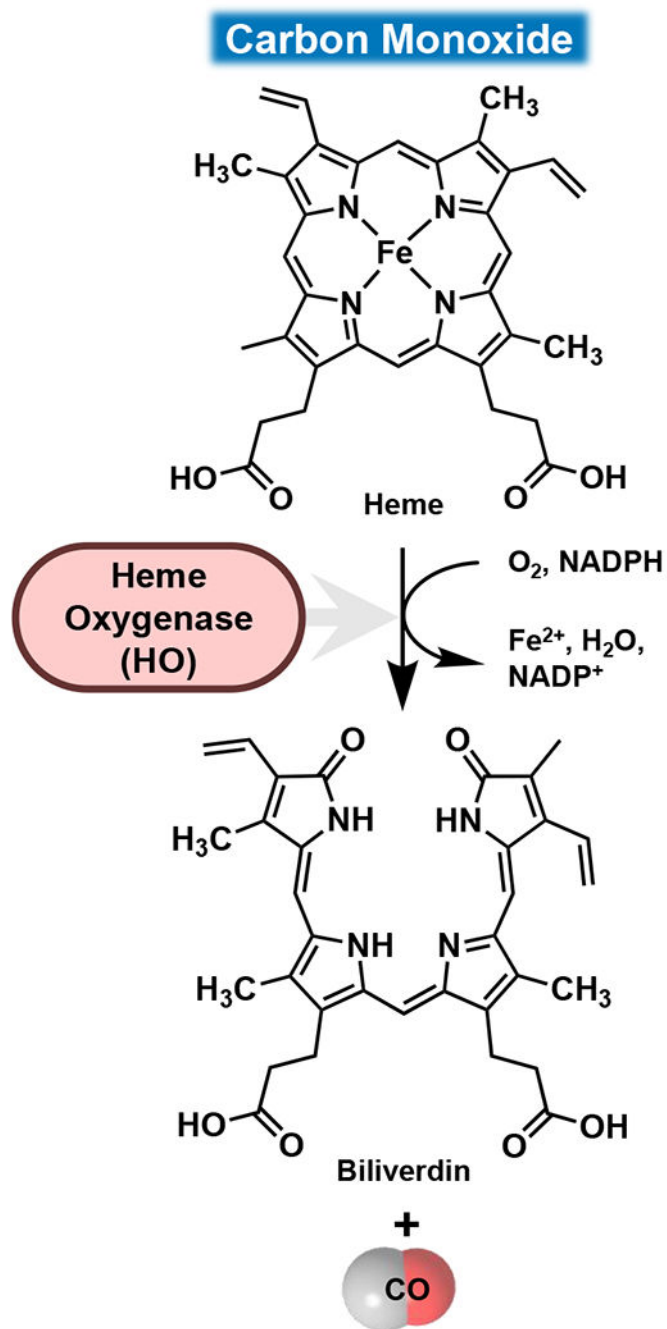


**Figure 2.** CO synthesis in reticuloendothelial cells of the liver, spleen, and bone marrow via the degradation of hemoglobin by heme oxygenase (HO).

## Hydrogen Sulfide

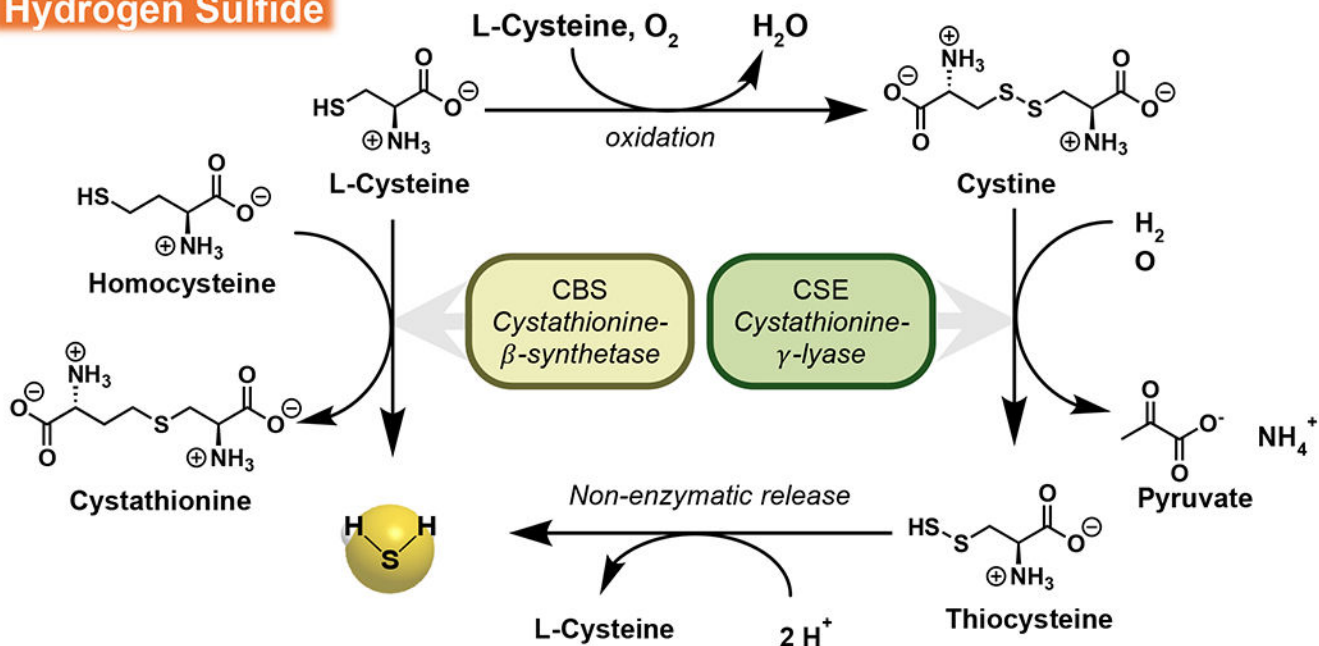


**Figure 3.** Pathways of biosynthesis for  $\text{H}_2\text{S}$ .  $\text{H}_2\text{S}$  is synthesized via L-cysteine catalysis in the mitochondria and cytosol by CAT and 3-MST, while CBS and CSE catalyze its production exclusively in the cell cytosol.

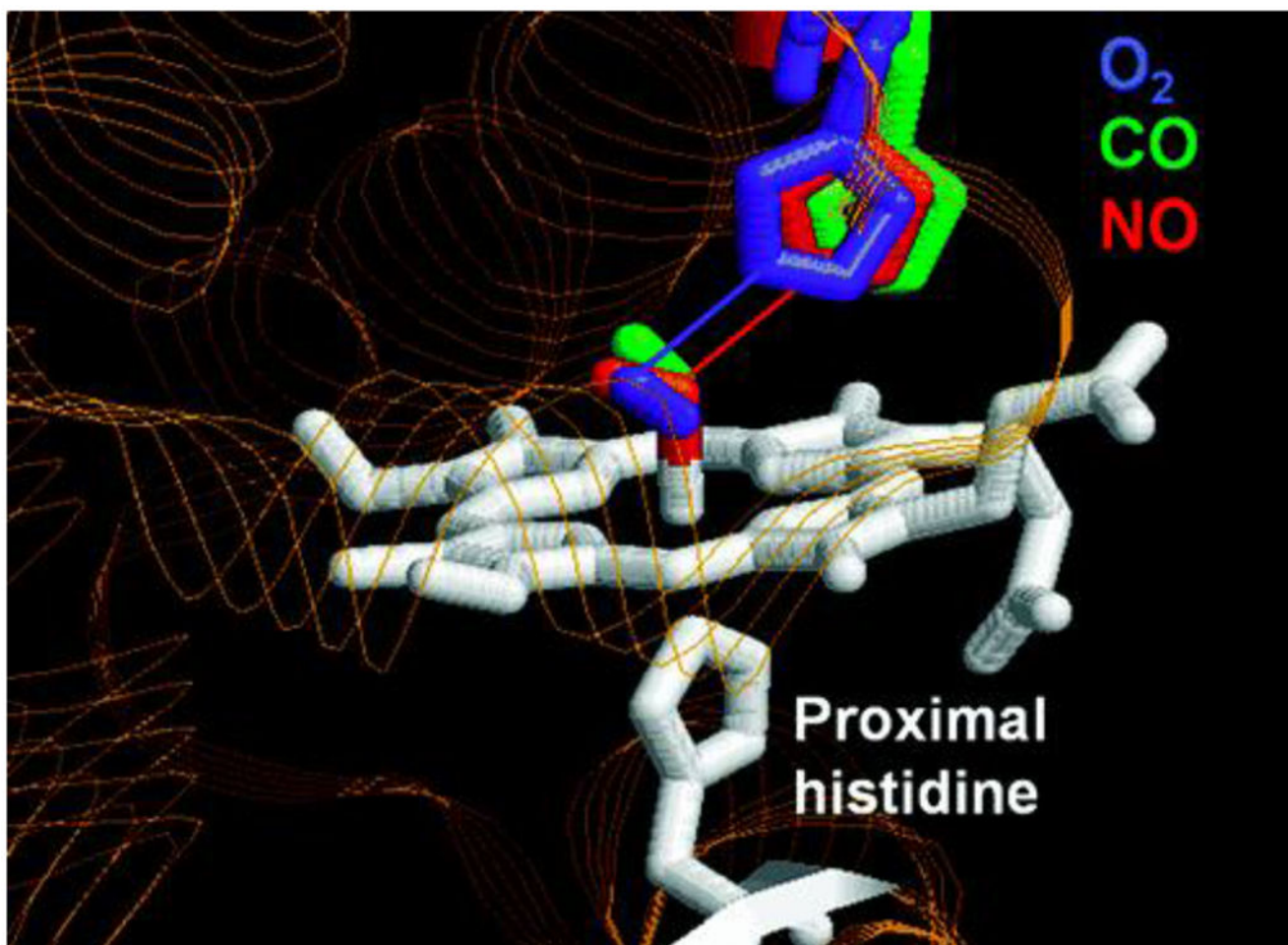


**Figure 4.** The impact of ligand geometry on the heme pocket of sperm whale myoglobin. Distinct positional changes at the distal histidine induced by different ligands – O<sub>2</sub>, CO, and NO – are shown. Each structure was determined by x-ray crystallography, and each structure is superposed on another. Hydrogen bonds, and interatomic distances  $< 3.0 \text{ \AA}$  are represented by lines. Reprinted with permission from Ref. 72. Copyright 1998 John Wiley and Sons.

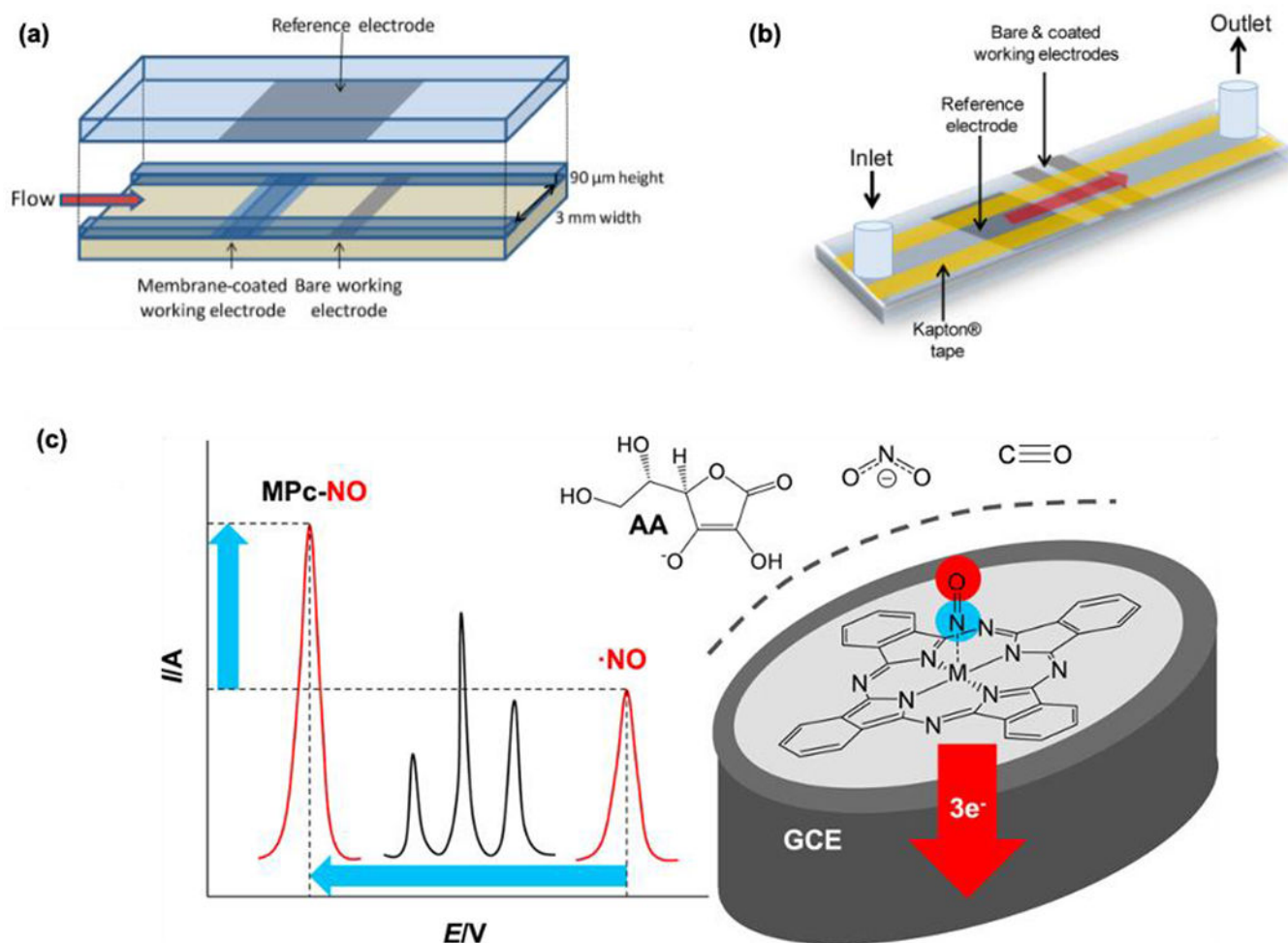


**Figure 5.** Examples of membrane-modified (a,b) and electrocatalyst-modified (c) electrochemical sensing devices. (a) and (b) show the channel construction (a) and overall device architecture (b) of an amperometric NO sensor coated with xerogel polymer membrane, demonstrating an 840 pM LOD and tested in blood and in-vivo monitoring for sepsis onset in a rodent model. The bottom device (c) is a glassy-carbon electrode (GCE) modified with a metallophthalocyanine (MPc) electrocatalyst. Differential pulse voltammetry showed  $\sim 1.5\times$  signal amplification for NO compared to bare GCE, and constant potential amperometry showed enhanced MPc-induced selectivity for NO over common interferents (e.g.,  $\text{NO}_2^-$ , ascorbic acid (AA), and CO). (a,b) Reproduced from Ref. 87. Copyright 2013 American Chemical Society. (c) Reprinted with permission from Ref. 88. Copyright 2018 Elsevier.

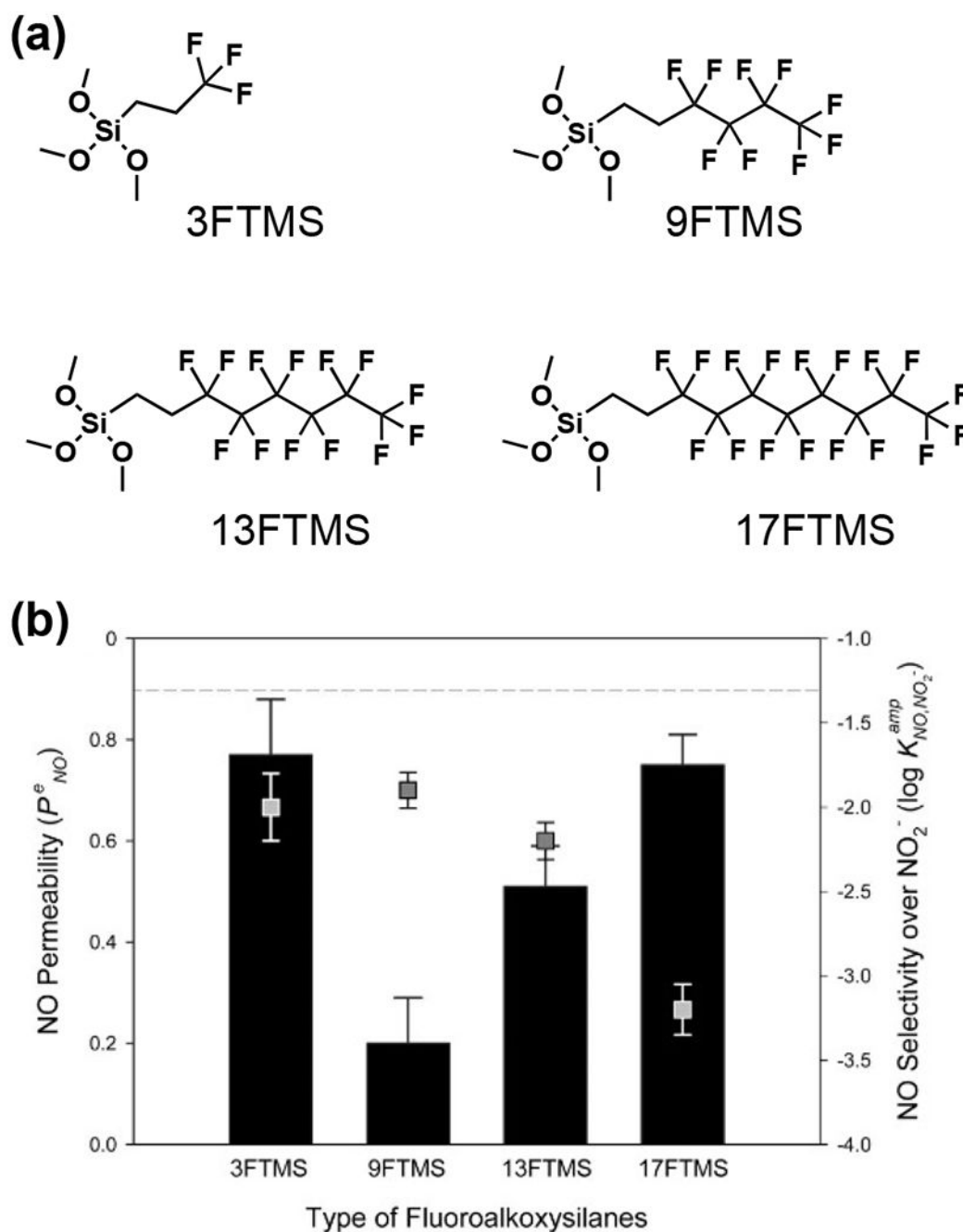


**Figure 6.**

(a) Structures of fluoroalkoxysilanes applied by Schoenfisch and colleagues: trifluoropropyltrimethoxysilane (3FTMS), nonafluorohexyltrimethoxysilane (9FTMS), (tridecafluoro-1,1,2,2-tetrahydrooctyl)trimethoxysilane (13FTMS), (heptadecafluoro-1,1,2,2-tetrahydrodecyl)trimethoxysilane (17FTMS). (b) NO permeability (bars, left axis) and selectivity over nitrite (points, right axis) as a function of the type of fluoroalkoxysilanes (20%, balance MTMOS). NO permeability is greatest when  $P^e_{NO}$  is high, and NO selectivity is the best when  $\log K_{NO,NO_2^-}$  is most negative; the 17FTMS



membrane demonstrates the most desirable sensing characteristics. (The dashed line indicates NO selectivity of the bare Pt electrode over nitrite, and data are represented as means  $\pm$  SD.) Reproduced from Ref. 110. Copyright 2008 American Chemical Society.

Author Manuscript

Author Manuscript

Author Manuscript

Author Manuscript

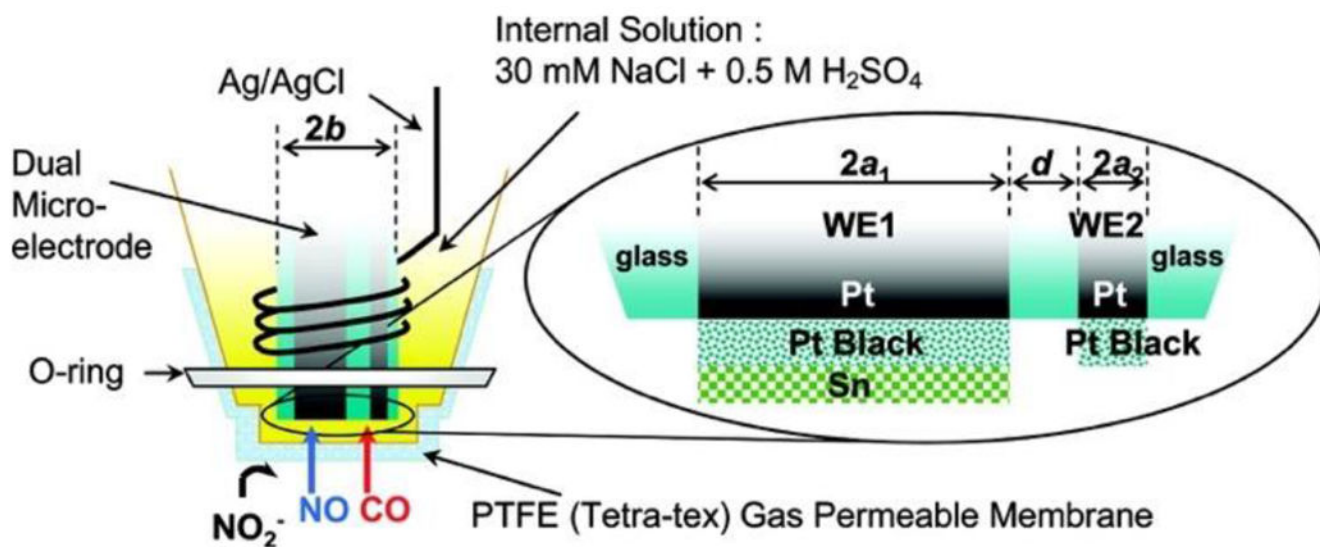


**Figure 7.** Schematic diagram of NO/CO dual microsensor from Ref. <sup>23</sup>. The dual microelectrode is composed of two working electrodes, WE1 and WE2, with dimensions  $a_1 = 125 \mu\text{m}$ ,  $a_2 = 12.5 \mu\text{m}$ ,  $b = 200\text{--}250 \mu\text{m}$ , and  $d = 30\text{--}50 \mu\text{m}$ . Reproduced Ref. 23. Copyright 2007 American Chemical Society.

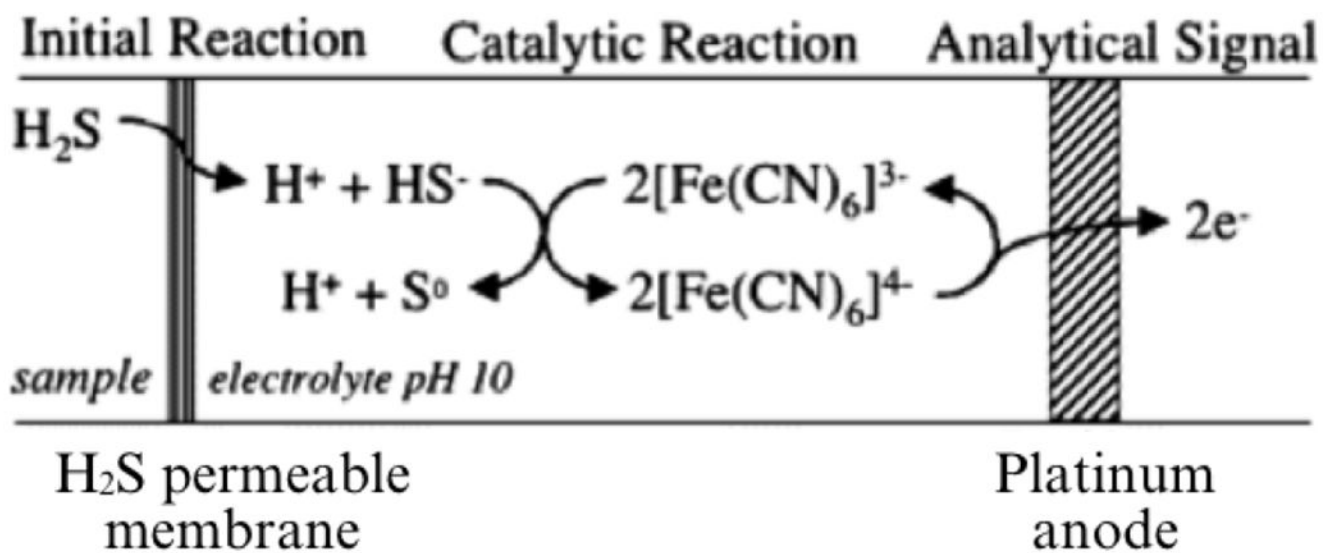


**Figure 8.** Redox chemistry of a polarographic  $\text{H}_2\text{S}$  sensor with  $\text{H}_2\text{S}$ -permeable silicone polymer membrane. Reprinted with permission from Ref. 97. Copyright 2005 Elsevier.

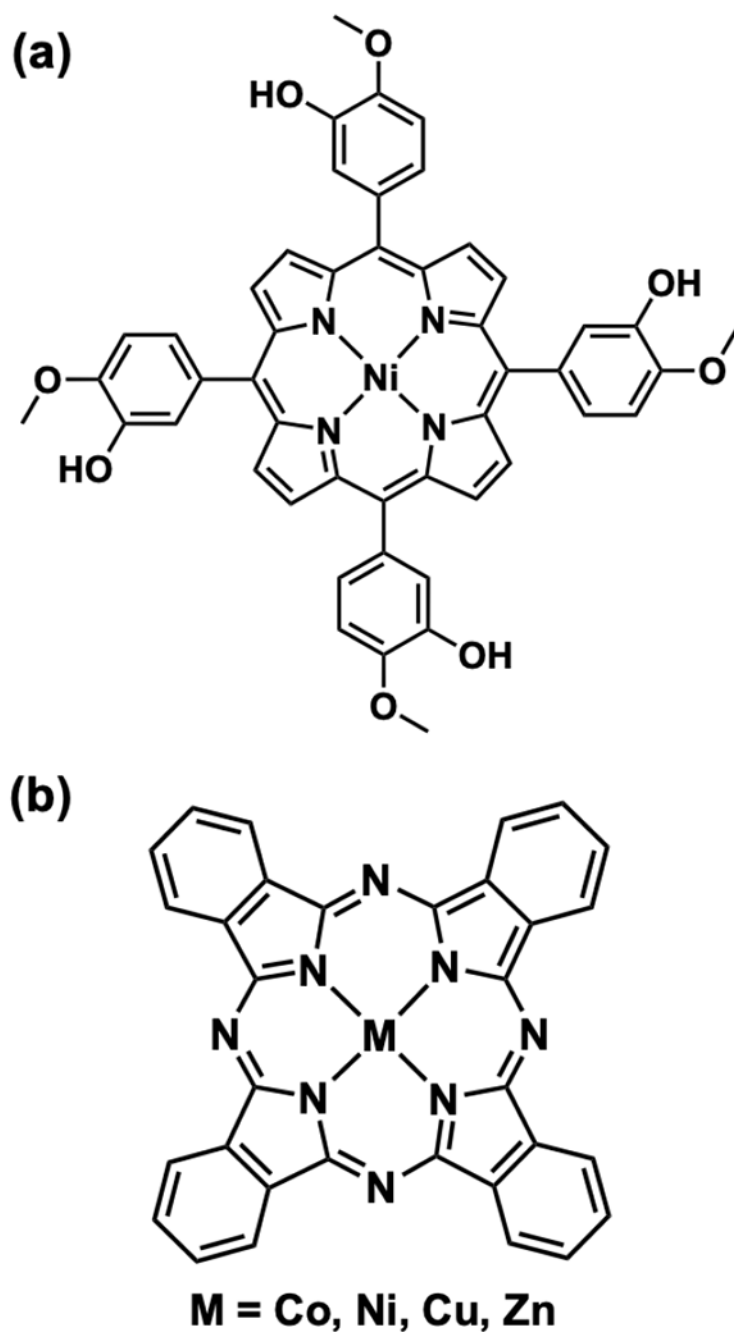


**Figure 9.** Metalloporphyrins and metallophthalocyanines used for NO detection. (a) Ni-porphyrin complex incorporated into an EPF for NO sensing. (b) Metallophthalocyanine macrocycles explored for NO detection.

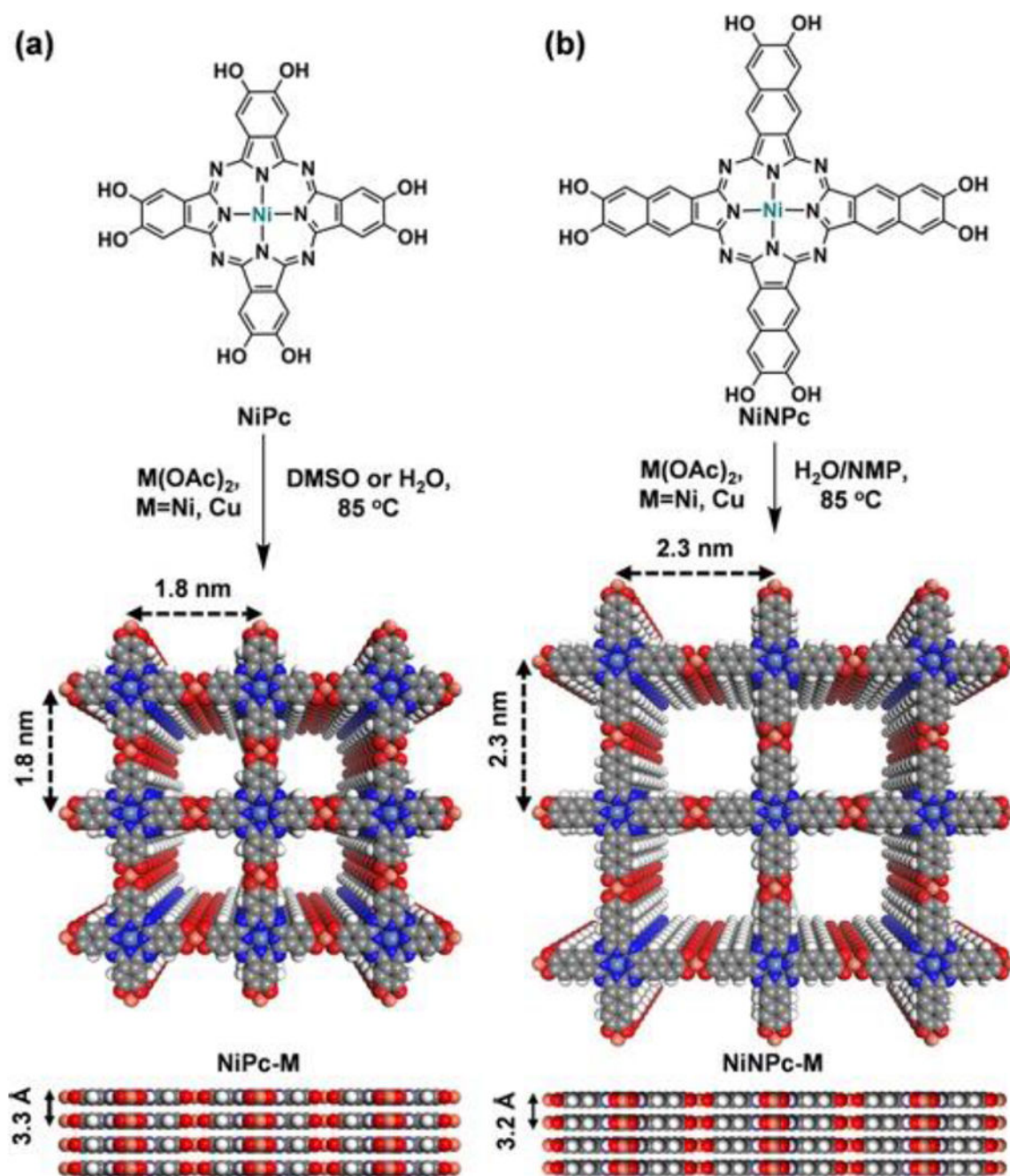


**Figure 10.**

The structure and synthesis of (a) NiPc and (b) NiNPc MPc-based two-dimensional MOFs. A 2 x 2 square grid form in eclipsed stacking mode is displayed, including both a top view (middle of figure) and side view (bottom of figure). Reprinted from Ref. 151. Copyright 2019 American Chemical Society.

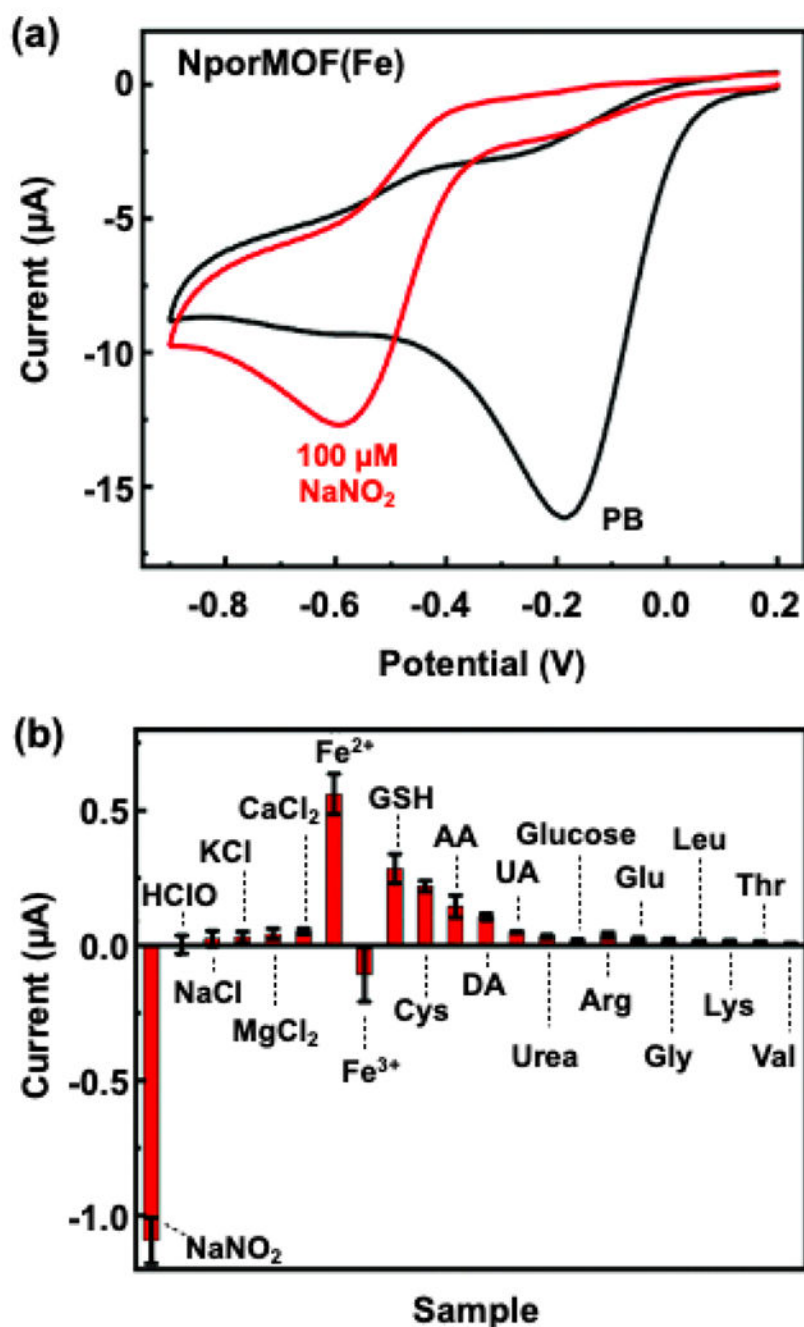


**Figure 11.**

(a) CV response of the NporMOF(Fe)-modified GCE in 10 mM phosphate buffer (PB), pH 2.5 (black) and 100 μM NaNO<sub>2</sub> added to buffer. (b) Current response of NporMOF(Fe) electrode in constant potential amperometry experiment to NaNO<sub>2</sub> (20 μM) and 21 interferences (all 200 μM): HClO, NaCl, KCl, MgCl<sub>2</sub>, CaCl<sub>2</sub>, Fe<sup>2+</sup>, Fe<sup>3+</sup>, glutathione (GSH), cysteine (Cys), ascorbic acid (AA), uric acid (UA), urea, glucose, arginase (Arg), glutamic acid (Glu), glycine (Gly), leucine (Leu), lysine (Lys), threonine (Thr), and valine (Val). All



experiments conducted at  $-0.55$  V in 10 mM PB, pH 2.5. Adapted with permission from Ref. 115. Copyright 2021 Royal Society of Chemistry.

Author Manuscript

Author Manuscript

Author Manuscript

Author Manuscript

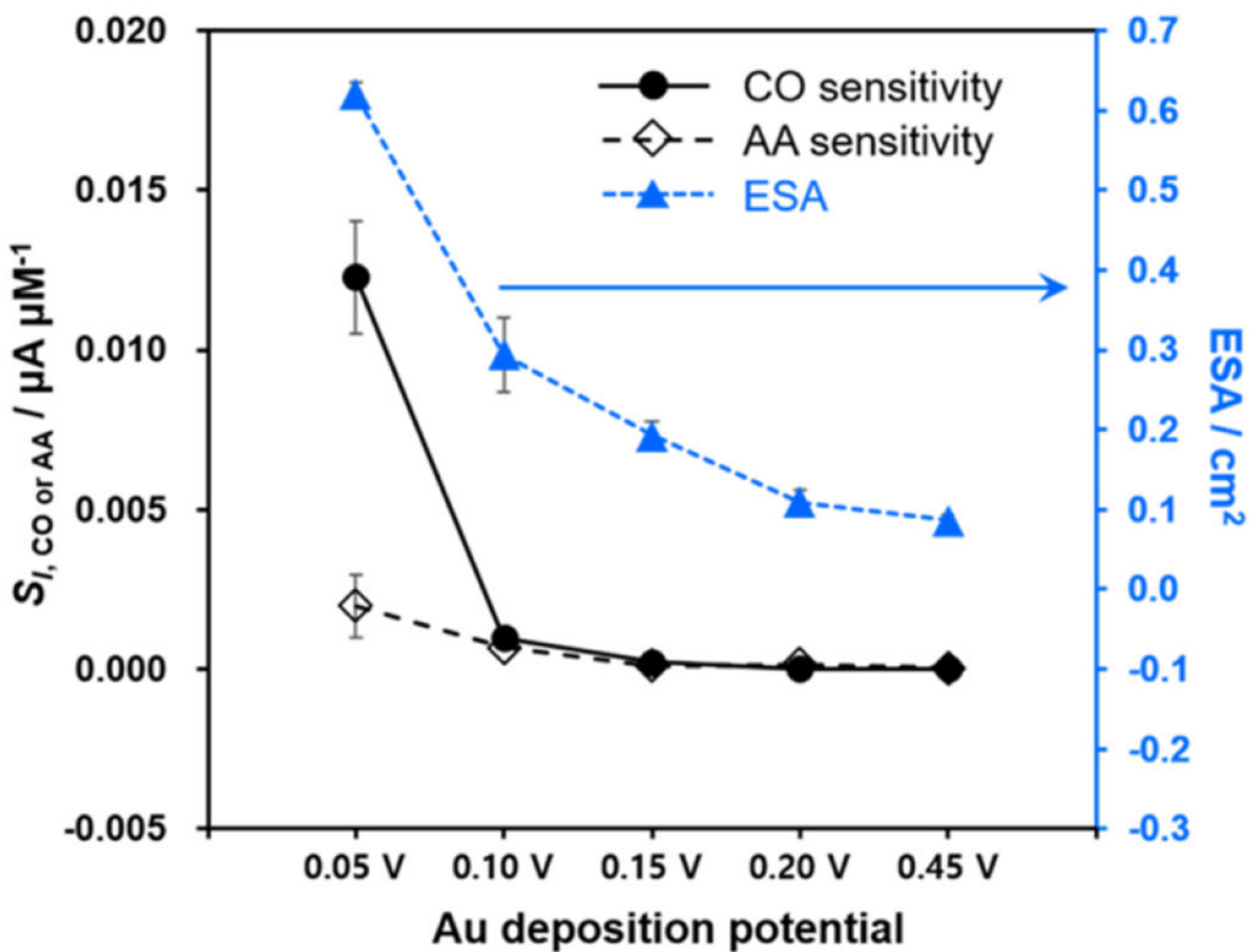


**Figure 12.** The current sensitivities of Au deposits to CO and AA along with the corresponding ESAs (electrode surface areas) depending on the deposition potential of Au ( $n = 5$ ). Reproduced from Ref. 94. CC BY 4.0.

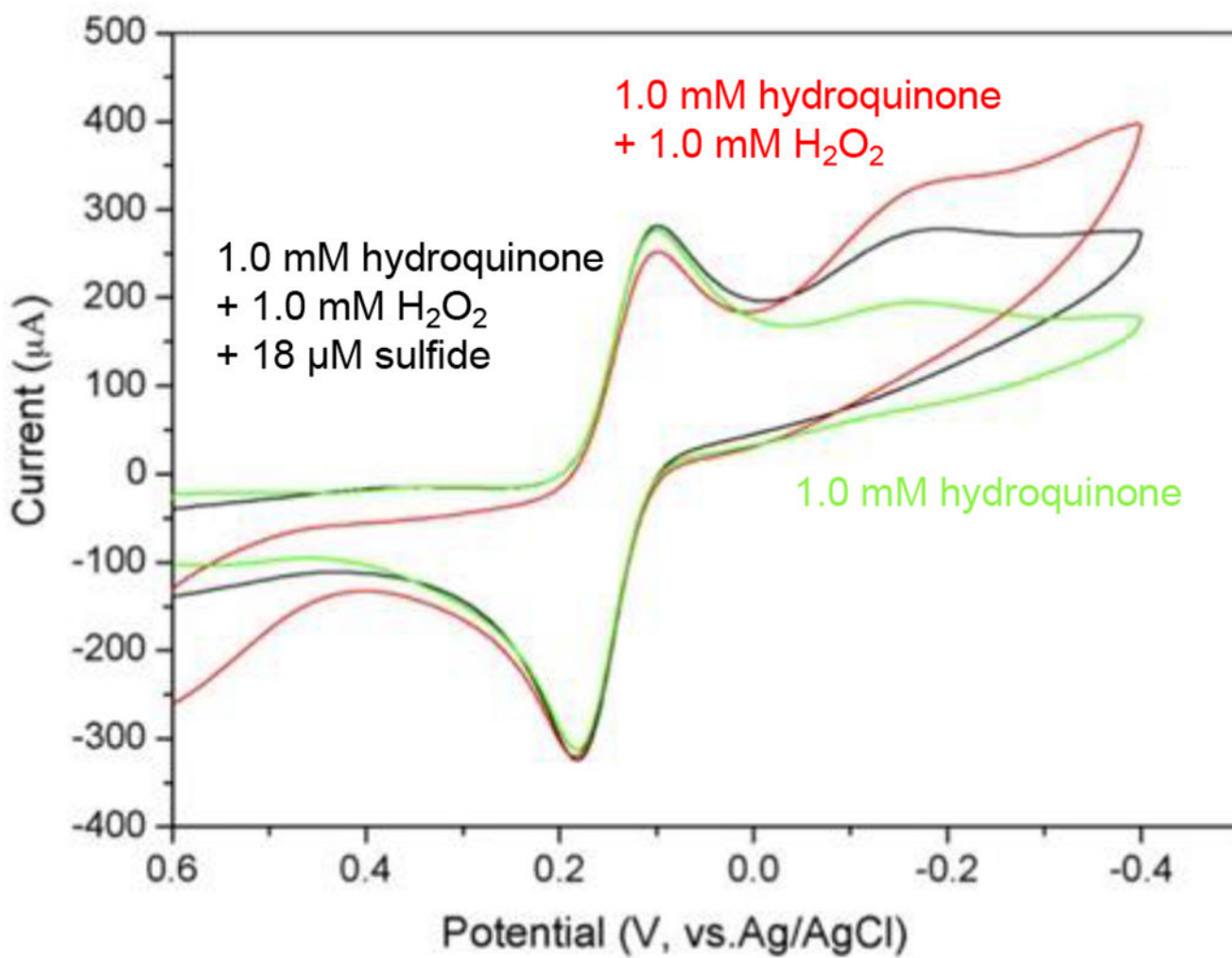


**Figure 13.**

Cyclic voltammograms of Au/MPS/PAH/PSS/PAH/(Con A/HRP)<sub>4</sub> electrode at different stages: the electrode in 0.2 mM PBS (pH 6.5) containing 1.0 mM hydroquinone; with 1.0 mM  $\text{H}_2\text{O}_2$  added; and with 18.0  $\mu\text{M}$  sulfide added; scan rate for all scans was 100 mV/s. Adapted with permission from Ref. 165. Copyright 2008 Elsevier.

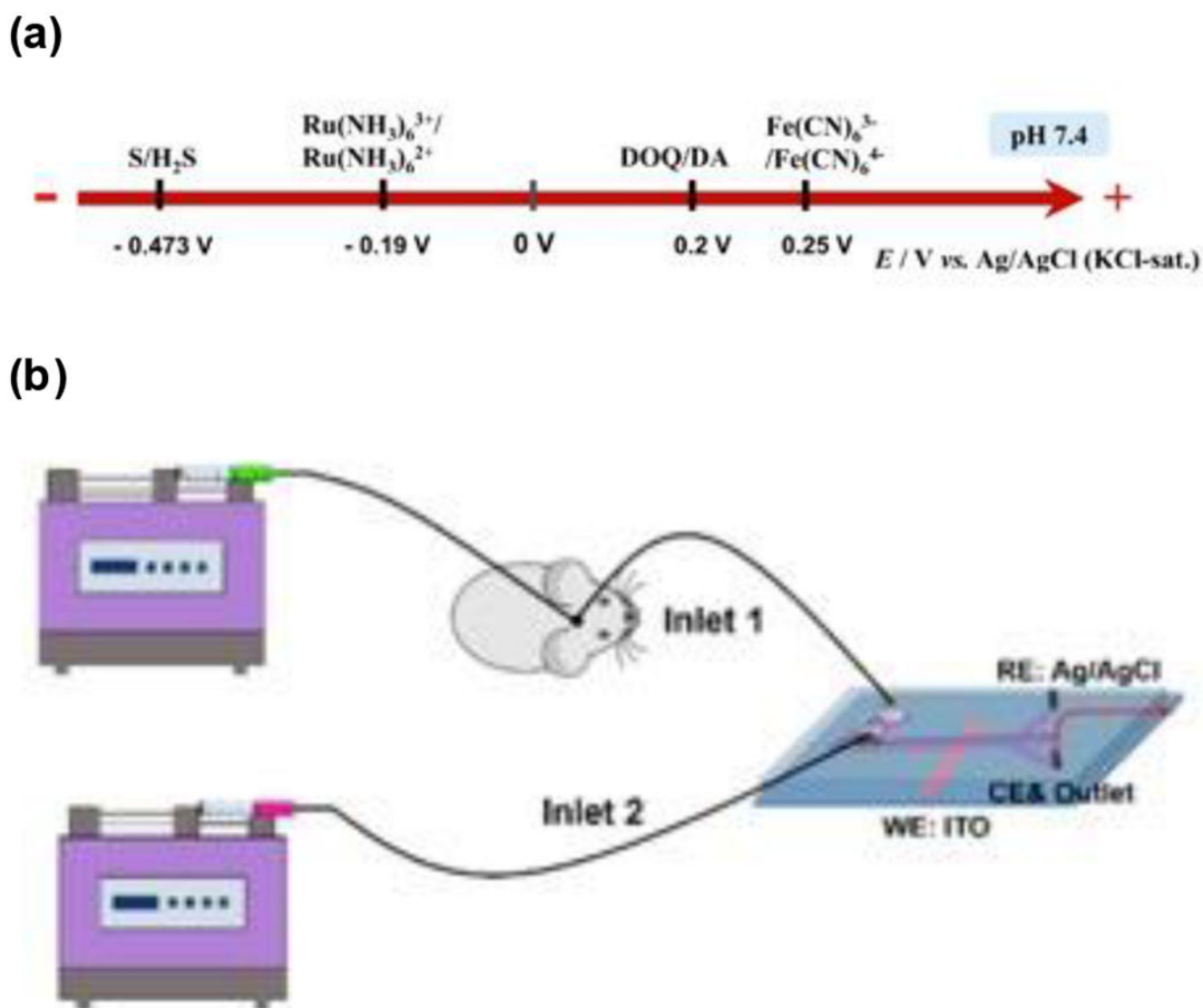


**Figure 14.** (a) Potentials of typical species related to hydrogen sulfide; (b) Schematic of the microchip-based online electrochemical system for measurement of hydrogen sulfide; Reproduced from Ref. 175. Copyright 2017 American Chemical Society.

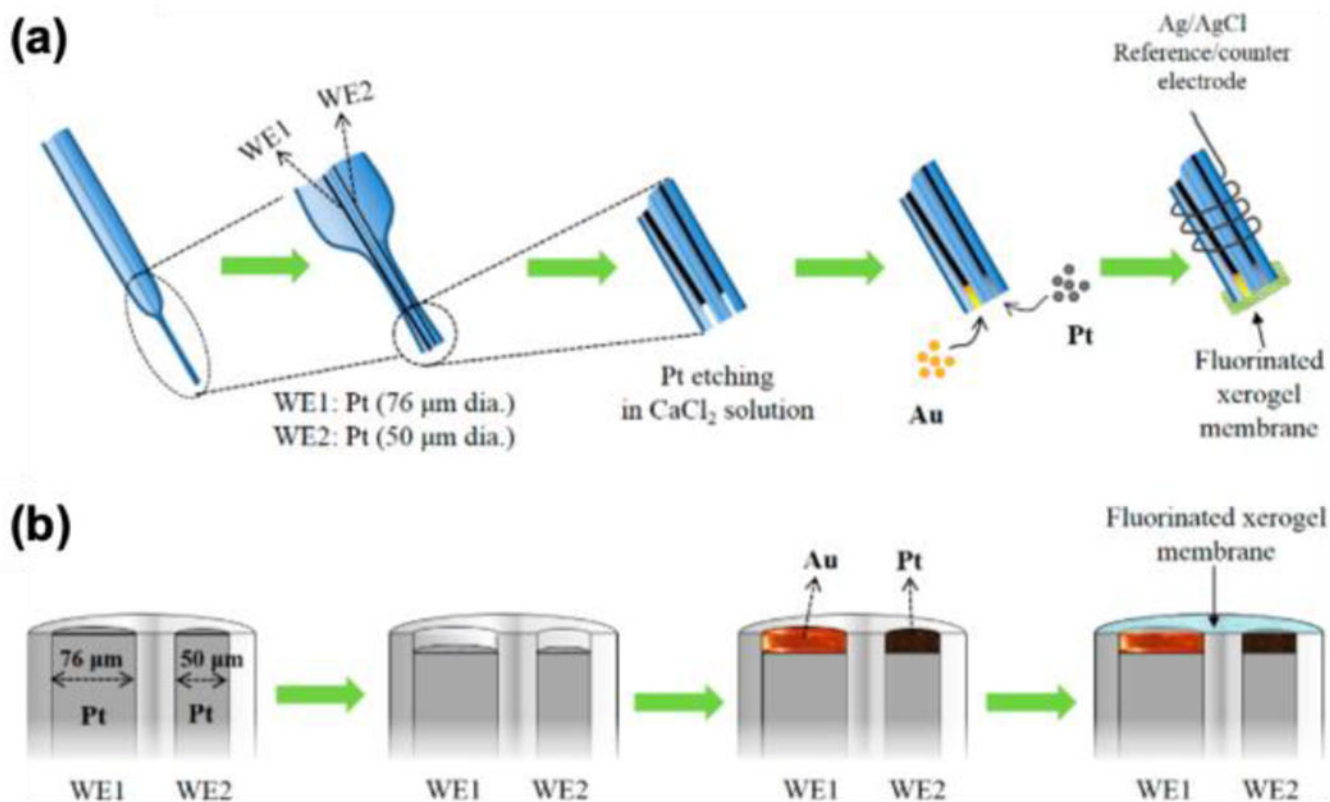


**Figure 15.**

An example multi-analyte detection from Ha and colleagues. (a) Schematic illustration for the preparation steps of an insertable NO/CO dual microsensor. (b) Cross-sectional views of a dual microelectrode during a course of the NO/CO dual sensor preparation. Reproduced from Ref. 116. Copyright 2016 American Chemical Society.

Table 1.

Physiological and physiochemical properties of gasotransmitters

Physiological Concentrations and Endogenous Locations*			
	NO	CO	H <sub>2</sub> S
Cell location/compartments	Tissue-specific cell cytosol, mitochondria	Multiple subcellular compartments, ER, PM, cell nucleus	Cell cytosol, mitochondria
Cell enzymatic systems	eNOS nNOS iNOS	HO-1 HO-2 HO-3	CBS CSE 3MST
Alternative endogenous mechanisms	NO <sub>2</sub> <sup>-</sup> , NO-buffers (GSNO, PtNO)	Reduction of thiosulfate, polysulfurated intermediates	None identified
Physiological cell concentration	10 <sup>-3</sup> – 10 <sup>-1</sup> μM	~2 nM	10 <sup>-3</sup> – 10 <sup>-1</sup> μM
Mobility in tissues (cm <sup>2</sup> ·s <sup>-1</sup> )	4.8 x 10 <sup>-5</sup>	3.3 x 10 <sup>-5</sup>	3.0 x 10 <sup>-6</sup>
Concentration in exhaled air <sup>**</sup>	10 – 50 ppb	0 – 6 ppm	0 – 1.3 ppm
Physiochemical Properties***			
	NO	CO	H <sub>2</sub> S
Molar mass (g/mol)	30.01	28.01	34.08
Dipole moment (D, Debye)	0.16	0.11	0.97
Solubility (g/100g H <sub>2</sub> O, 20 °C)	0.0062	0.0028	0.40
Diffusion coefficient in H <sub>2</sub> O (x10 <sup>-5</sup> cm <sup>2</sup> ·s <sup>-1</sup> 20°C)	2.07	2.03	1.75
I <sup>st</sup> ionization energy (eV)	9.26	14.01	10.46

Abbreviations: ER, endoplasmic reticulum; PM, plasma membrane; eNOS, endothelial nitric oxide synthase; nNOS, neuronal nitric oxide synthase; iNOS, inducible nitric oxide synthase; HO, heme oxygenase; CBS, cystathione-β-synthase; CSE, cystathione-γ-lyase; 3MST, 3-mercaptopyruvate-sulfurtransferase; D, diffusion rate (cm<sup>2</sup>·s<sup>-1</sup>); GSNO, nitrosated glutathione; PtNO, nitrosated/nitrosylated endogenous proteins.

\* Values from Ref.16.

\*\* Concentrations ranges for healthy person. Values from Ref. 17.

\*\*\* Values from Ref. 7 and references within.



**Table 2.** Selected examples of electrochemical detection: NO, CO, and H<sub>2</sub>S in biological applications

Electrode Material ( <i>Features</i> )	Target analyte	Method	Limit of detection	Linear dynamic range	Sensitivity	Selectivity	Ref.
CuTAPc-MCOF@AgNPs ( <i>electrocatalyst</i> )	NO	CV	12.6 nM (S/N=3)	0.18 - 17.1 μM	29.1 μA μM <sup>-1</sup> cm <sup>-2</sup>	No interference (signal change <5%) from 1 mM KCl, NaNO <sub>2</sub> , Na <sub>2</sub> SO <sub>4</sub> , glucose, CaSO <sub>4</sub> , CuSO <sub>4</sub> , H <sub>2</sub> O <sub>2</sub> , UA, DA, AA	114
nano-metalloporphyrinic metal-organic framework (NporMOF(Fe)) ( <i>electrocatalyst, multi-analyte</i> )	NO, H <sub>2</sub> O <sub>2</sub>	CV	1.3 μM	5 μM to 200 μM	n/a	Qualitatively selective against 20 physiological interferents with current response negligible at NO reduction potential	115
bioresorbable substrate (copolymer of poly(L-lactic acid) and poly(trimethylene carbonate), Au nanomembrane electrodes, poly(eugenol) film ( <i>membrane, solid contact WE only</i> ))	NO	LSV (bias voltage of +0.8 V)	3.97 nmol	0.01–100 μM	5.29 nA μM <sup>-1</sup>	Qualitatively selective against glucose, sodium nitrite, sodium nitrate, ascorbic acid and uric acid.	103
Au-deposited Pt microdisk (WE1, 76 μm) Pt/black-deposited Pt disk (WE2, 50 μm), fluorinated xerogel membrane (dual-electrode sensing system) ( <i>membrane, solid contact, WE only, multi-analyte</i> )	NO CO	Amperometric; oxidation of CO at WE1 (+0.2 V vs Ag/AgCl) and NO at WE2 (+0.75 V vs Ag/AgCl)	~6.0 nM of NO ~180 nM of CO (S/N=3)	0.020–2.0 μM for NO 0.18–9.0 μM for CO	0.1338 μA μM cm <sup>-2</sup> NO 0.2656 μA μM cm <sup>-2</sup> CO	log K <sub>CO<sub>2</sub></sub> <sup>amp</sup> between -3.03 and -4.16 for nitrite, AA, DA, H <sub>2</sub> O <sub>2</sub> , and H <sub>2</sub> S	116
ITO microelectrode array/πGO-FeTCP/ATPA ( <i>electrocatalyst</i> )	NO	CPA at +0.75 V vs. Ag/AgCl in 100 mM PBS	55 pM in PBS and 90 pM in cell medium (S/N = 3)	0.020–2.0 μM	37.6 μA μM <sup>-1</sup> cm <sup>-2</sup>	selectivity ratios for NO against AA = 113; DA = 96; UA = 158; and NO <sub>2</sub> <sup>-</sup> = 117	117
Pt/APTES/XG ( <i>membrane, solid contact, all electrodes, microfluidic</i> )	NO	CPA at +700 mV vs. Ag/AgCl	840 pM	840 pM - 100 μM	1.4 pA nM <sup>-1</sup>	No interference (signal change <5%) over NO <sub>2</sub> <sup>-</sup> , AA, AC, UA, H <sub>2</sub> S, NH <sub>4</sub> <sup>+</sup> , NH <sub>3</sub> , ONOO <sup>-</sup> (selectivity coefficients -5.3, -4.2, -4.0, -5.0, -6.0, -5.8, -3.8, -1.5, and -4.0, respectively)	87
Pt microdisks, Ag/AgCl reference electrode, poly(tetrafluoroethylene) membrane *dual-electrode sensing system: Pt/Sn (WE1) and Pt-Fe(III) (WE2) ( <i>membrane, Shibuk-style, multi-analyte</i> )	NO, CO	LSV; oxidation of NO at WE2 +0.75 V; CO at WE1 +0.70 V, (vs Ag/AgCl) in 30 mM NaCl and 0.5 M H <sub>2</sub> SO <sub>4</sub>	< 2 nM for NO at WE1, <10 nM for CO at WE1	2 nM - 6 μM for NO, 10 nM - 6 μM for CO	1.59 ± 0.47 nA μM <sup>-1</sup> at WE1 for NO, 1.29 ± 0.35 nA μM <sup>-1</sup>	No significant response to 100 μM acetaminophen, 100 μM UA, 100 μM nitrite, 100 μM ascorbic acid, 50 μM DA	19
Au/poly(eugenol)/poly(phenol) ( <i>membrane, solid contact, WE only, multi-analyte</i> )	NO, ONOO <sup>-</sup>	Amperometric; 0.8 V vs. Ag/AgCl in 100 mM PBS	27 nM (S/N = 3)	0.1 - 7 μM	0.56 pA nM <sup>-1</sup>	Not quantified	118
Pt microdisk; Ag/AgCl CE/ref.; Tetra-tex membrane *dual-electrode sensor: platinumized/Sn deposited Pt electrode (WE1), platinumized Pt	CO, NO	Amperometric; oxidation of NO (WE1 and 2) and CO (WE1) at 0.7 V for	<5 nM for CO, ~1 nM for NO	0.18 - 120 μM for CO, 0.1 - 7 μM for NO	19.8 ± 3.11 nA μM <sup>-1</sup> for CO, 9.6 μM <sup>-1</sup> for NO	No significant responses to 500 μM nitrite, AA, UA, DA, AC (at -0.7 V and -0.85 V vs. Ag/AgCl)	23

Electrode Material (Features)	Target analyte	Method	Limit of detection	Linear dynamic range	Sensitivity	Selectivity	Ref.
electrode (WE2) (membrane, Shibuki-style, multi-analyte)		WE1, 0.85 V for WE2 vs Ag/AgCl			$\pm 1.5$ nA $\mu\text{M}^{-1}$ for NO		
GCE with electrodeposited Au nanoparticles (electrocatalyst)	CO	Amperometric (LSV, CPA)	n/a	0 - 18.2 $\mu\text{M}$	0.013 $\mu\text{A}$ $\mu\text{M}^{-1}$	Selectivity coefficients $\log K_{\text{CO}_2/\text{amp}}$ for AA, -0.714; GABA, -3.768; $\text{NO}_2^-$ -3.665	94
Reduced graphene oxide-molybdenum disulfide nanohybrid (RGO-MoS2) and poly(o-phenylenediamine) (POPD) (electrocatalyst, membrane, solid contact WE only)	H <sub>2</sub> S	Amperometric (CV, CPA)	1 nM	12.5 nM-1.2 mM	0.0172 $\mu\text{A}$ $\mu\text{M}^{-1}$	Qualitatively selective against dopamine, ascorbic acid, cysteine, uric acid, glutathione, Na <sub>2</sub> S <sub>2</sub> O <sub>3</sub> , Na <sub>2</sub> S <sub>2</sub> O <sub>4</sub> , NO <sub>3</sub> <sup>-</sup> , NO <sub>2</sub> <sup>-</sup> , and H <sub>2</sub> O <sub>2</sub> .	119
Gold nanowire (AuNW) and carbon nanotube (CNT) films embedded in poly(dimethylsiloxane) (PDMS) (electrocatalyst)	H <sub>2</sub> S	CV	3 nM	5 nM - 24.9 $\mu\text{M}$	Not quantified	Selective against dopamine, glutathione, cysteine, and Na <sub>2</sub> SO <sub>3</sub> (1 $\mu\text{M}$ each, 0.3 V, pH 7.4)	101

Abbreviations: CuTAPe-MCOF@AgNPs = metallo-copper phthalocyanine-based covalent-organic framework (CuTAPe-MCOF) with silver nanoparticles; WE = working electrode; CE = counter electrode; AA = ascorbic acid; UA = uric acid; AC = acetaminophen; APTES = (3-aminopropyl)triethoxysilane; XG = xerogel polymer; 5-HIAA = 5-hydroxyindole-3-acetic acid; 5-HT = serotonin; DA = dopamine; DOPAC = 3,4-dihydroxyphenylacetic acid; HVA = homovanillic acid; rGO = reduced graphene oxide; APBA = 3-aminophenylboronic acid; FeTCP = porphyrin; MOFs = metal-organic framework; PCA = principal component analysis; GO = graphene oxide